RT magnet design, fabrication and testing

Attilio Milanese

CAS course on Normal- and Superconducting Magnets
19 Nov. – 2 Dec. 2023
St. Pölten, Austria

If you want to know more…

1. D. Tommasini, Practical Definitions & Formulae for Normal Conducting Magnets
2. Special CAS on magnets, Bruges, Jun. 2009
3. Lectures about magnets in JUAS (Joint Universities Accelerator School
4. Lectures about magnets in previous general CAS
5. N. Marks, Magnets for Accelerators, JAI (John Adams Institute) course, Jan. 2015
6. J. Tanabe, Iron Dominated Electromagnets
7. And many many more!!

Thanks in particular to Davide Tommasini, Thomas Zickler and the colleagues of the TE-MSC-NCM (MNC) section at CERN!

Introduction

We have many normal conducting magnets at CERN, many of them can be considered "references"…

NORMA

The CERN Normal Conducting Magnets database

The portal with information about the magnets, their components and activities linked to their operation and maintenance.

https://norma-db.web.cern.ch

(link available within CERN)

NORMA DATABASE

MAGNET ADVANCED SEARCH

| Found 4551 results. Page 58 of 304.

Previous 50 51 52 53 54 55 56 57 58 59 60 61 62 63 64 65 Next

Magnet	Status	Condition	Location
PXMBHEDWWP-E2000001 *Type W-01*	Installed	Not Checked	AD , *slot* DI.BHZ6064
PXMBHEDWWP-E2000002 *Type W-02*	Installed	Not Checked	AD , *slot* DI.BHZ6065
PXMBHEDWWP-E2000003 *Type W-03*	Installed	Certified Good (2020-01-08)	AD , *slot* DI.BHZ6045
PXMBHEDWWP-E2000004 *Type W-04*	Installed	Certified Good (2020-01-08)	AD , *slot* DI.BHZ6044

4551 installed
315 design codes

PS main unit magnets: operated (with several consolidation campaigns) since 1959

MPS/Int. DL 63-13
31.5.1963

EDMS 1262033
268 pages

CERN. Genève. Division du synchrotron à protons.

THE CERN PROTON SYNCHROTRON MAGNET

SPS main bending magnets

2.0 T, 5.8 kA

vertical gap 39 mm (MBA) or 52 mm (MBB)

MCB (HB2) dipoles, East Area and North Area

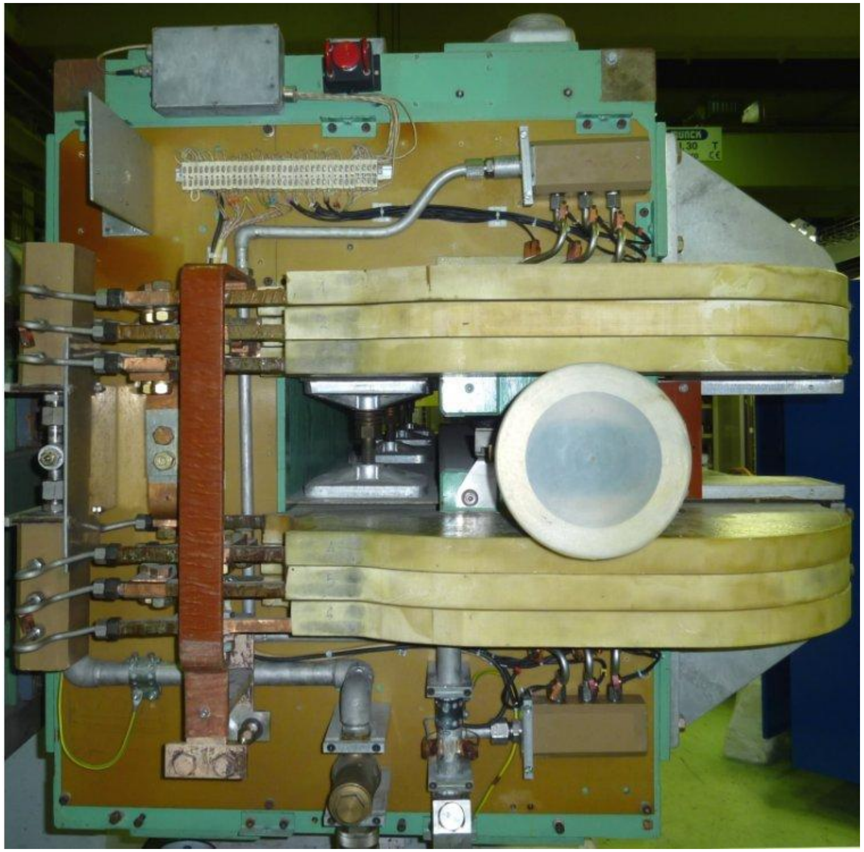

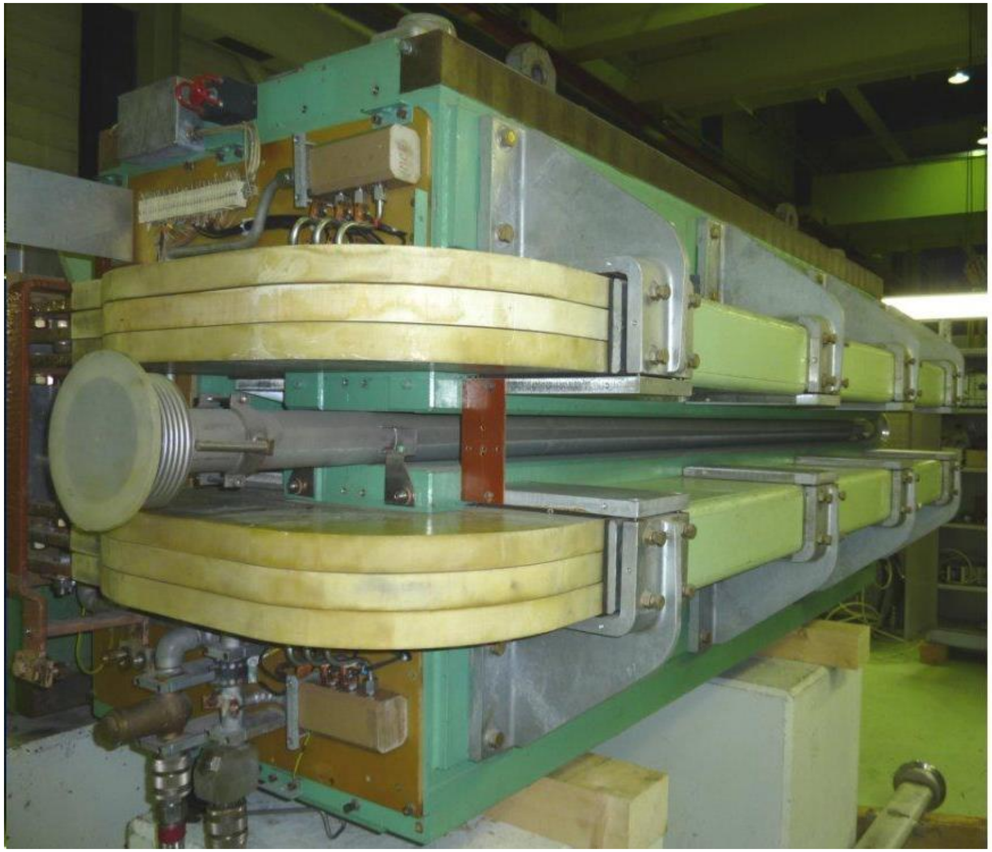

1.74 T, 880 A
vertical gap 80 mm

SPS main quadrupoles

22 T/m, 2.1 kA
aperture diameter 88 mm

Q200 L quadrupoles, East Area

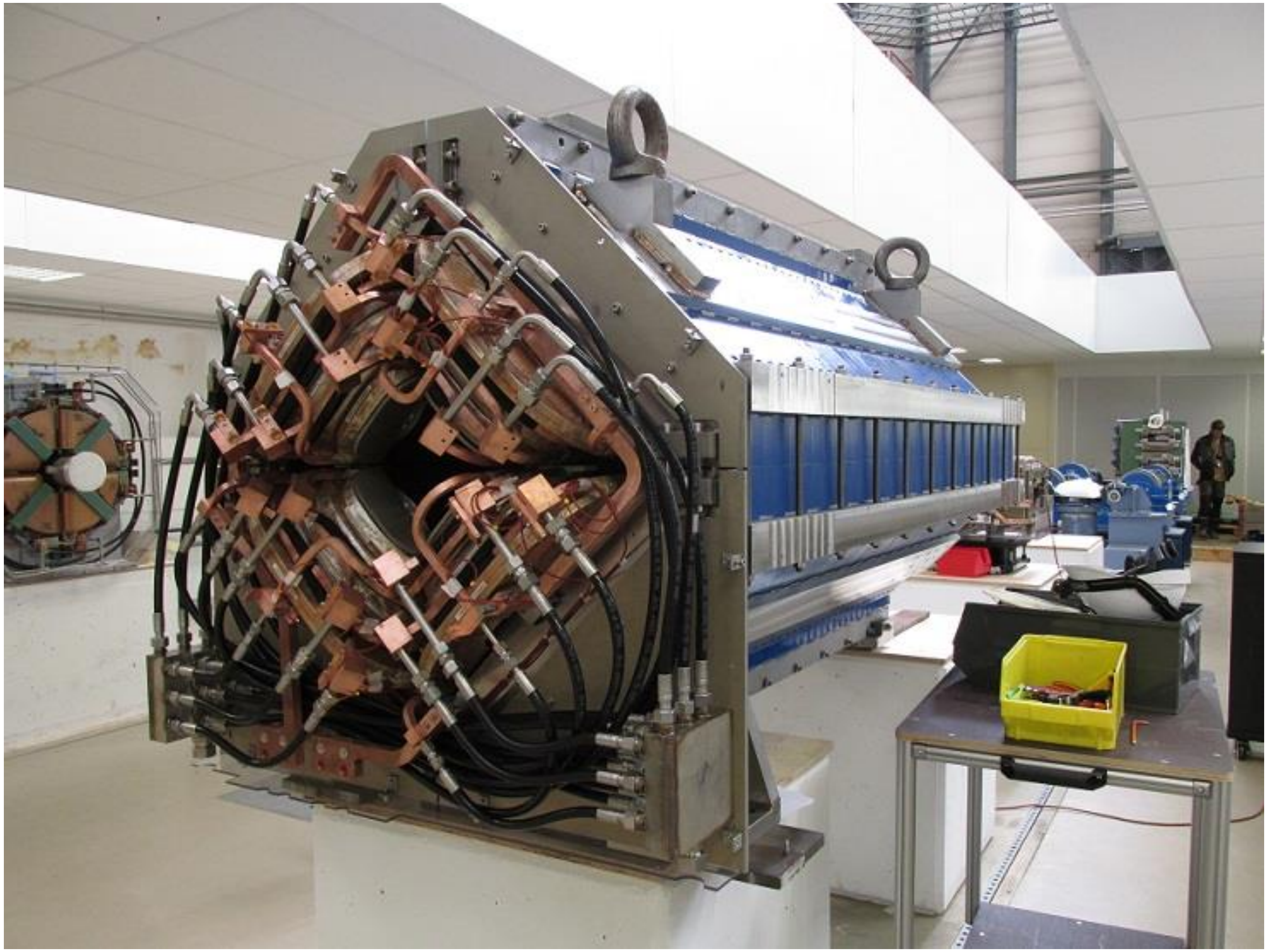

11.85 T/m, 800 A
aperture diameter 200 mm

SESAME combined function main bending

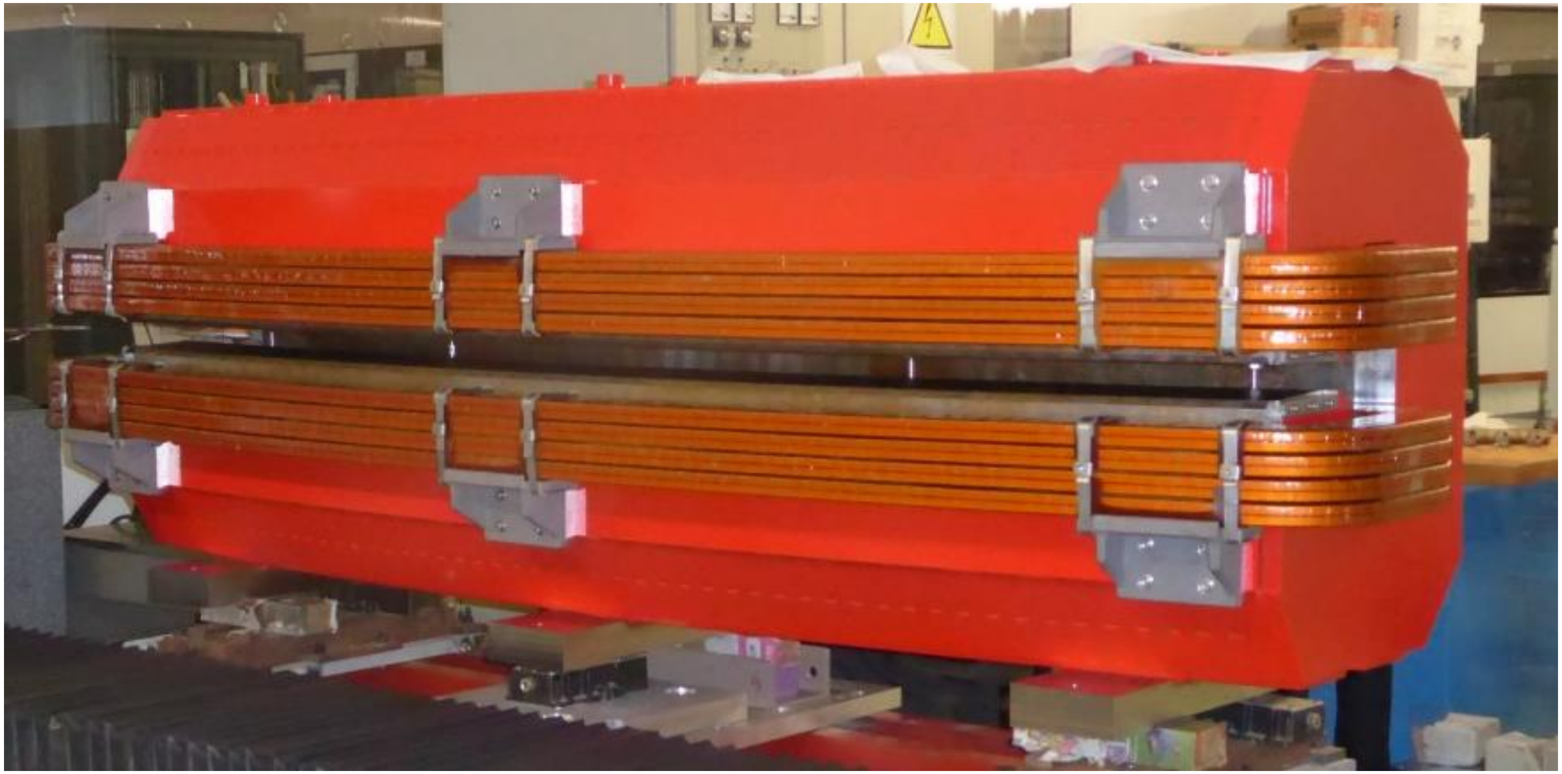

1.46 T, -2.79 T/m, 494 A
vertical gap 40 mm

MQW twin quadrupoles for LHC

35 T/m, 710 A
aperture diameter 46 mm

MDX L 150 correctors, East Area

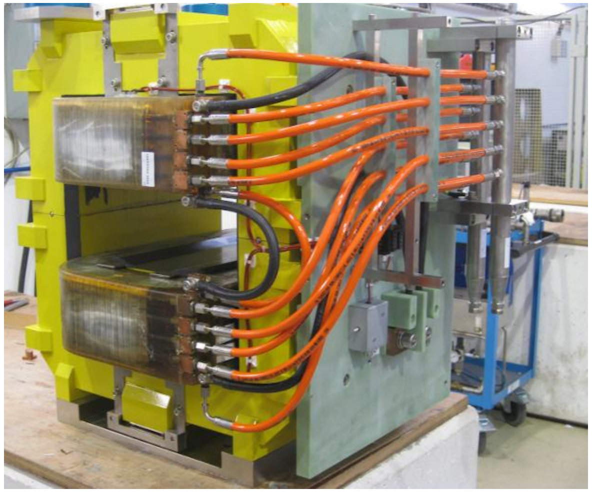
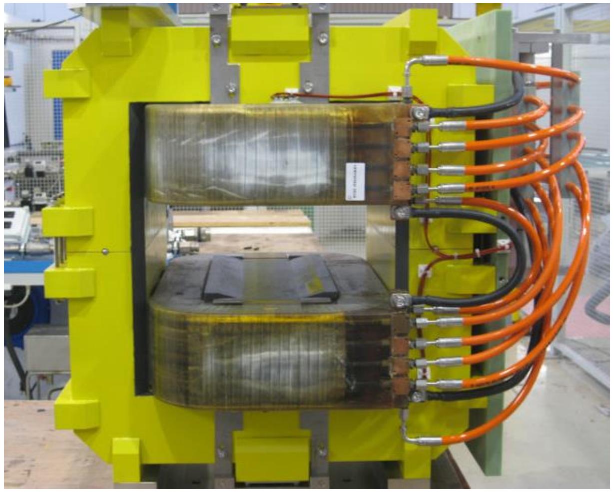


0.70 T, 240 A
vertical gap 150 mm

H+V correctors: HIE Isolde and AWAKE electron line

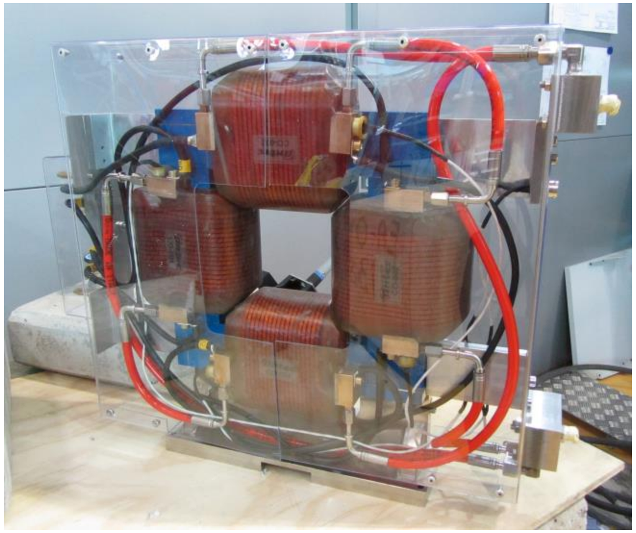

9.1 mT·m, 48 A
gap 92 × 92 mm

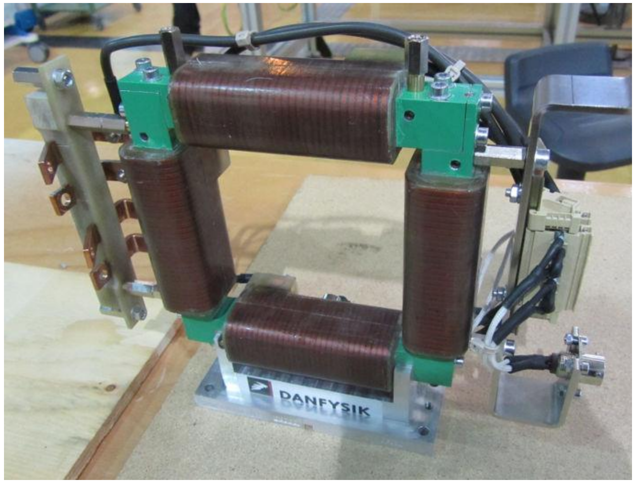

0.414 mT·m, 5 A
gap 100 × 100 mm

SESAME sextupoles (with embedded correctors)

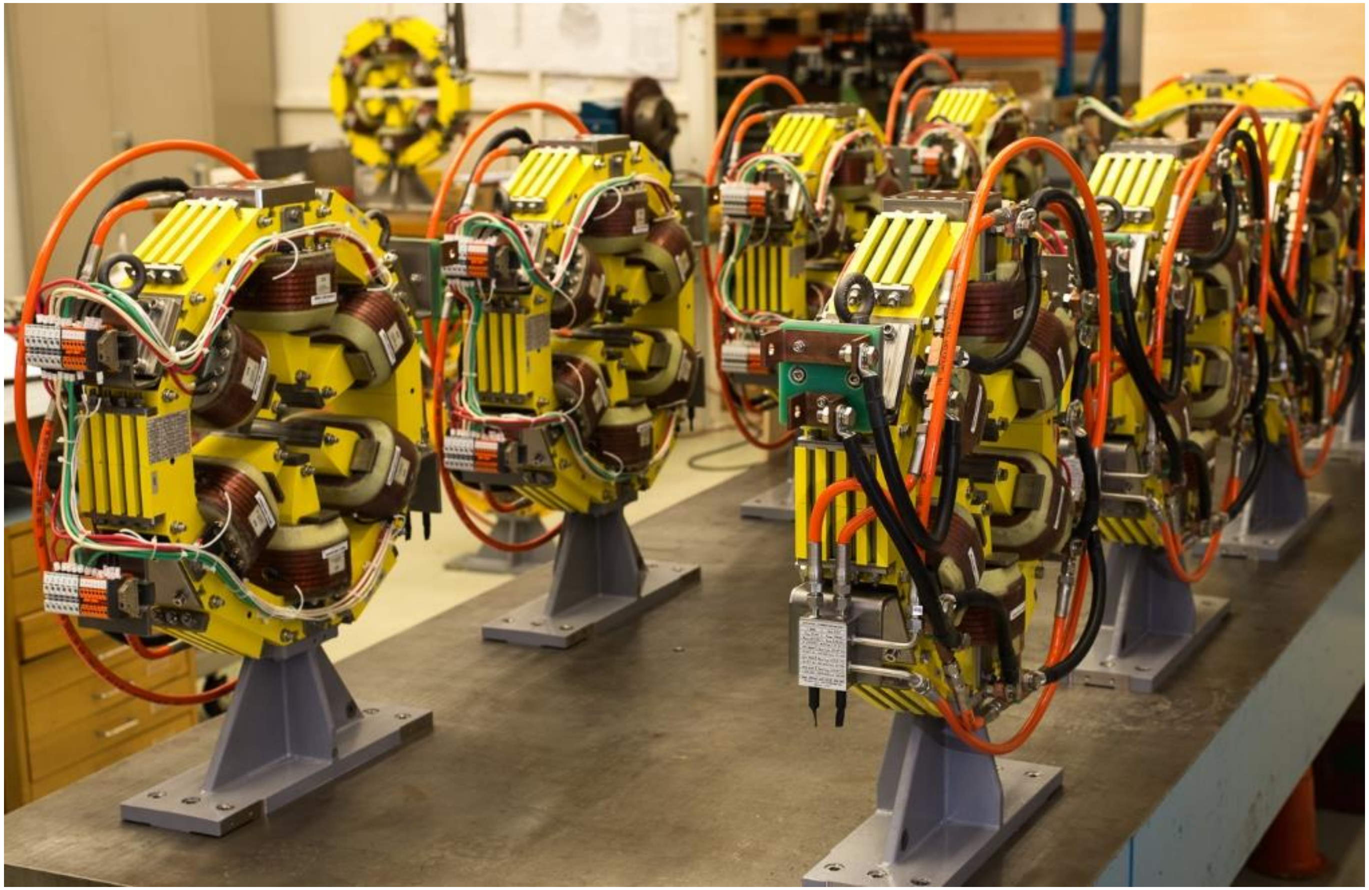

220 T/m^2, 223 A
aperture diameter 75 mm

Type 610 sextupoles, PS

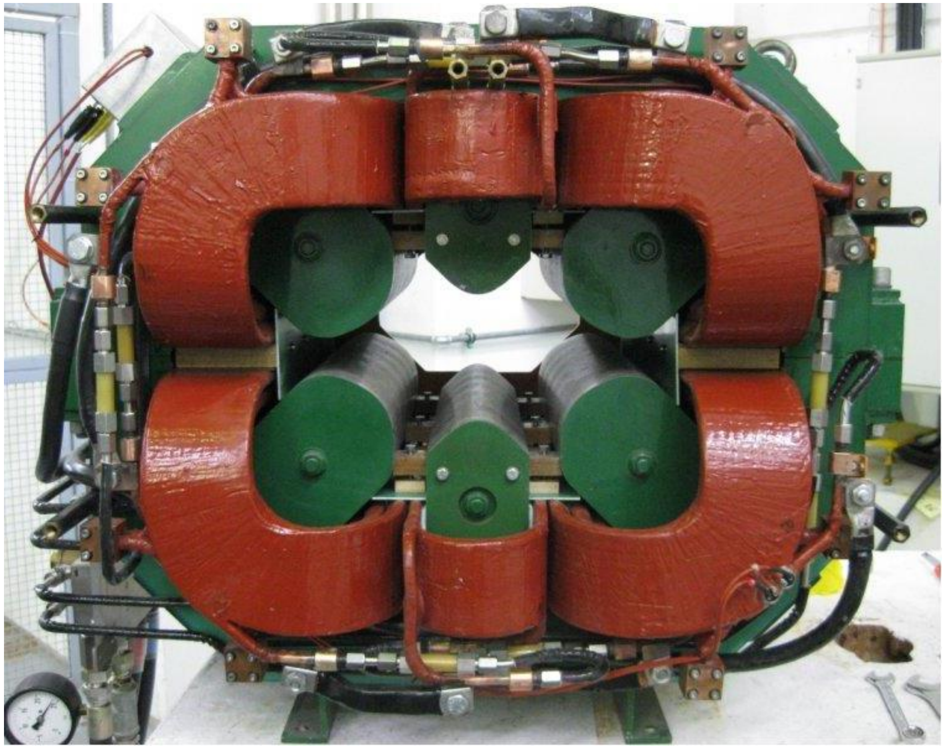

150 A

non-circular aperture, 350 mm × 112 mm

MTE octupoles, PS (Multi-Turn Extraction)

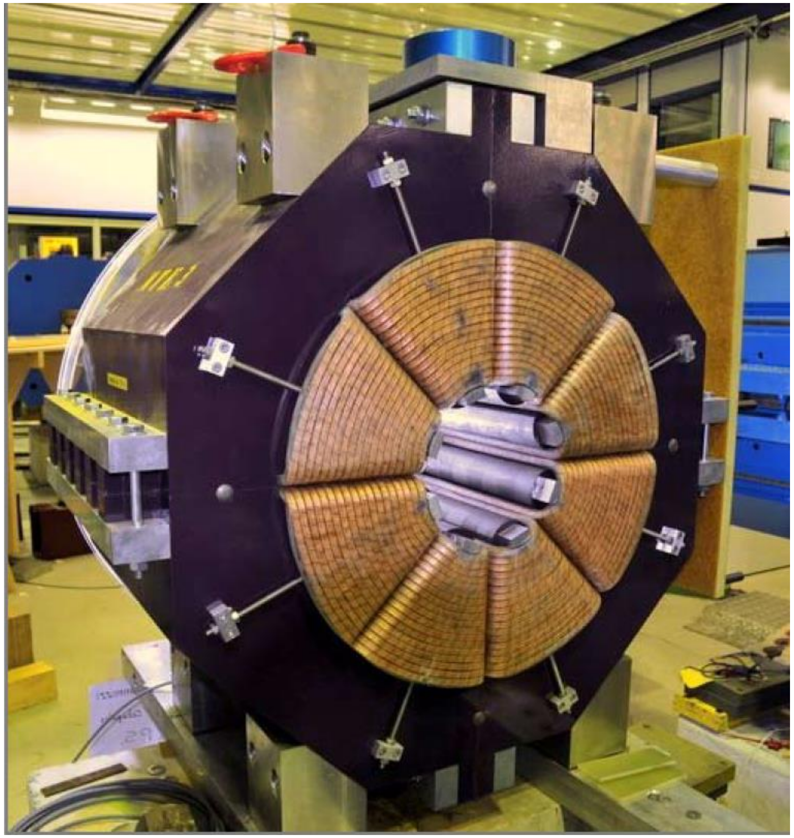

$14360\ T/m^3$, 700 A
aperture diameter 140 mm

SR facilities : storage ring dipoles

	ELETTRA	ALS	ESRF	ANKA	ASP	ALBA	SOLEIL	SPRING-8	SLS	DIAMOND
Bending radius [m]	5.5	∞	23.37	5.56	∞	7.05	5.36	39.27	5.73	7.16
N. of magnets	24	36	64	16	28	32	32	88	36	48
Dipole field [T]	1.21	1.35	0.86	1.5	1.3	1.42	1.71	0.68	1.4	1.4
Gradient [T/m]	2.86	5.19	0	0	3.35	5.65	0	0	0	0
Gap [mm]	70	50	54	41	42	36	37	64	41	46.6
Current [A]	1420	924	700 ?	660	695	530	538	1090	557	1337

ANKA

ALBA

ELETTRA

SLS

SPRING-8

SOLEIL

DIAMOND

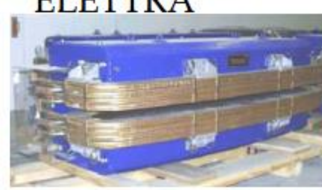

CLS

Gap=45 mm B= 1.35 T G= 3.8T/m

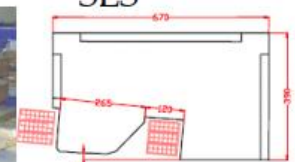

ASP

SPEAR3

Gap = 50 mm B= 1.4 T G= 3.6 T/m

Experimental magnets: LHCb dipole

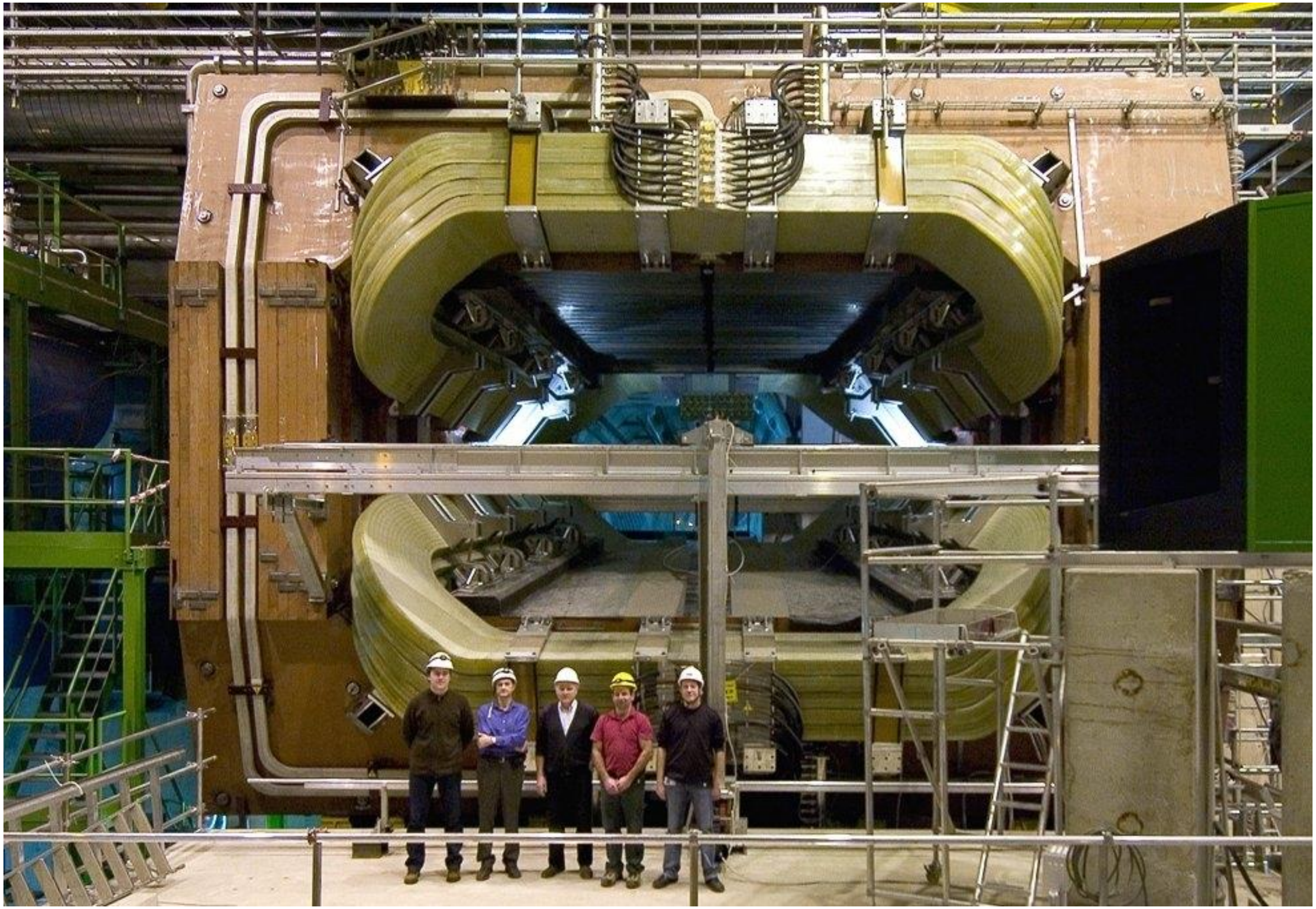

Experimental magnets: L3 / ALICE solenoid – the largest resistive magnet?

CONSTRUCTION OF THE L3 MAGNET

F. Wittgenstein[1], A. Hervé[1], M. Feldmann[1], D. Luckey[2] and I. Vetlitsky[3]

1 CERN, European Organization for Nuclear Reseach, CH–1211 Geneva 23, Switzerland
2 Massachussetts Institute of Technology (MIT), Boston, MA 02115, USA
3 Institute of Theoretical and Experimental Physics (ITEP), Moscow 117259, USSR

Inside radius	5930	mm
Width of the coil	890	mm
Outside radius	7900	mm
Total length	14000	mm
Power at the taps	4.2	MW
Central field	0.5	T
Coil contribution	0.36	T
Stored energy	150	MJ
Amper turns	5	MAt
Rated current	30	kA
Current density	55.5	A/cm^2
Cooling water	150	m^3/h
Coil weight (Al)	1100	t
Shielding weight	6700	t

Twin dipole short model for FCC-ee

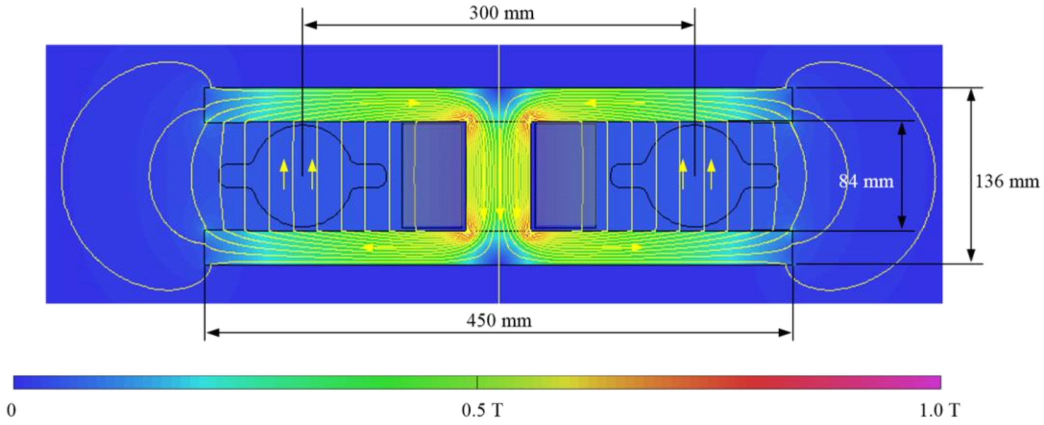

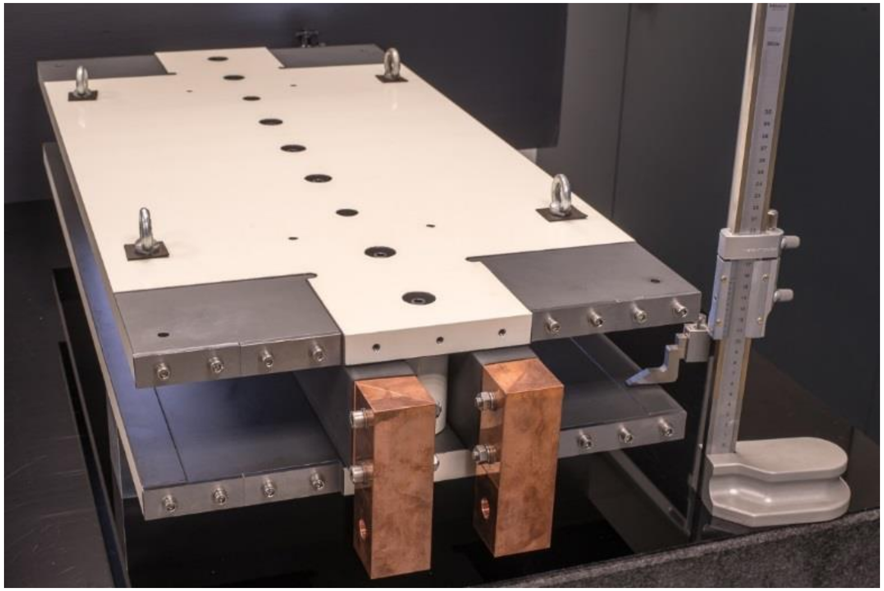

54.3 mT, 3.65 kA
vertical gap 84 mm

Twin quadrupole short model for FCC-ee

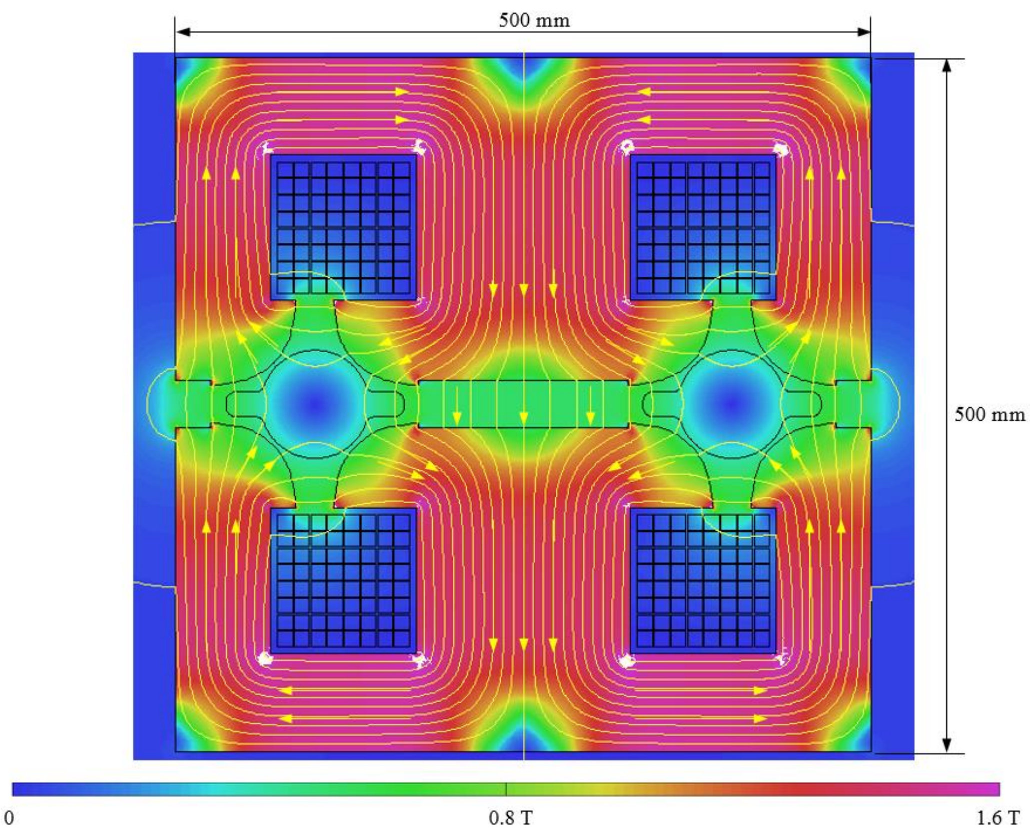

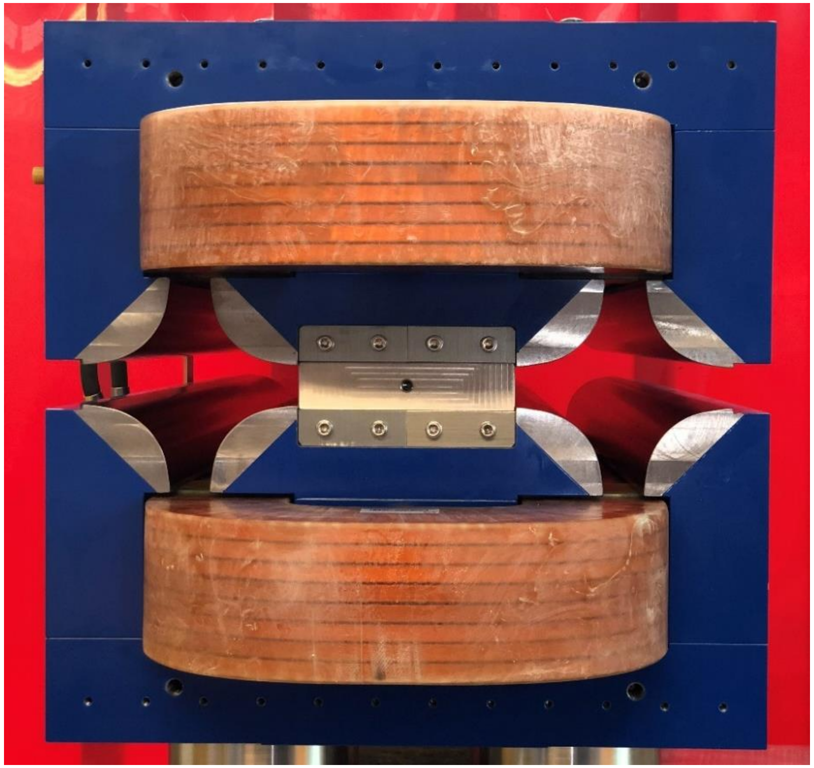

10 T/m, 222 A
aperture diameter 84 mm

And so much more is out there… see also the bonus slides

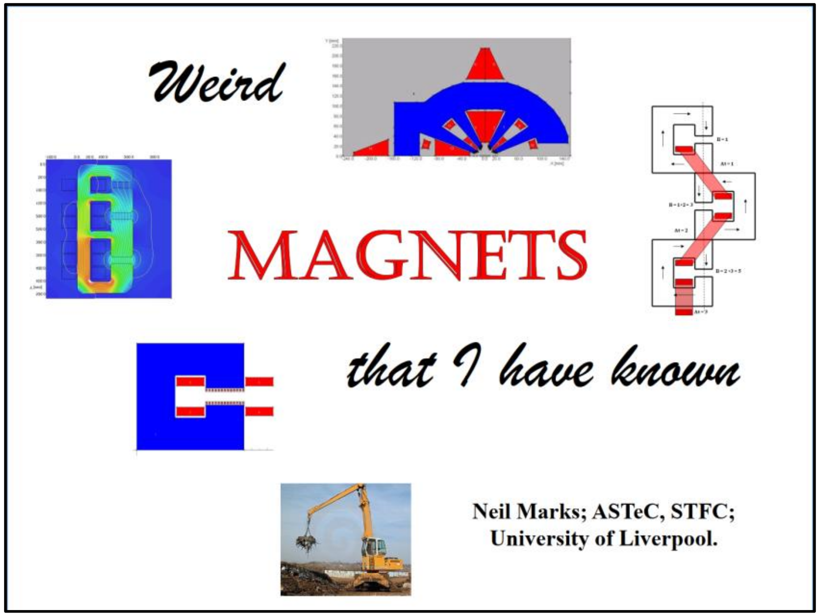

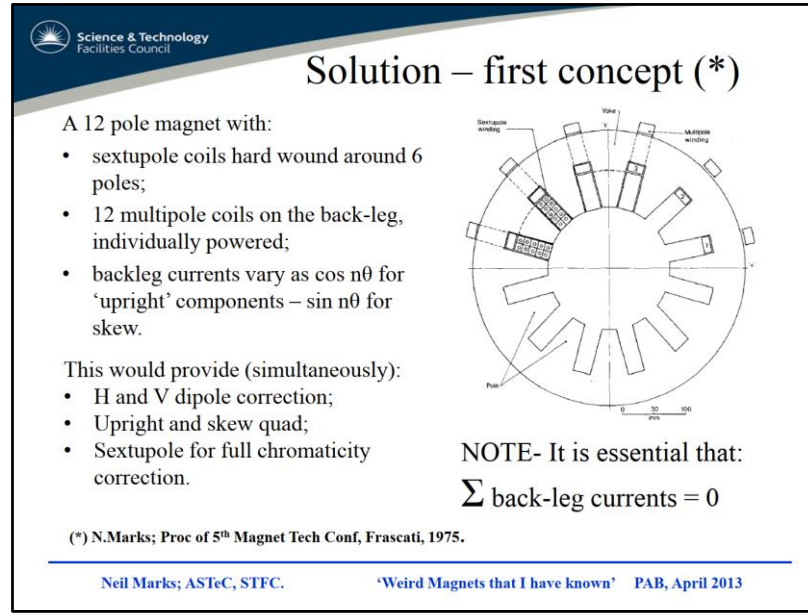

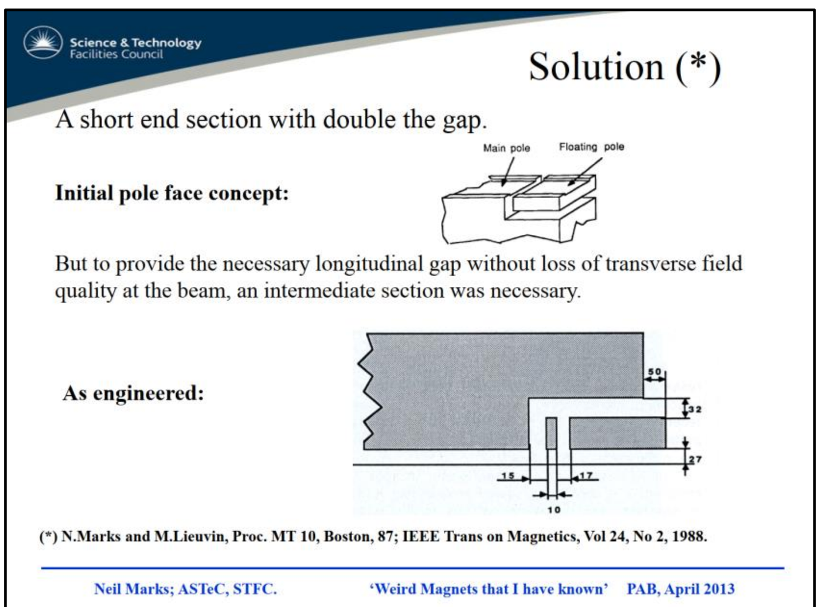

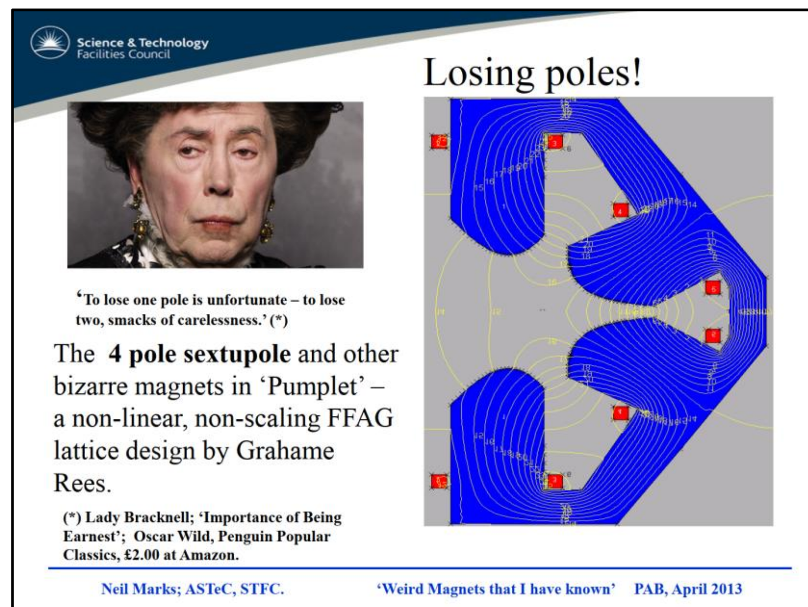

Conclusions (introduction)

There is a long tradition and experience with room temperature magnets in accelerators

We did not look at cyclotrons, FFAGs, synchrocyclotrons, etc.

There are many types of resistive magnets: dipoles, quadrupoles, combined function, sextupoles, octupoles, solenoids, experimental magnets, wigglers, undulators, etc.

We focus on dipoles and quadrupoles

Most of them are iron dominated, with coils wound from copper (or aluminum) conductor

There are coil dominated RT magnets, but they are more of a niche

Requirements

Input parameters

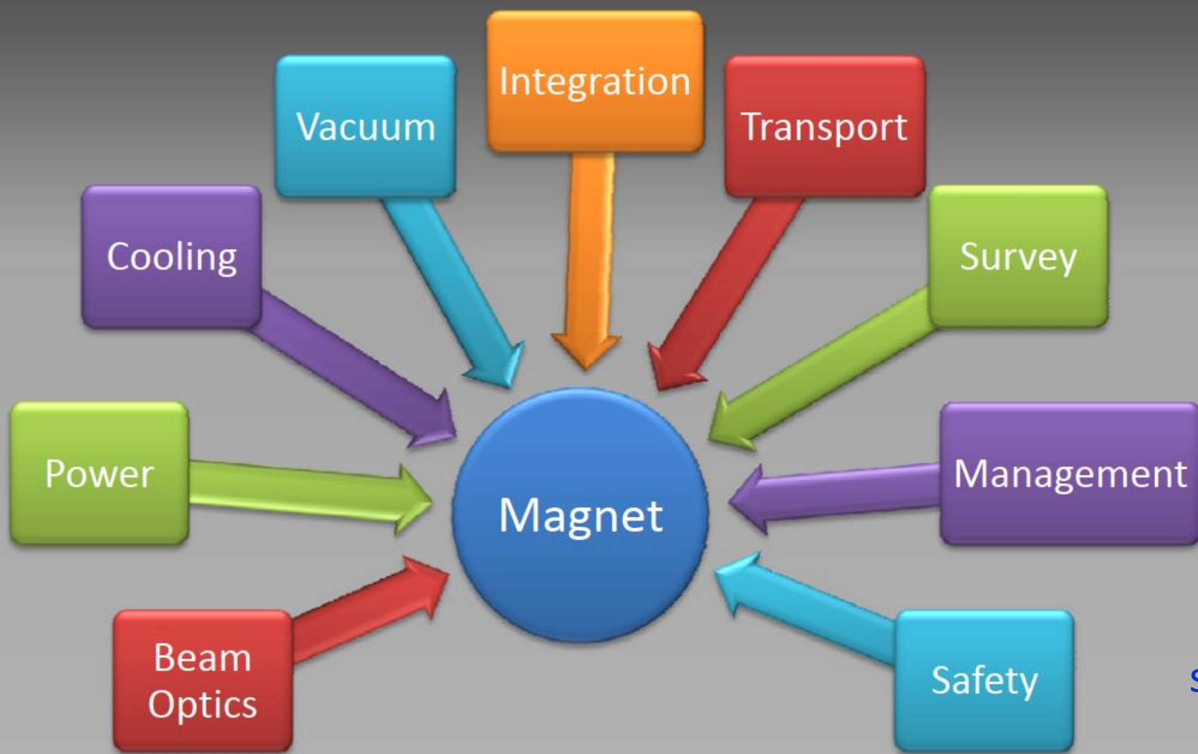

cost & schedule

procurement

QA/QC

A magnet is not a stand-alone device!

General requirements

Magnet type and purpose	• Dipole: bending, steering, extraction • Quadrupole, sextupole, octupole • Combined function, solenoid, special magnet
Installation	• Storage ring, synchrotron light source, collider • Accelerator • Beam transport lines
Quantity	• Installed units • Spare units (~10 %) spare magnets / coils

Performance requirements

Beam parameters	
	• Type of beam, energy range and deflection angle (k-value) • Integrated field (gradient) • Local field (gradient) and magnetic length

Sometimes there might be ambiguity in the communication between beam physicists and magnet engineers: typical examples are the strength of a sextupole (factor of 2 difference) or field quality (like field homogeneity vs. gradient homogeneity in a quadrupole).

Performance requirements

Operation mode

- Continuous
- Pulsed-to pulse modulation (ppm)
- Ramped – ramp rate (T/s)
- Fast pulsed

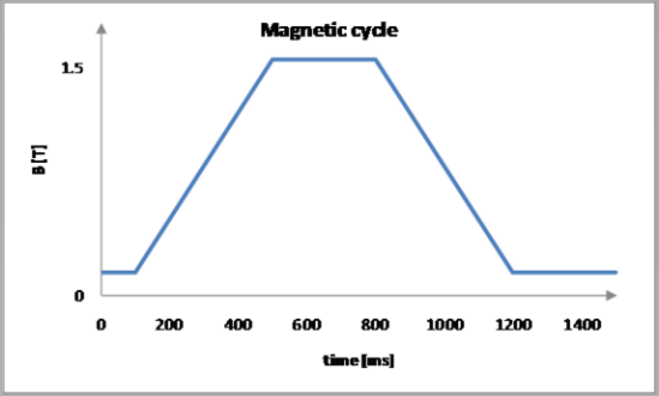

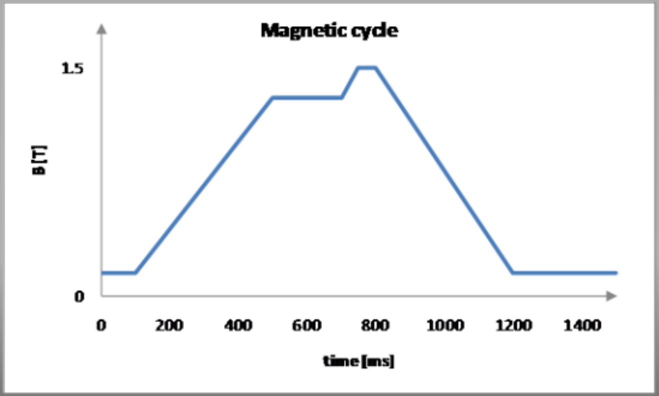

Performance requirements

Field quality

- Homogeneity (uniformity)
- Allowed harmonic content
- Stability & reproducibility
- Settling time (time constant)

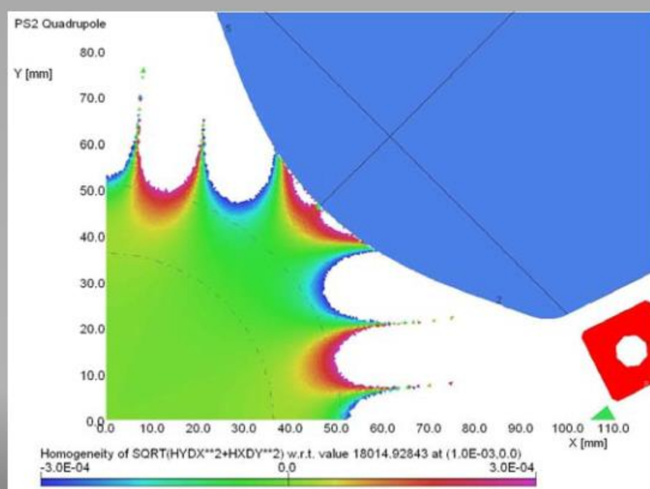

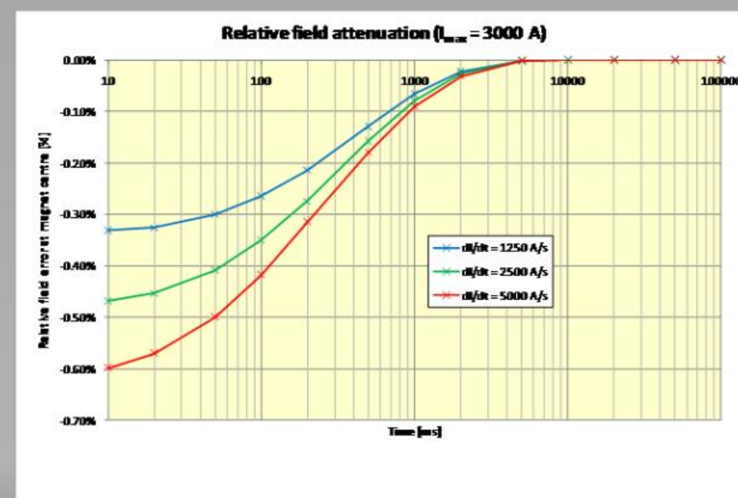

Physical requirements

Geometric boundaries	• Available space • Transport limitations • Weight limitations
Accessibility	• Crane • Connections (electrical, hydraulic) • Alignment targets
Aperture	• Physical aperture • 'Good field region'

Interfaces

Equipment linked to the magnet is defining the boundaries and constraints

Power converter	• Max. current • Max. voltage • Pulsed/dc
Cooling	• Max. flow rate and pressure drop • Water quality (aluminium/copper circuit) • Inlet temperature • Available cooling power
Vacuum	• Size of vacuum chamber • Space for pumping ports, bake out • Captive vacuum chamber

Environmental aspects

Other aspects, which can have an influence on the magnet design

Environment temperature	• Risk of condensation • Heat dissipation into the tunnel
Ionizing radiation	• High radiation levels require radiation hard materials • Special design to allow fast repair/ replacement
Electro-magnetic compatibility	• Magnetic fringe fields disturbing other equipment (beam diagnostics) • Surrounding equipment perturbing field quality
Safety	• Electrical safety earthing, protection covers • Interlocks

Conclusions (specifications)

Make sure you know which magnet you have to design, build, test, install

- Ideally before starting the design… though some iterations in the early phases are normal

Make sure this is validated by all colleagues

- A specification and a preliminary design document can help, this depends also on the size of the project

Yoke design

2D

The design of the yoke usually starts in 2D, considering several aspects

- Pole tip
- Back or return legs
- Space for coils
- Integration: overall dimensions, weight
- Construction and assembly considerations
- Confinement of stray field
- Field trimming after magnetic measurements
  - integrated strength (main component)
  - integrated field quality
- Different ferromagnetic materials
  - solid vs. laminated
  - iron based, usually electrical steel, but also ARMCO® and cobalt-iron alloys (in very specific cases)

These are the most common types of resistive dipoles (cartoon representation)

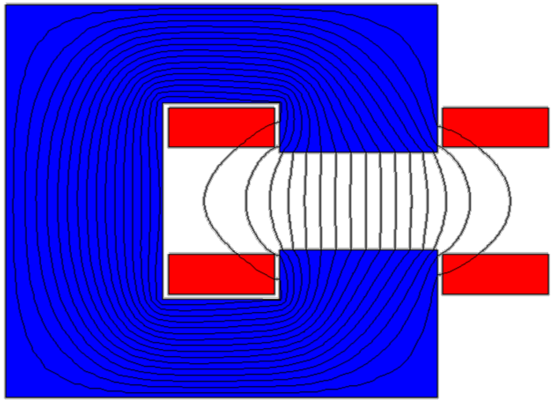

C

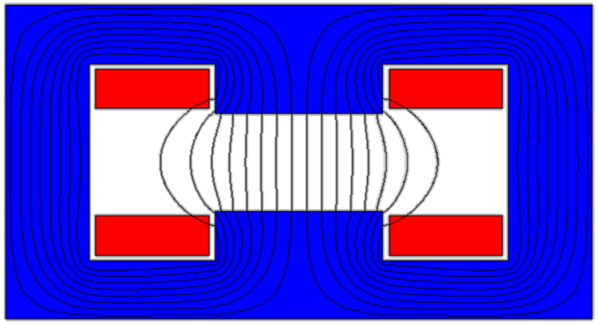

H

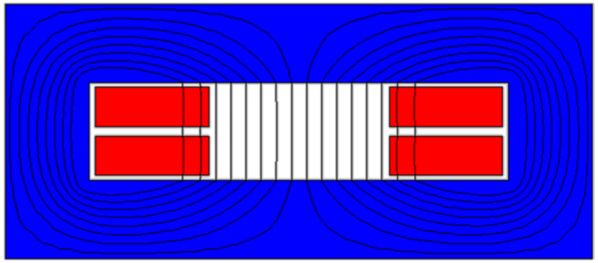

window frame
(O)

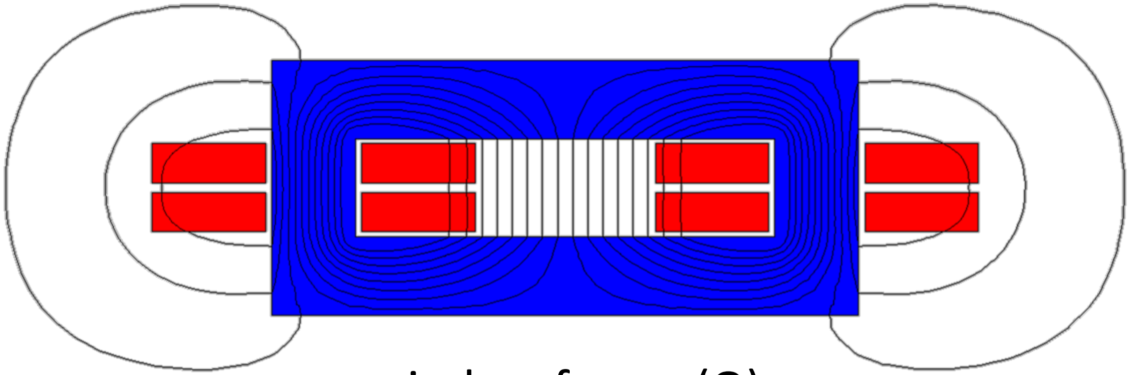

window frame (O)
with windings on both backlegs

These are the most common types of resistive quadrupoles (cartoon representation)

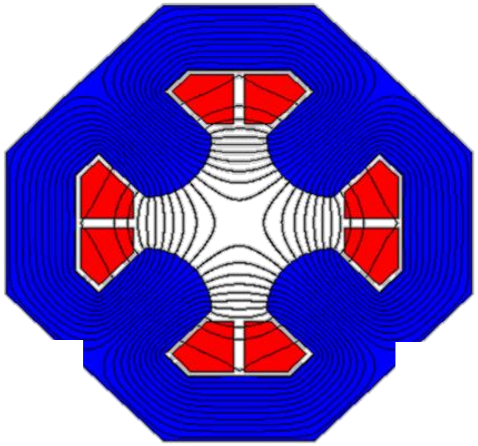

standard quadrupole

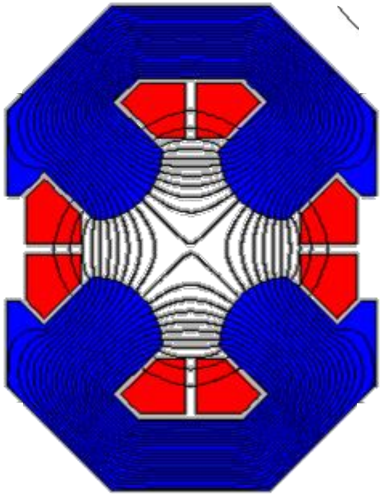

figure-of-8
(useful because narrow)

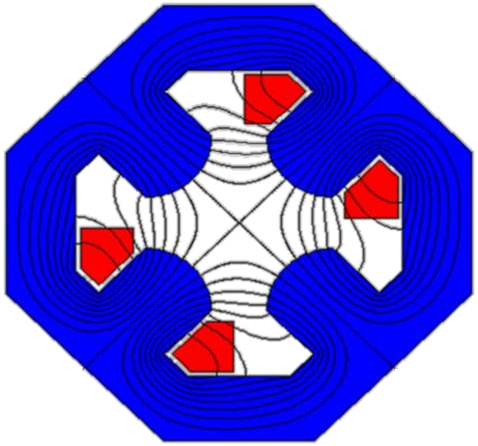

quadrupole
with half the coils
(maybe not so common)

Reminder: the allowed / not-allowed harmonics refer to some terms that shall / shall not cancel out thanks to design symmetries

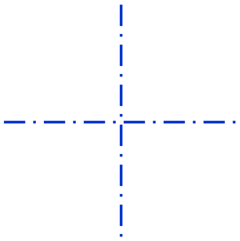

fully symmetric dipoles (ex. H)

allowed: B_1, b_3, b_5, b_7, b_9, etc.

half symmetric dipoles (ex. C)

allowed: B_1, b_2, b_3, b_4, b_5, etc.

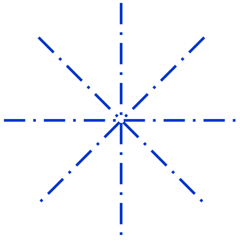

fully symmetric quadrupoles

allowed: B_2, b_6, b_{10}, b_{14}, b_{18}, etc.

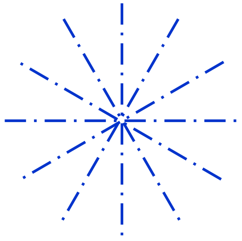

fully symmetric sextupoles

allowed: B_3, b_9, b_{15}, b_{21}, etc.

Out of curiosity, the table lists the allowed multipoles for the different layouts of the dipole (cartoon) examples

	C-shape	H-shape	O-shape
b_2	1.4	0	0
b_3	-88.2	-87.0	0.2
b_4	0.7	0	0
b_5	-31.6	-31.4	-0.1
b_6	0.1	0	0
b_7	-3.8	-3.8	-0.1
b_8	0.0	0	0
b_9	0.0	0.0	0.0

b_n multipoles in units of 10^{-4} at R = 17 mm

NI = 20 kA, h = 50 mm, w_{pole} = 80 mm

The magnetic circuit is dimensioned so that the pole is wide enough for field quality, and there is enough room for the flux in the return legs

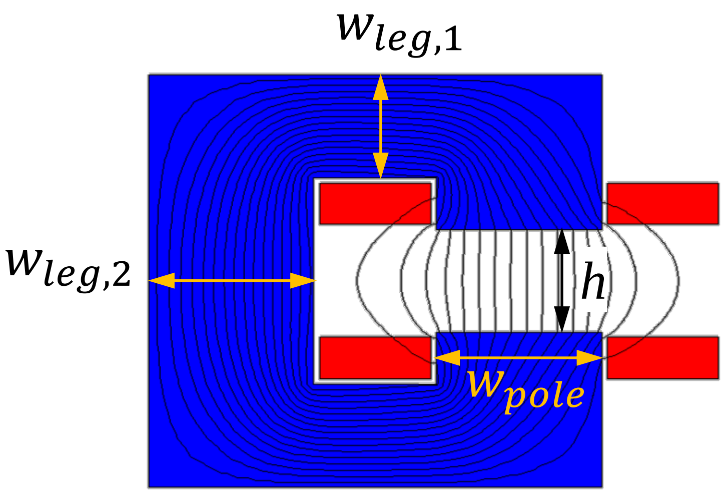

$$w_{pole} \cong w_{GFR} + 2.5h$$

$$B_{leg} \cong B_{gap} \frac{w_{pole} + 1.2h}{w_{leg}}$$

The BH response of the yoke material in an important parameter

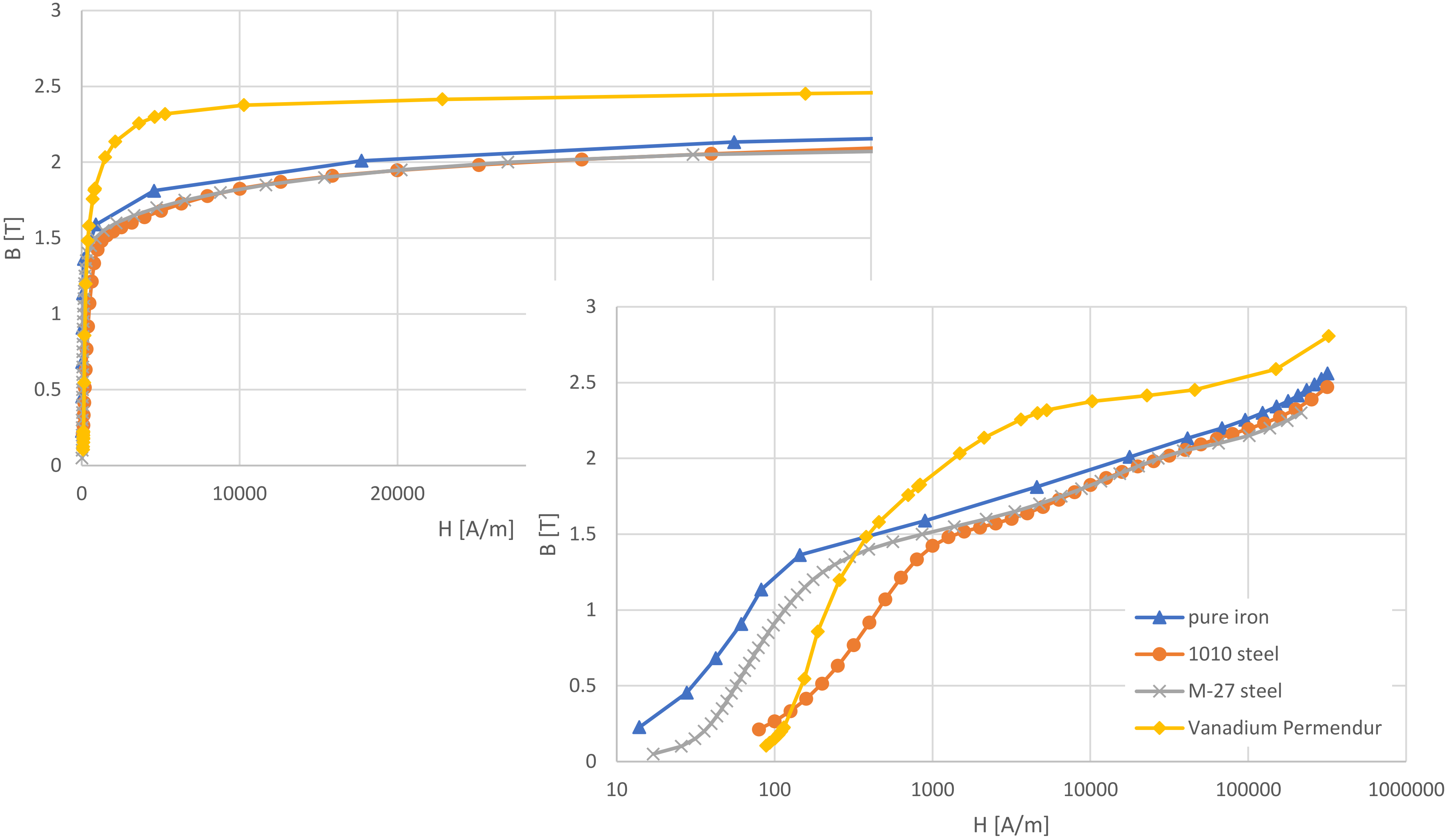

Below a didactic example of yoke optimization for a dipole

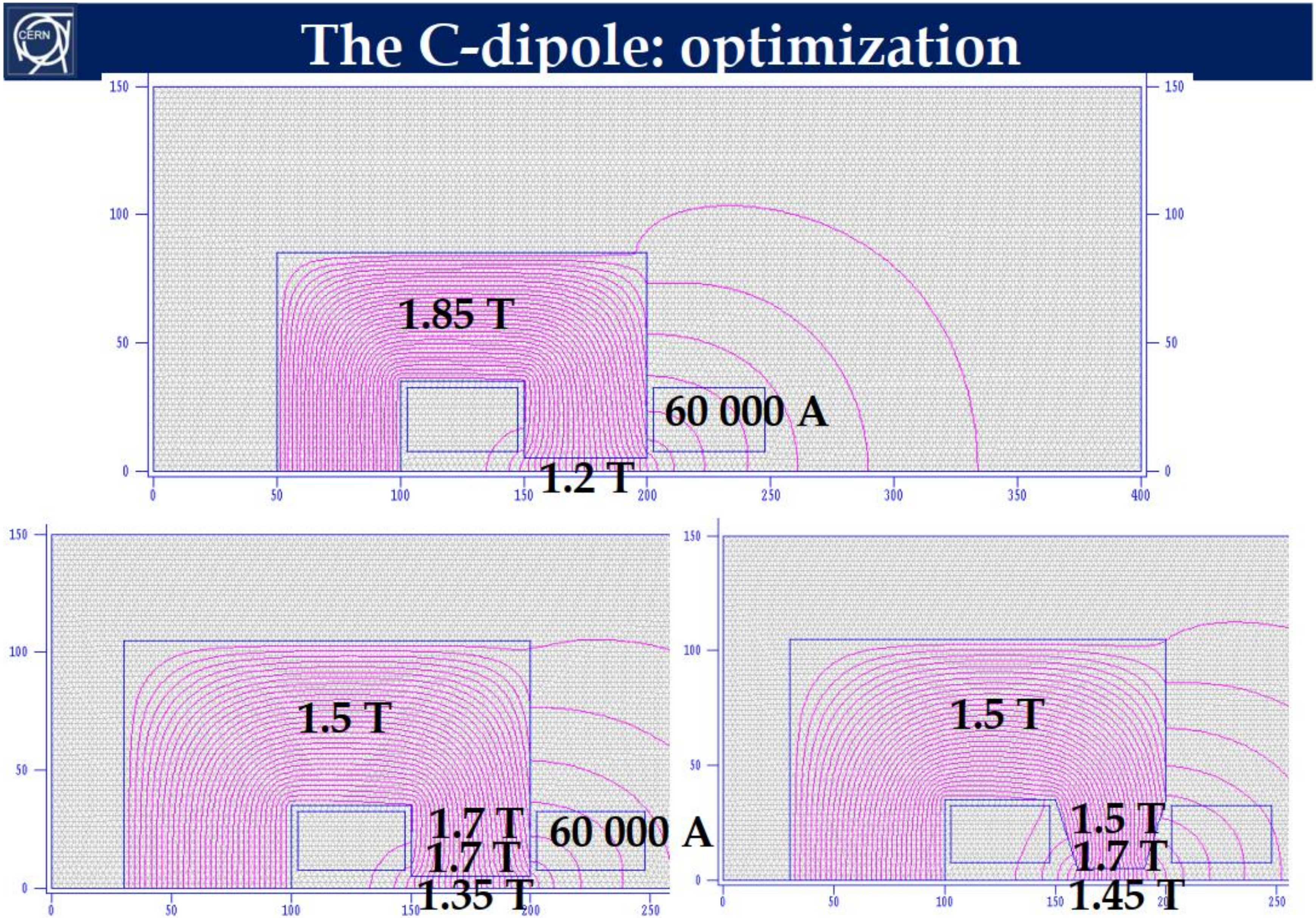

The high field target is 2.0 T, at the limit but doable (standard iron, reasonable Ampere-turns, reasonable size of yoke, field quality at various currents)

SPS @ 450 GeV

bending	$B = 2.0$ T
quadrupole	$B_{pole} = 21.7*0.044 = 0.95$ T

TI2 / TI8 (transfer lines SPS to LHC, @ 450 GeV)

bending	$B = 1.8$ T
quadrupole	$B_{pole} = 53.5*0.016 = 0.86$ T

PS @ 26 GeV

combined function bending	$B \approx 1.5$ T

This is the (average) transfer function field B vs. current I for the SPS main dipoles

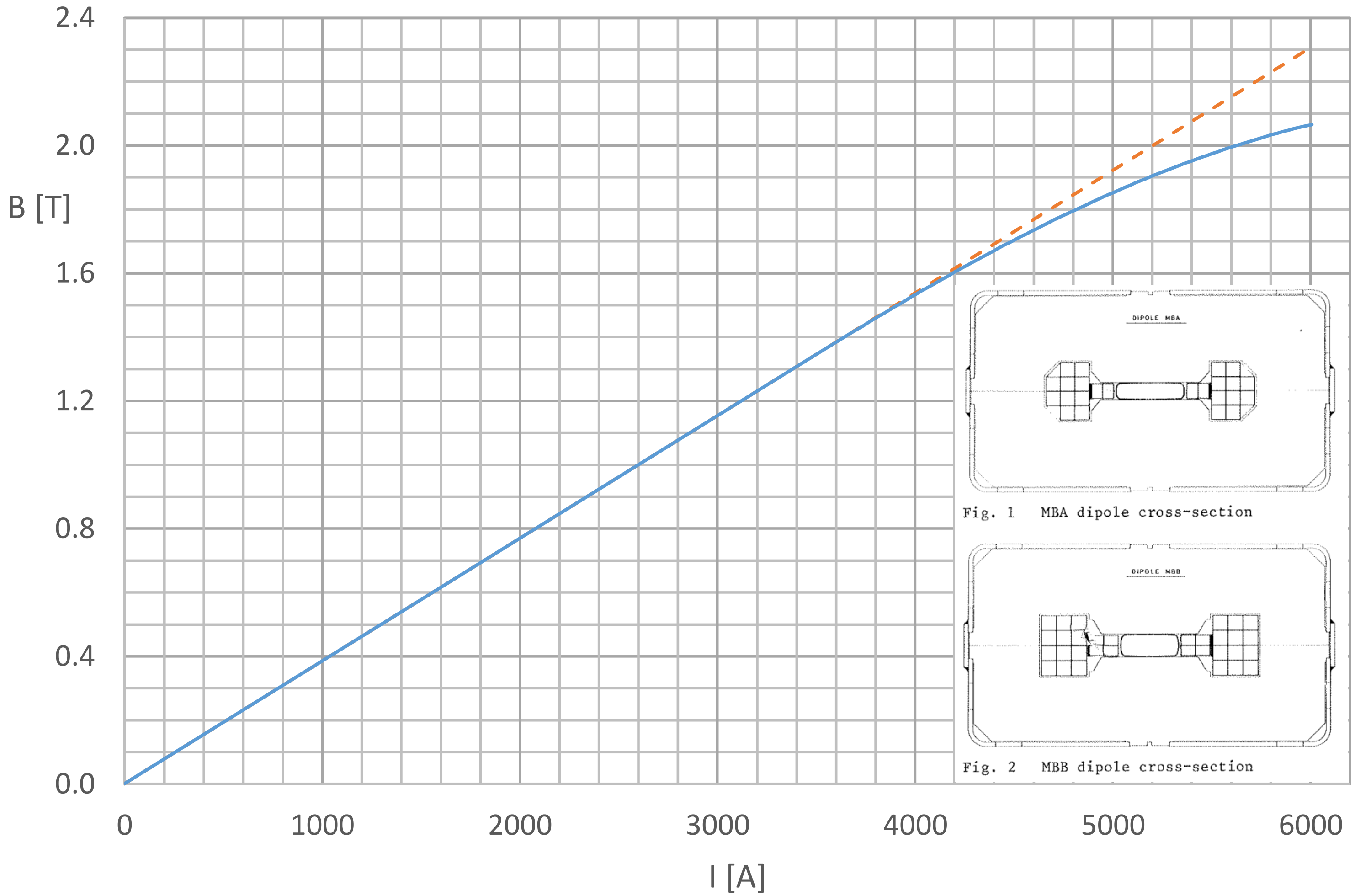

What about low field? This is another challenge, typically a few tens of mT

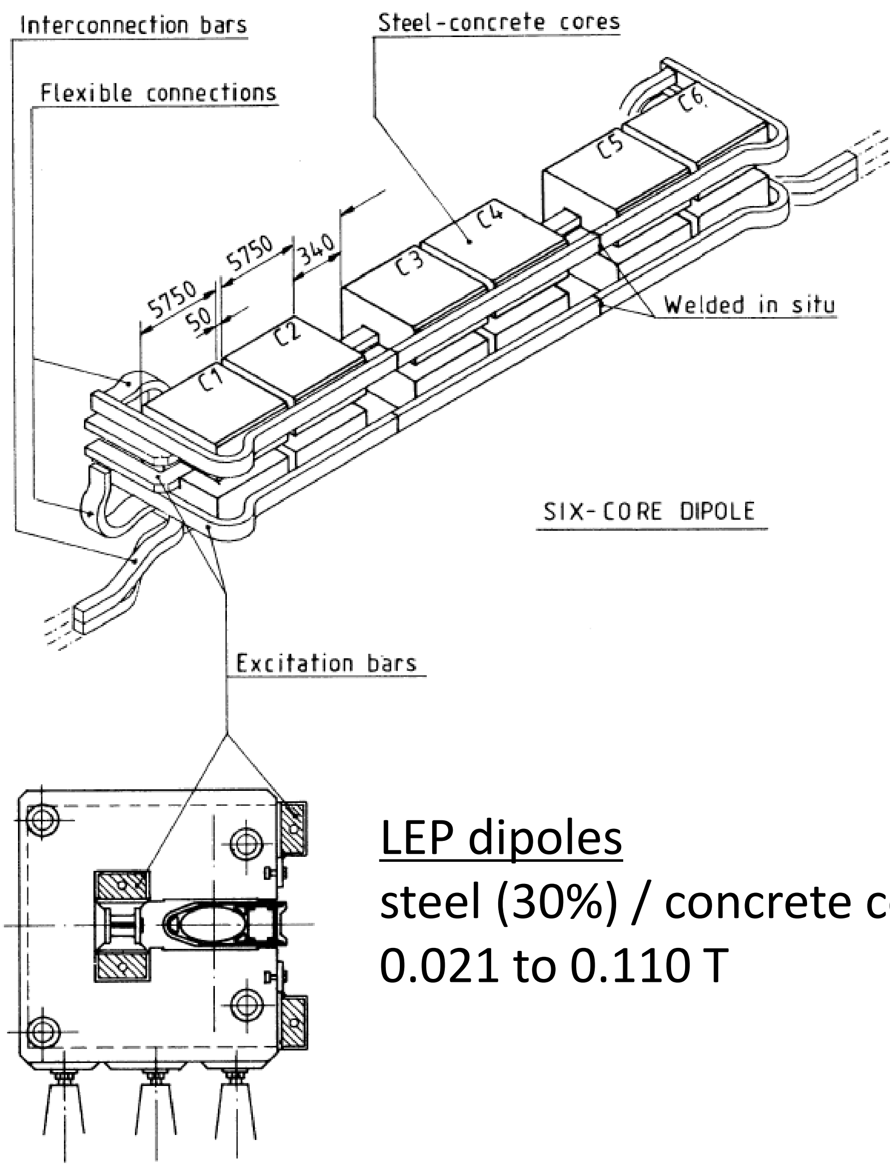

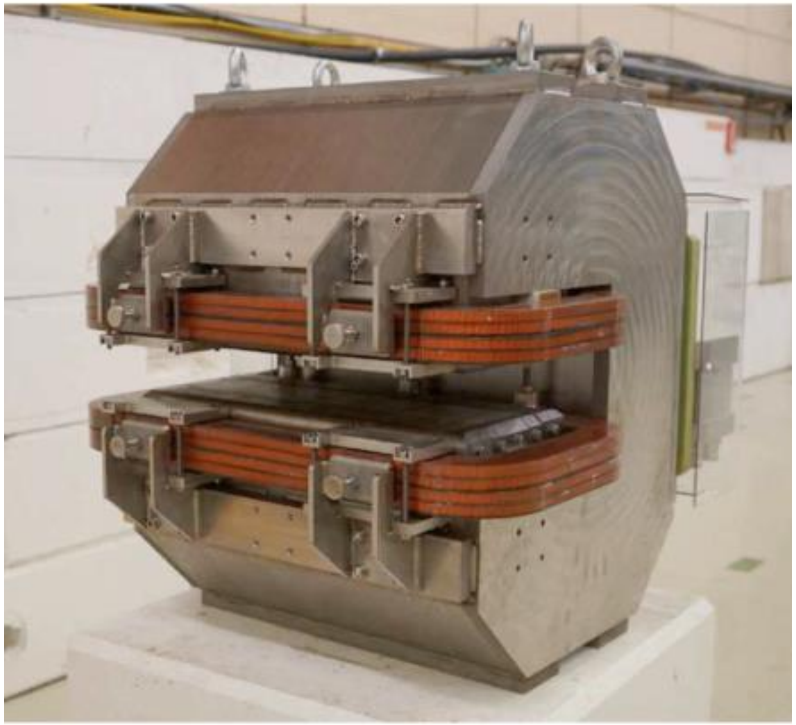

<u>LEP dipoles</u>
steel (30%) / concrete cores
0.021 to 0.110 T

<u>ELENA dipoles</u>
prototypes with diluted / not diluted cores
0.36 to 0.05 T

The ideal poles are curves of constant scalar potential

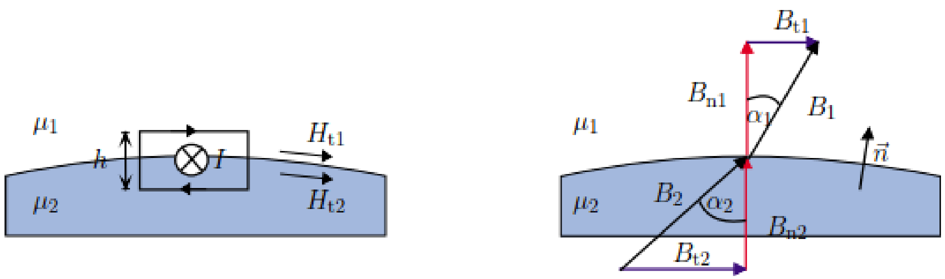

If we apply Ampère's law in the integral form

$$\oint \vec{H} \cdot d\vec{s} = \int_A \vec{J} \cdot d\vec{A}, \tag{30}$$

to the loop displayed in fig. 4 (left), and let $h \to 0$, then the enclosed current is zero, as in an infinitesimal small rectangle there cannot be a current flow. Therefore

$$H_{t1} = H_{t2}, \tag{31}$$

i.e.,

$$\vec{n} \times (\vec{H}_1 - \vec{H}_2) = 0. \tag{32}$$

Because of $\oint \vec{B} \cdot d\vec{A} = 0$ we get at the interface

$$B_{n1} = B_{n2}, \tag{33}$$

i.e.,

$$\vec{n} \cdot (\vec{B}_1 - \vec{B}_2) = 0. \tag{34}$$

Now

$$\frac{\tan\alpha_1}{\tan\alpha_2} = \frac{\frac{B_{t1}}{B_{n1}}}{\frac{B_{t2}}{B_{n2}}} = \frac{\mu_1 H_{t1}}{\mu_2 H_{t2}} = \frac{\mu_1}{\mu_2}. \tag{35}$$

For $\mu_2 \gg \mu_1$ it follows that $\tan\alpha_1 \gg \tan\alpha_2$. Therefore for all angles $\pi/2 > \alpha_2 > 0$ we get $\tan\alpha_1 \approx 0$, see also fig. 4 (right). The field exits vertically from a highly permeable medium into a medium with low permeability. We will come back to this point when we discuss ideal pole shapes of conventional magnets.

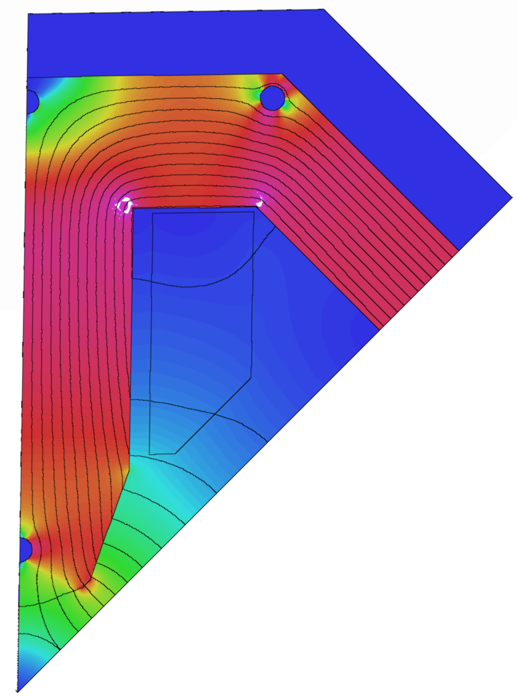

The ideal poles for a dipole, a quadrupole, a sextupole, etc. are curves of constant scalar potential, of infinite length

dipole

$\rho \sin(\theta) = \pm h/2$ | $y = \pm h/2$ | straight line

quadrupole

$\rho^2 \sin(2\theta) = \pm r^2$ | $2xy = \pm r^2$ | hyperbola

sextupole

$\rho^3 \sin(3\theta) = \pm r^3$ | $3x^2 y - y^3 = \pm r^3$

combined function dipole + quadrupole: translated hyperbola
(that is, a pure quadrupole with a horizontal offset)

dipole quadrupole sextupole

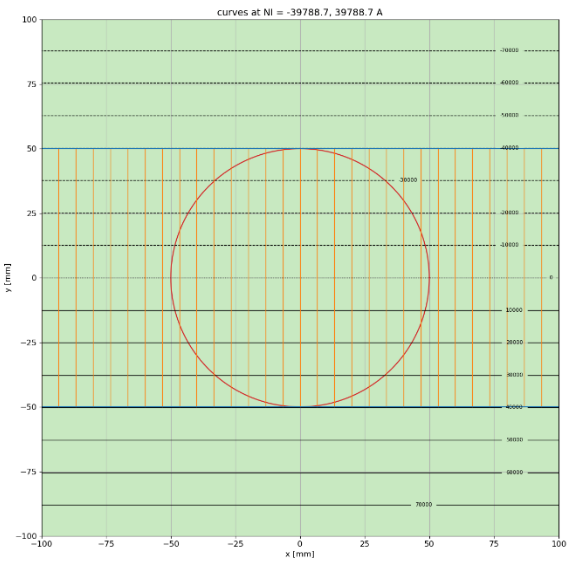

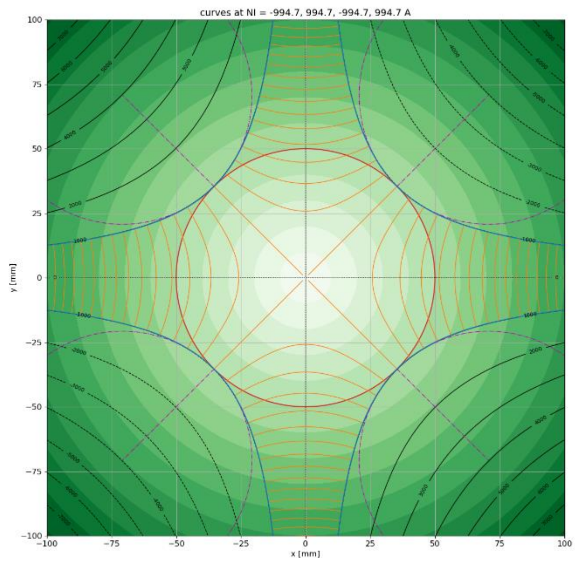

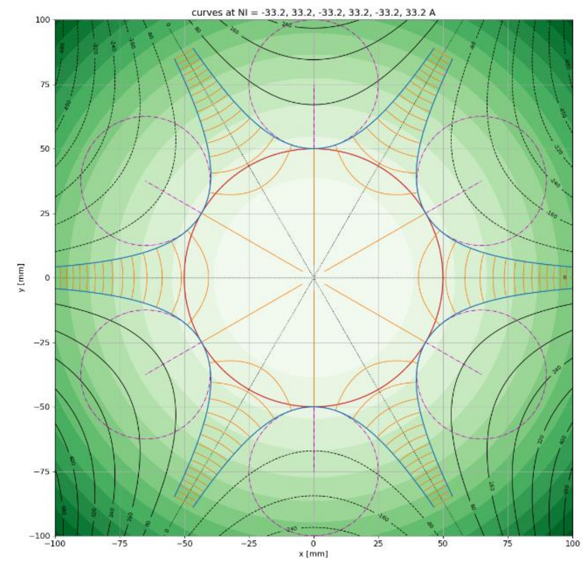

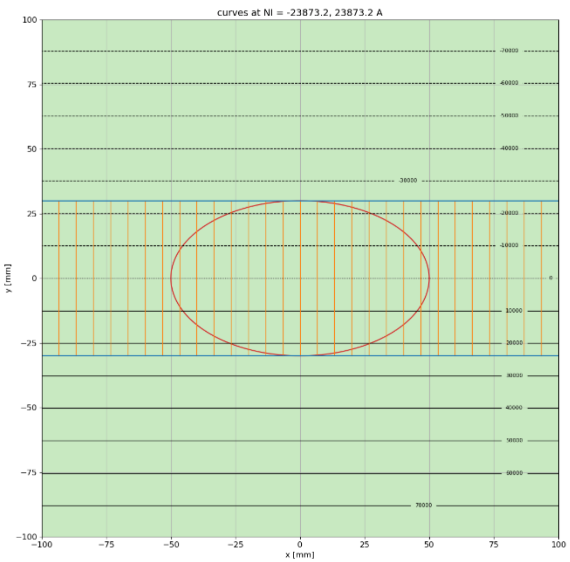

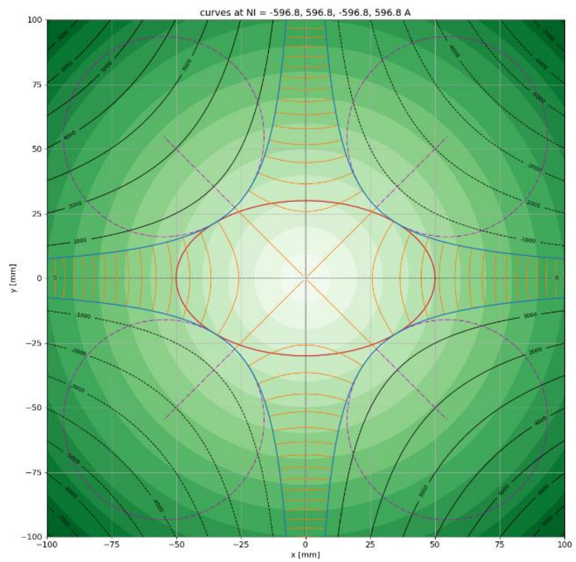

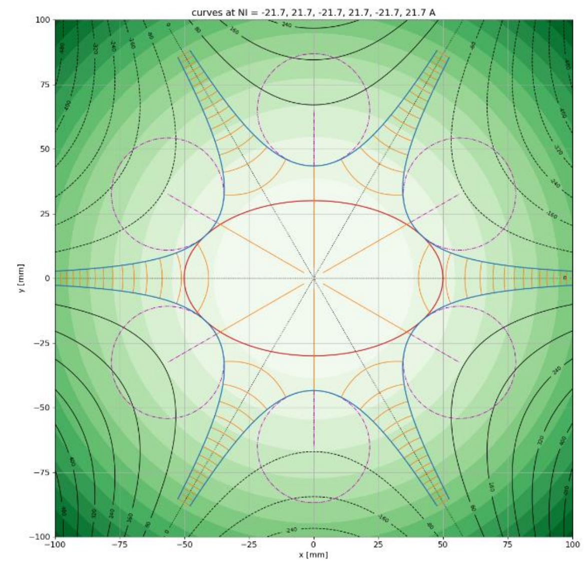

Ideal poles can be found for any linear combination of multipole terms (also tangent to non-circular apertures)

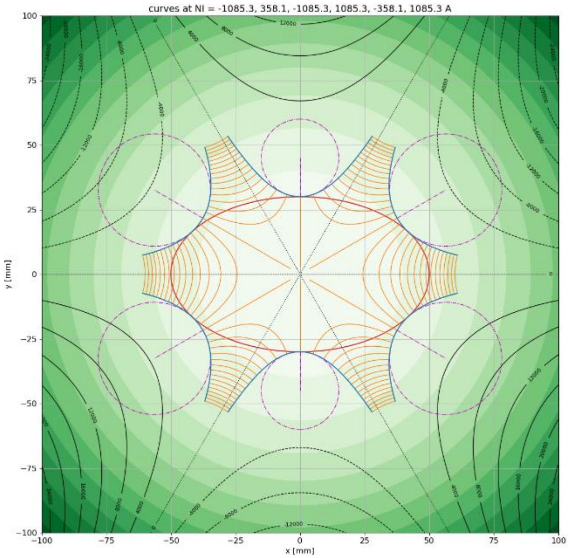

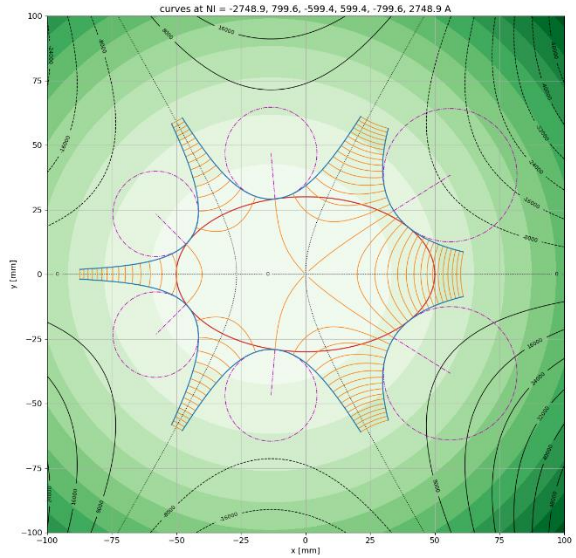

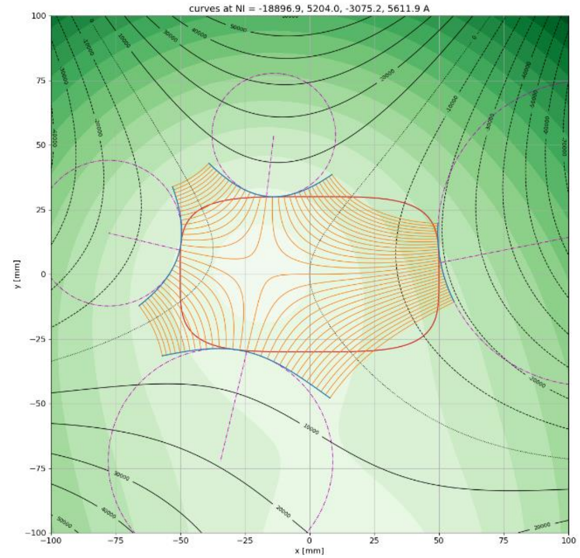

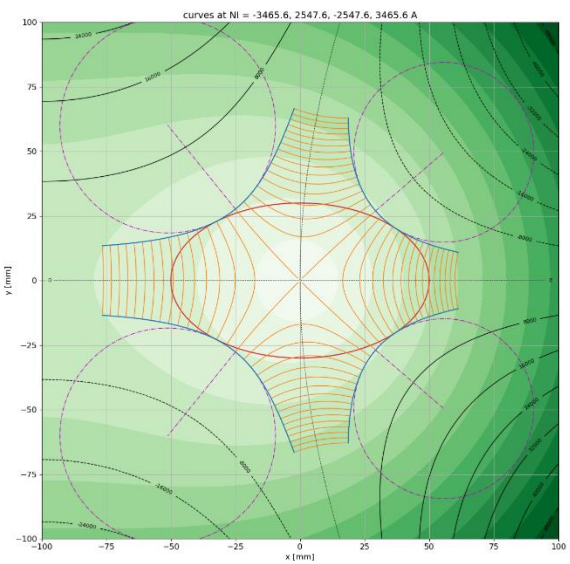

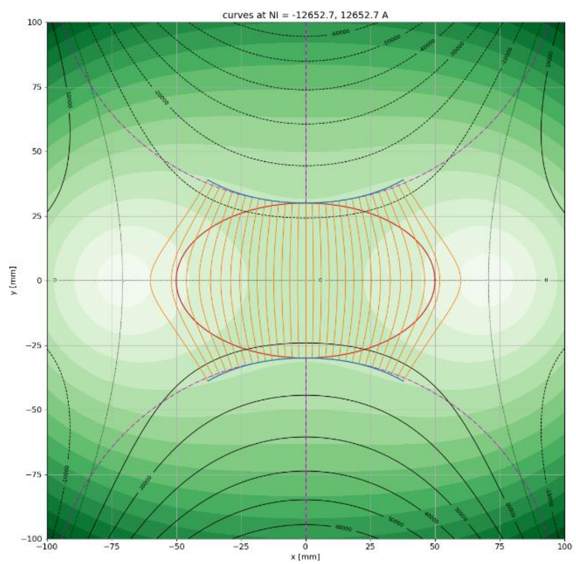

Tracking magnetic equipotential curves for general combinations of multipolar fields

EDMS 2792136

(with Python script producing list of points or a DXF file)

The osculating circle at the pole tip can also be a starting point

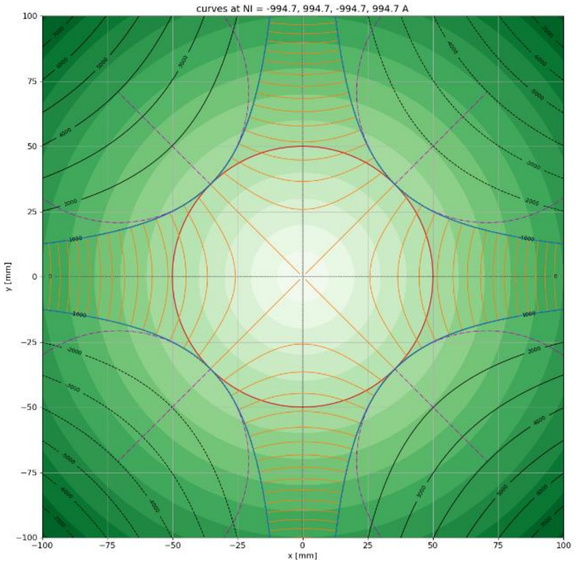

quadrupole: $R_{fit} = r$

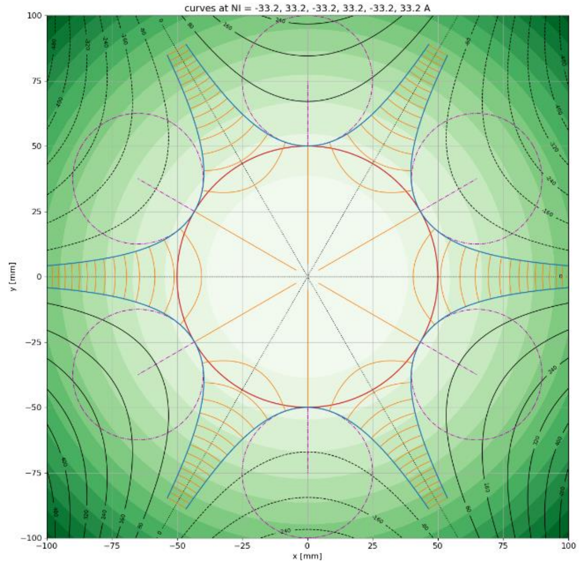

sextupole: $R_{fit} = r/2$

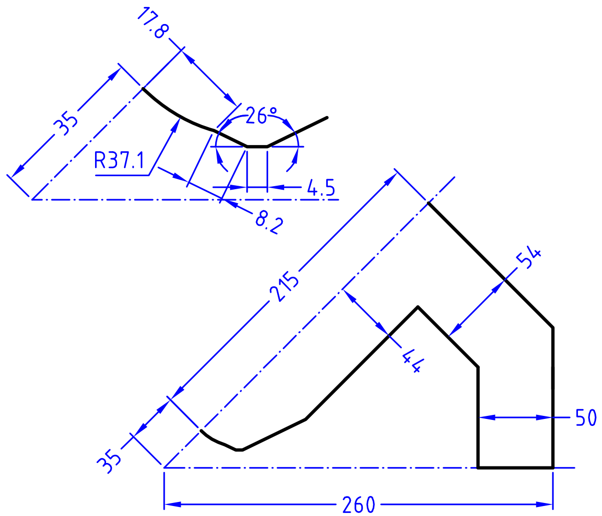

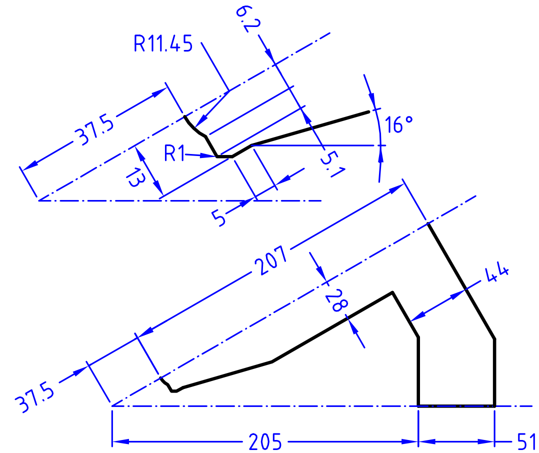

Pole profiles are even used for logos of large laboratories…

Ideal poles are a (useful) starting point to design the pole tip, nowadays we have 2D (and 3D) simulation tools

CERN-PS/JPB 7
April 2, 1954.

SHAPING OF MAGNET POLES FOR GENERATION OF UNIFORM GRADIENTS

J.P. Blewett

In the design of magnet poles for alternating-gradient synchrotrons it is usually assumed that the pole shape will be a section of a rectangular hyperbola. Although this makes a good first approximation it is in error for four reasons :

i) No present designs include the neutral pole which is an essential unit of the hyperbolic configuration.

ii) The hyperbolic contour is not continued to infinity but is cut off at boundaries close to the operating field region.

iii) The magnetising coil in all practical designs is sufficiently close to the useful field that it introduces perturbations of the field pattern.

iv) Effects of finite magnet permeability are not included.

Every magnet designer has his / her preference: below the pole tip of the SESAME quadrupoles vs. the hyperbola

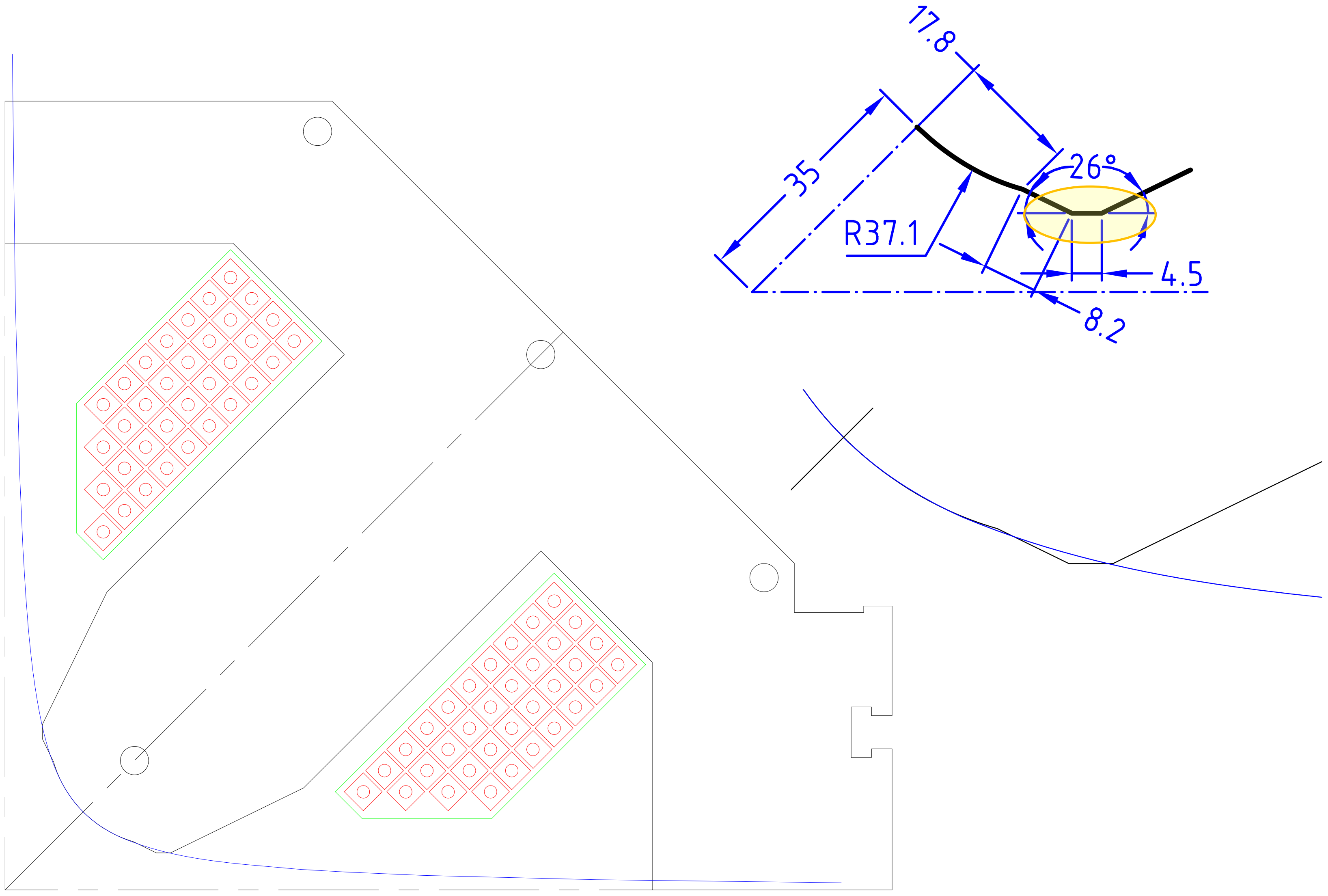

Below the example of the LEP main bending magnets, also with side pole shims

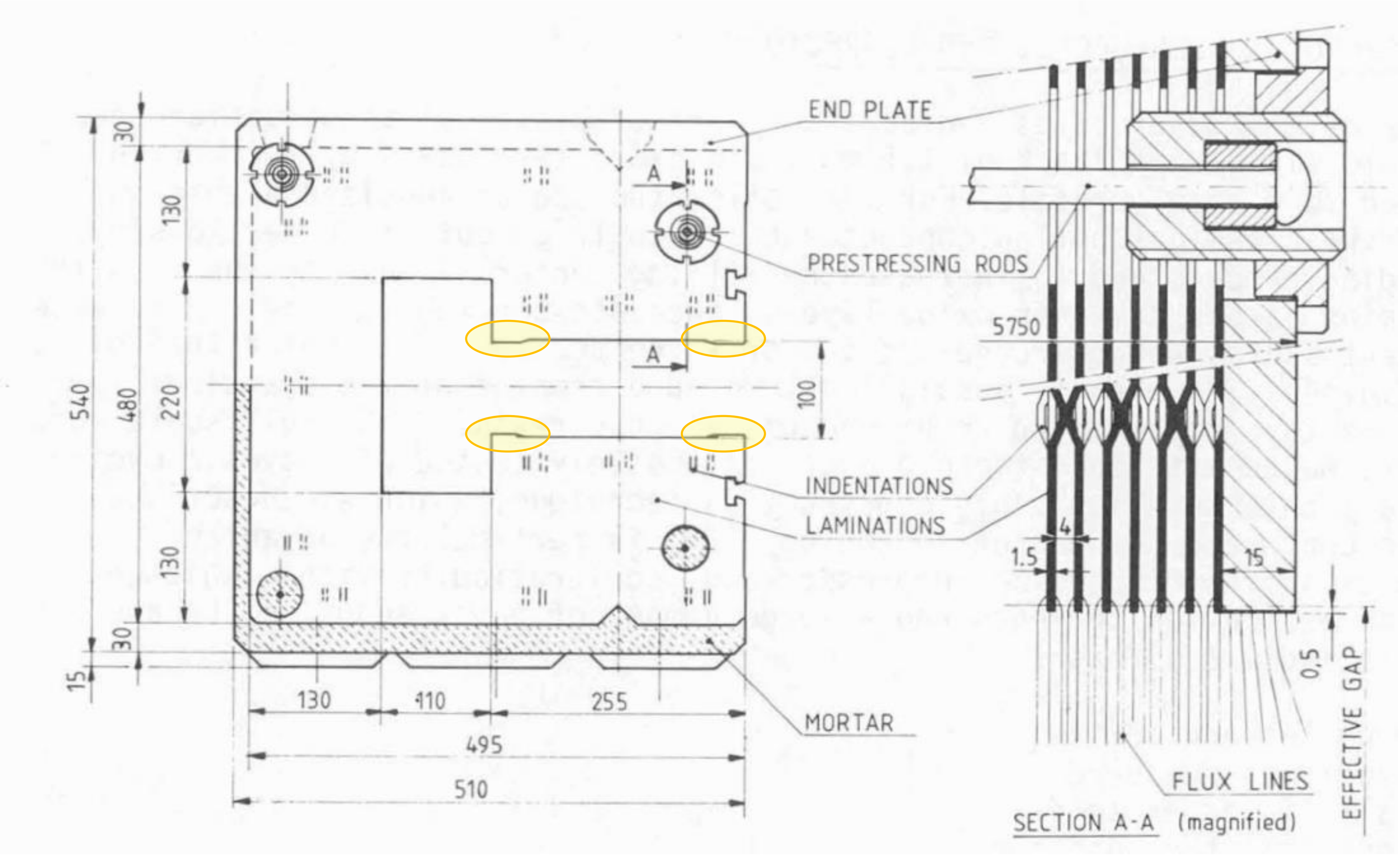

Some authors give guidelines: ex. for dipoles

Dipole Magnet Field Quality

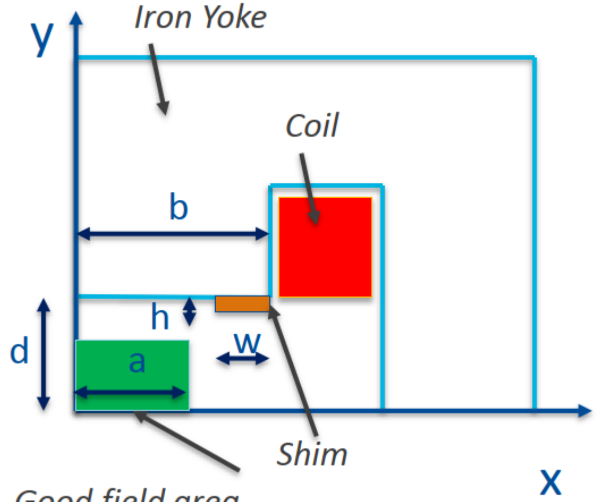

Good field area
B=By=const in the ideal dipole

Shim area: $S=0.021*d^2$

This relation is good for w/d in the range of 0.2 – 0.6.

Field in the magnet midplane:
$B=Bo(1+b1*x+b2*x^2+...)$
Without shims the good field area width is:
- for 1% field homogeneity a=(b-d);
- for 0.1% field homogeneity a=(b-2d).
The good field area could be extended by adding shims:
- for 1% field homogeneity a=(b-d/2);
- for 0.1% field homogeneity a=(b-d).

For gap fields above 0.8 T used more smooth shims to reduce iron saturation effects in pole edges and shim areas.

Fermilab

Some authors give guidelines: ex. for quadrupoles

Quadrupole Magnets

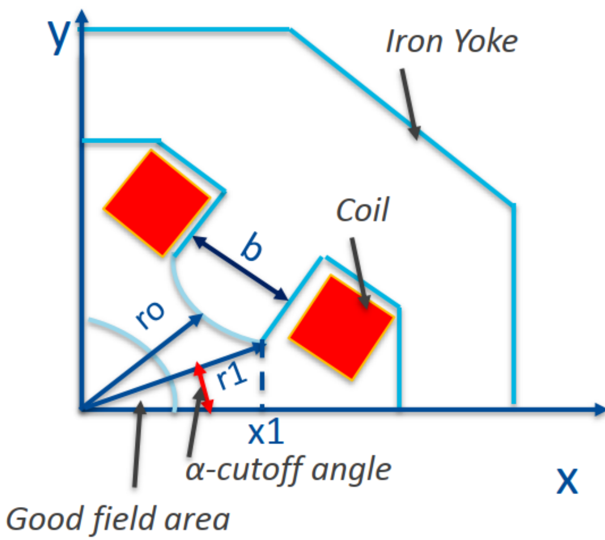

At α= 18° the first undesired multipole b5 vanishes.
*r1=1.122*ro, x1=1.077*ro*
Field gradient at μ=∞ :
G=dBy/dx=b1=const
*By=G*x, G=2μo*Iw/ro²*

Field in the magnet midplane:
*B=Bo(1+b1*x+b2*x²+…)*
For the quadrupole Bo=0,
*The ideal quadrupole field : B=b1*x generated by a hyperbolic pole profile: x*y=ro²/2*
*The quadrupole half gap ampere-turns: (Hp+Ho)/2*ro=Iw, or at Ho=0;*
Quadrupole coil ampere-turns:
*Hp*ro/2+Hfe*Lfe=Iw,*
*Bp*ro/2μo+Bfe/μ*Lfe=Iw.*
Hfe, Bfe –defined as for dipoles, but because of field gradient the flux through the yoke two times lower.

Some authors give guidelines: whole chapter (40 pages) in J. Tanabe's book

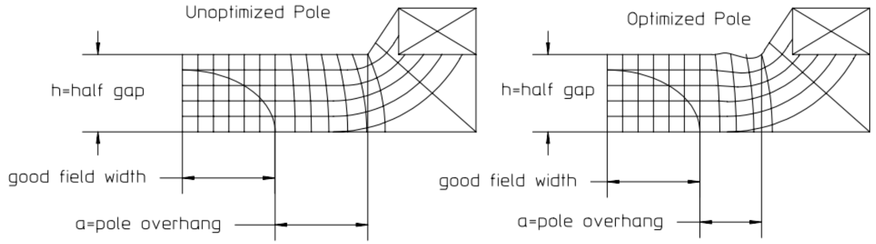

Optimized Pole

The expressions for the potential field quality and the pole overhang required to achieve a specified field quality for an optimized pole are given in eqs. (3.2) and (3.3).

$$\left(\frac{\Delta B}{B}\right)_{optimized} = \frac{1}{100}\exp\left[-7.17\left(x-0.39\right)\right] \tag{3.2}$$

$$x_{optimized} = \frac{a}{h} = -0.14\ln\frac{\Delta B}{B} - 0.25 \tag{3.3}$$

Unptimized Pole

The expressions for the potential field quality and the pole overhang required to achieve a specified field quality for an unoptimized pole are given in eqs. (3.4) and (3.5).

$$\left(\frac{\Delta B}{B}\right)_{unoptimized} = \frac{1}{100}\exp\left[-2.77\left(x-0.75\right)\right] \tag{3.4}$$

$$x_{unoptimized} = \frac{a}{h} = -0.36\ln\frac{\Delta B}{B} - 0.90 \tag{3.5}$$

The size of these side shims can depend on the field level and on the BH characteristics of the material

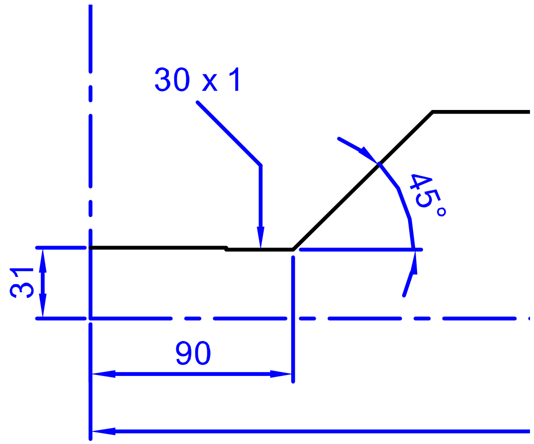

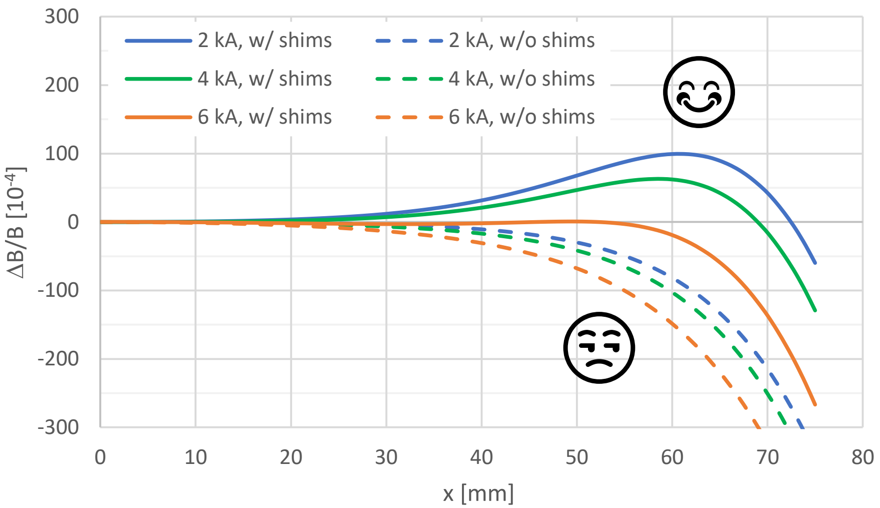

2 kA, 0.96 T

4 kA, 1.63 T

6 kA, 1.90 T

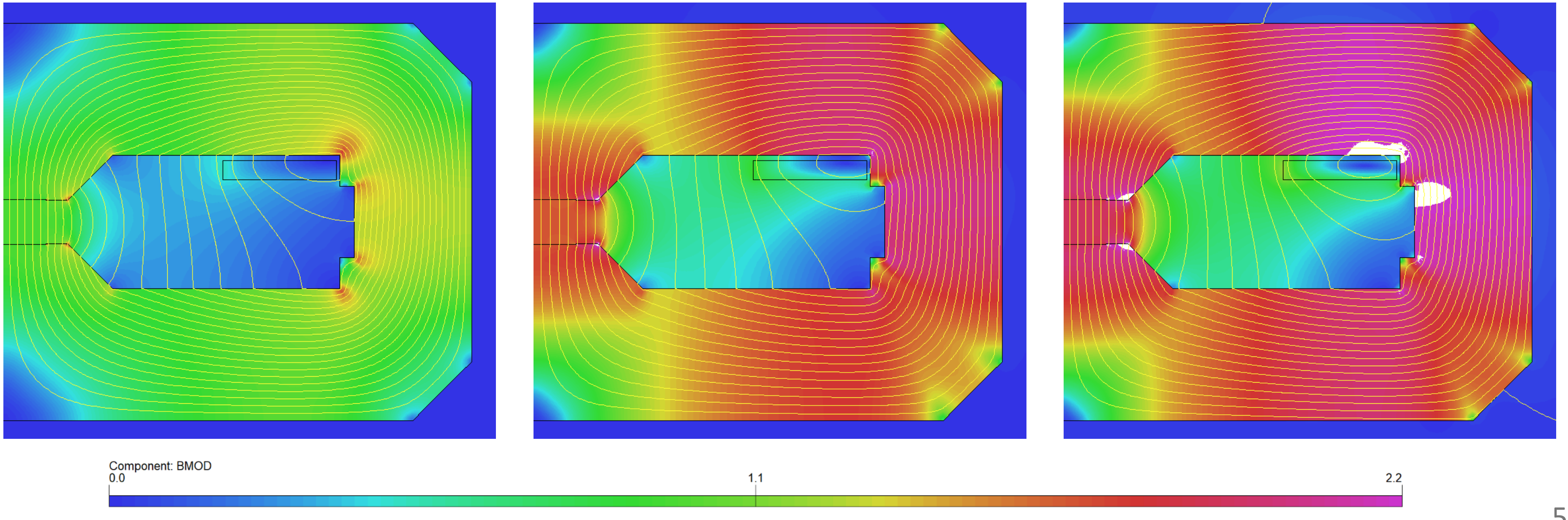

Conclusions (yoke design 2D)

The yoke shall be dimensioned considering various aspects

- There is not a unique solution
- Several magnet layouts are possible
- Pole width, pole tip profile, side shims: the starting point is often given by the curves of constant scalar potential

The material of the yoke is ferromagnetic with $\mu_r >> 1$

- In most cases, electrical steel

The maximum (reasonable) field for a dipole is 2.0 T

- In most cases, we prefer to stay below, in the 1.5 T region

Forces in the iron are (usually) not a main concern

Yoke design

3D

In 3D, the longitudinal dimension of the magnet is described by a magnetic length

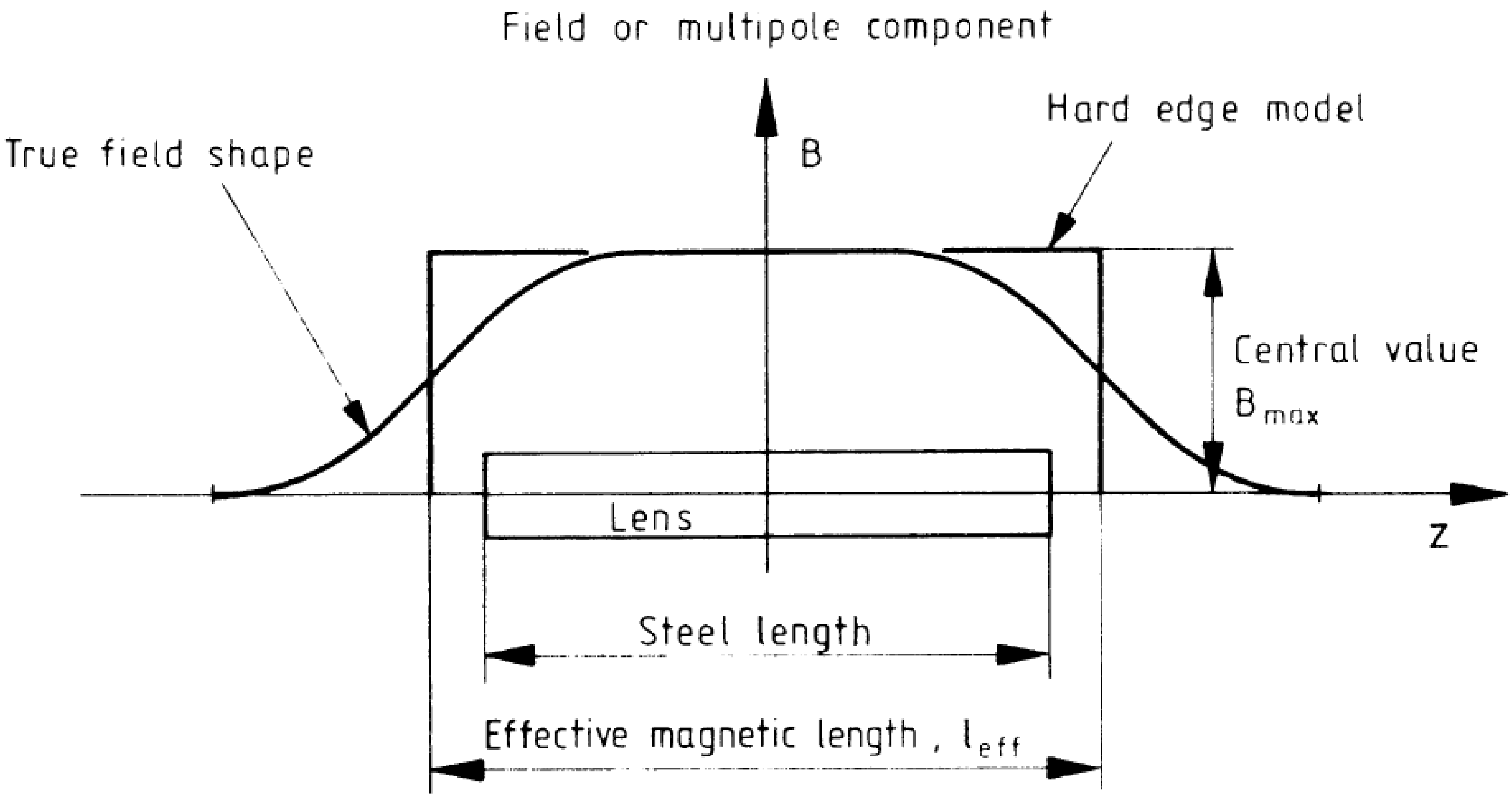

$$l_m B_0 = \int_{-\infty}^{\infty} B(z)dz$$

The magnetic length can be estimated at first order with simple formulae

$$l_m > l_{Fe}$$

dipole

$l_m \cong l_{Fe} + h$ $\qquad h$

quadrupole

$l_m \cong l_{Fe} + 2/3r$ $\qquad r$ aperture radius

sextupole

$l_m \cong l_{Fe} + r/2$ $\qquad r$ aperture radius

There are many different options to terminate the poles in 3D, depending on the type of magnet, its field level, personal preferences, etc.

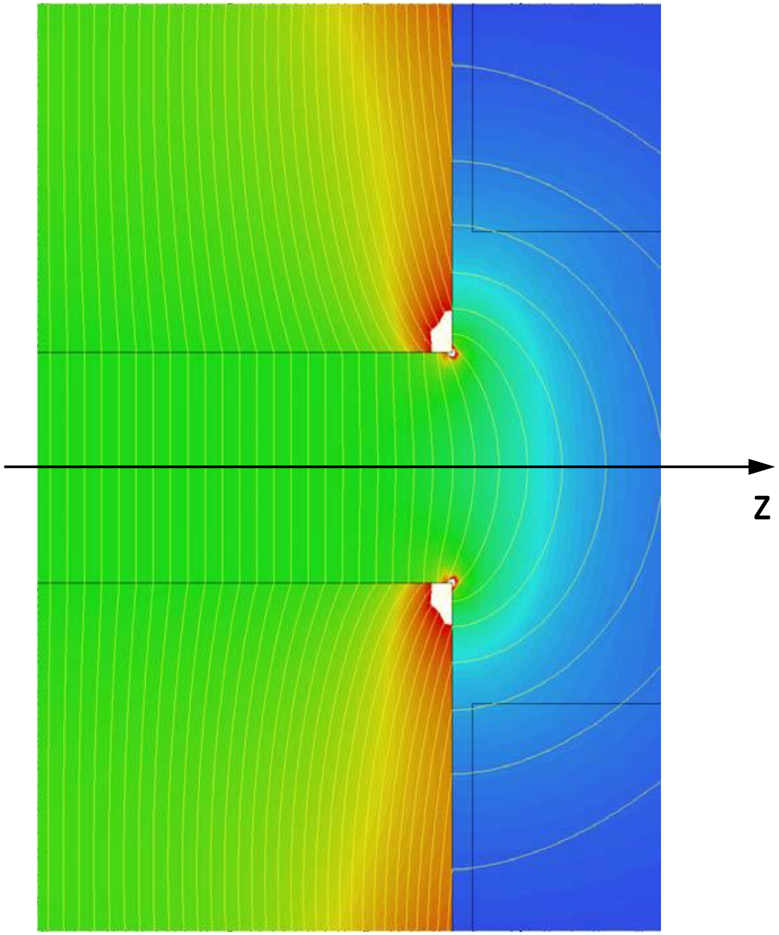

abrupt

rounded (DIAMOND dipole)

shims (SPS MB)

Shims and washers on quadrupole ends for the AA quads

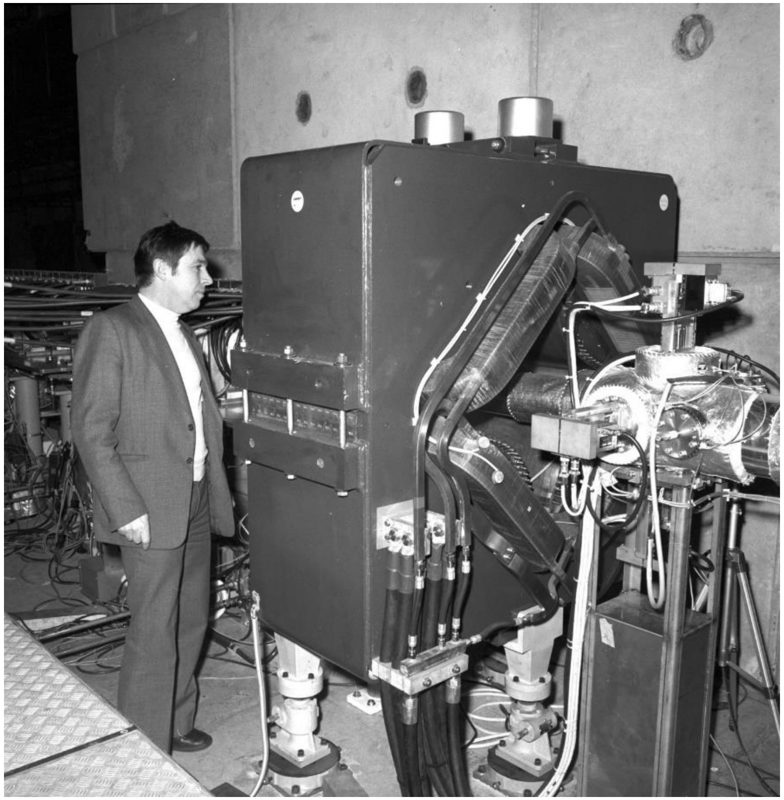

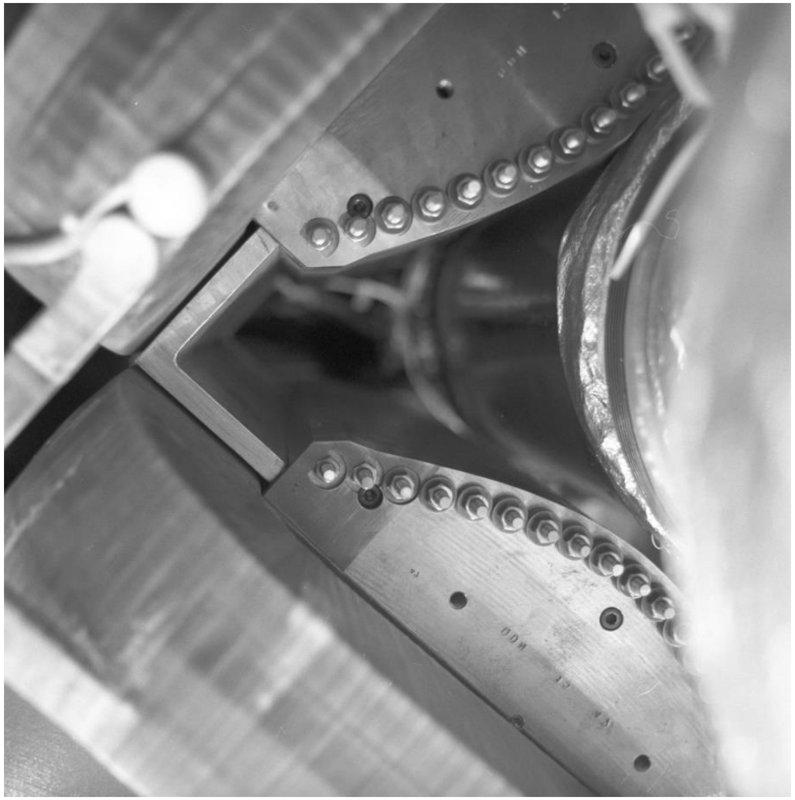

In some cases, a ferromagnetic plate delimits the field in the longitudinal direction: ex. SOLEIL dipole

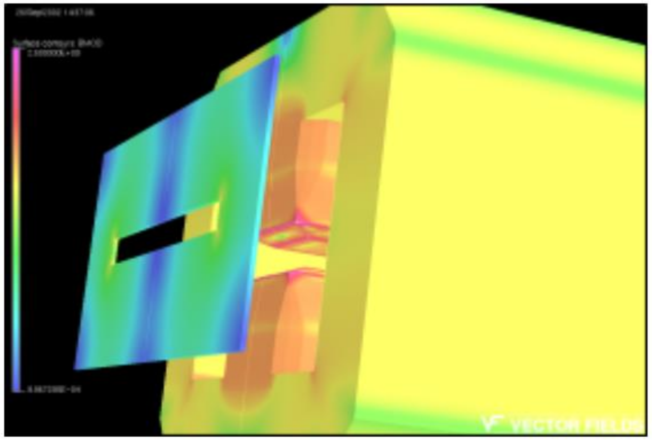

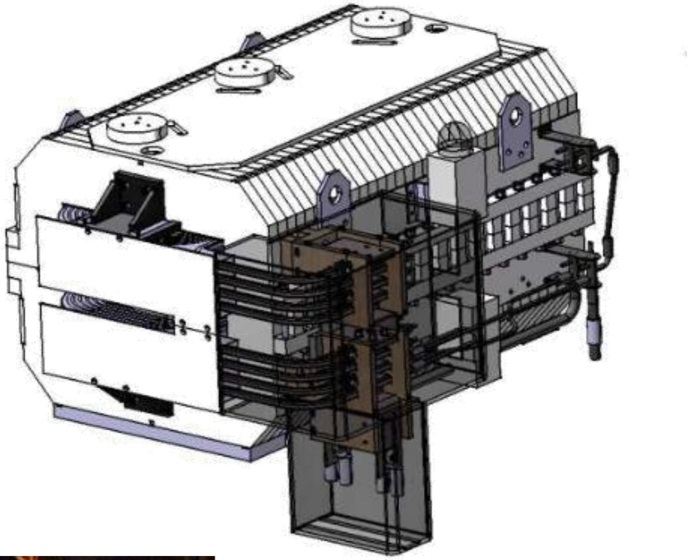

Some machines are very crowded, also in the longitudinal direction: see latest light sources, ex. ESRF-EBS

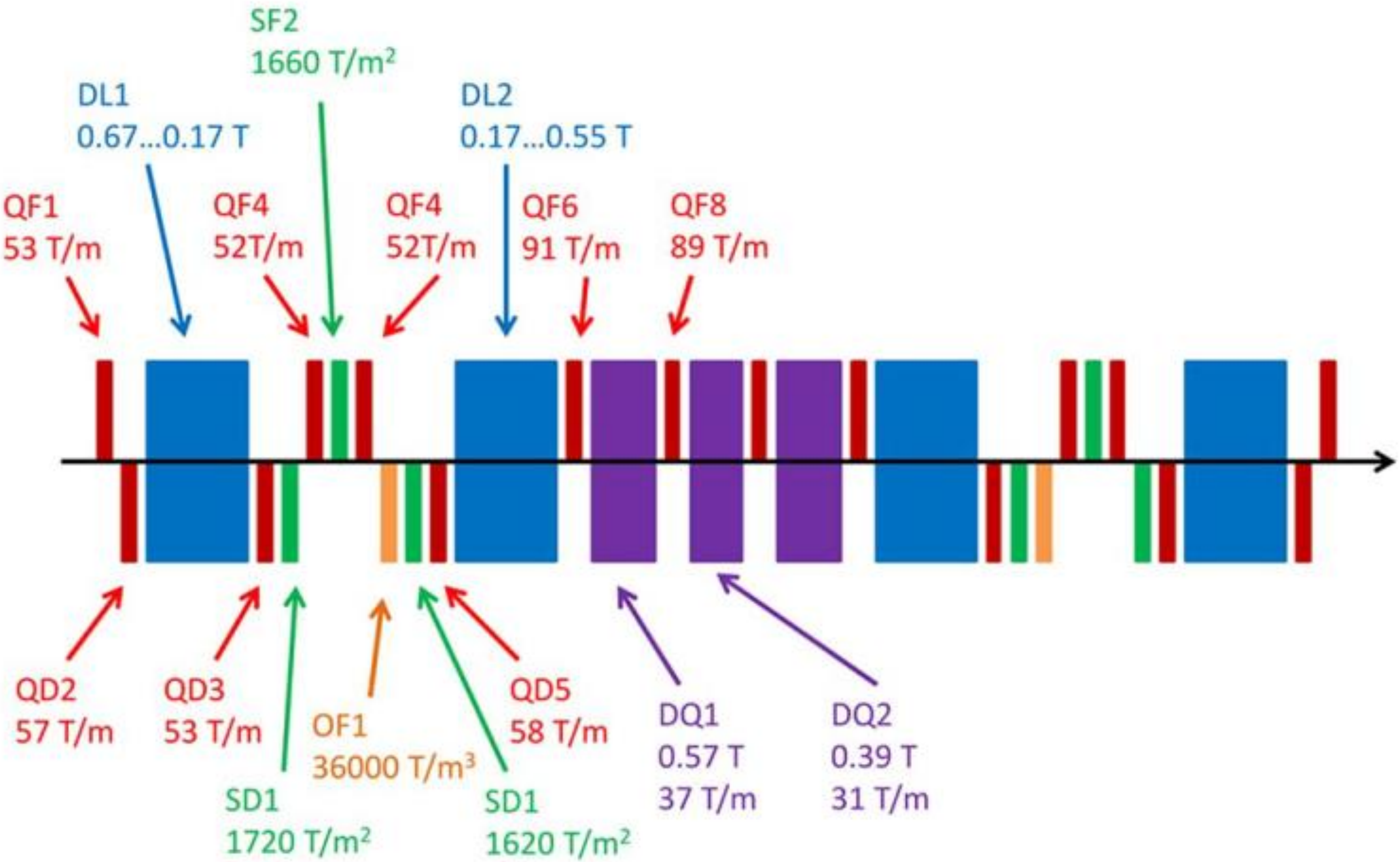

Fig. 1. Schematic view of the magnets of one cell: dipoles with longitudinal gradient (DL), quadrupoles (QF, QD), combined dipole–quadrupoles (DQ), sextupoles (S), and octupoles (O). Corrector magnets are not shown.

SESAME main bending: three degrees of freedom to correct integrated field, quadrupole and sextupole (if needed), after magnetic measurements

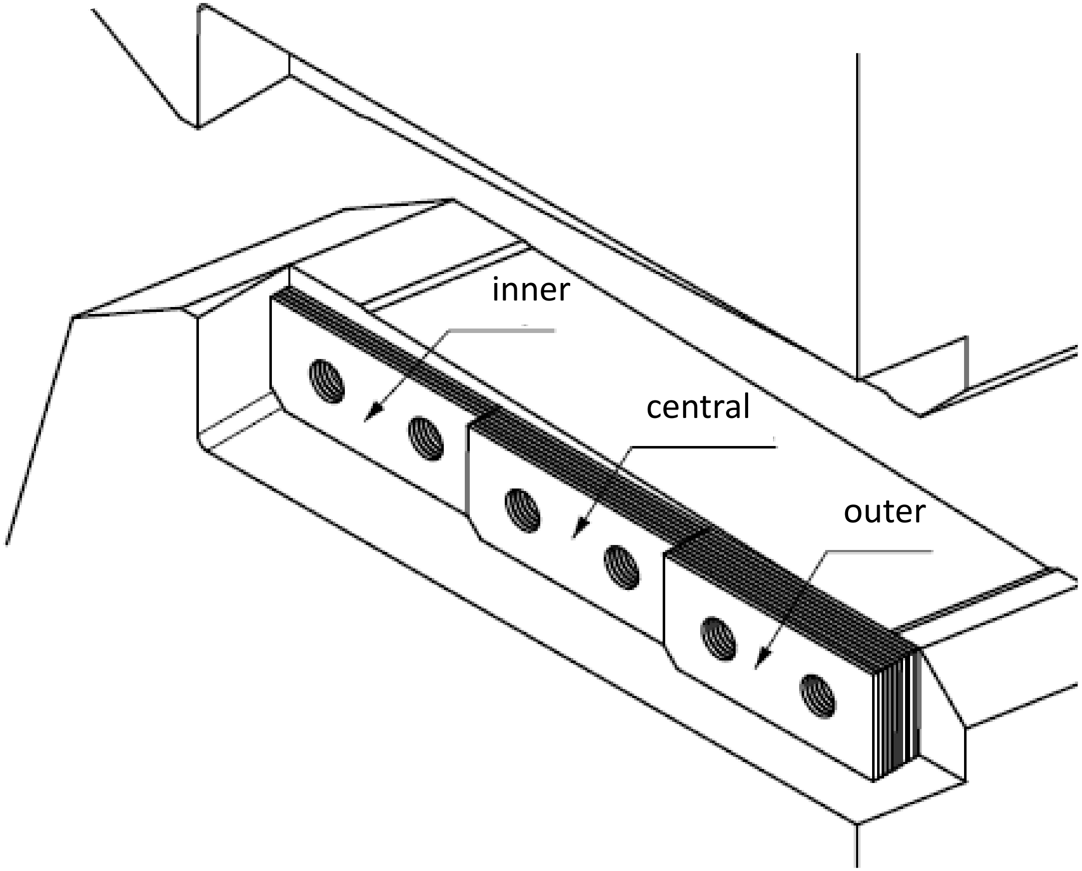

SESAME quadrupoles: same cross-section, different end chamfers (45°) to cancel the first allowed harmonic

QF
280 mm

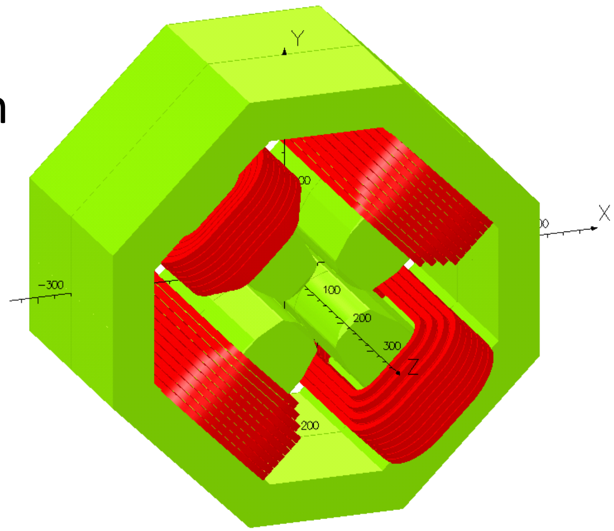

QD
100 mm

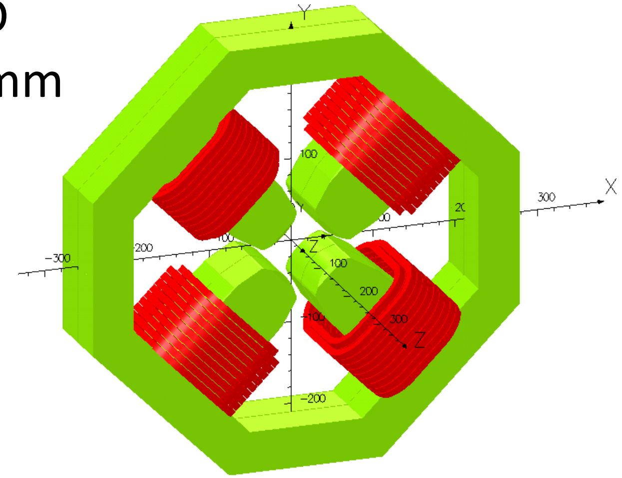

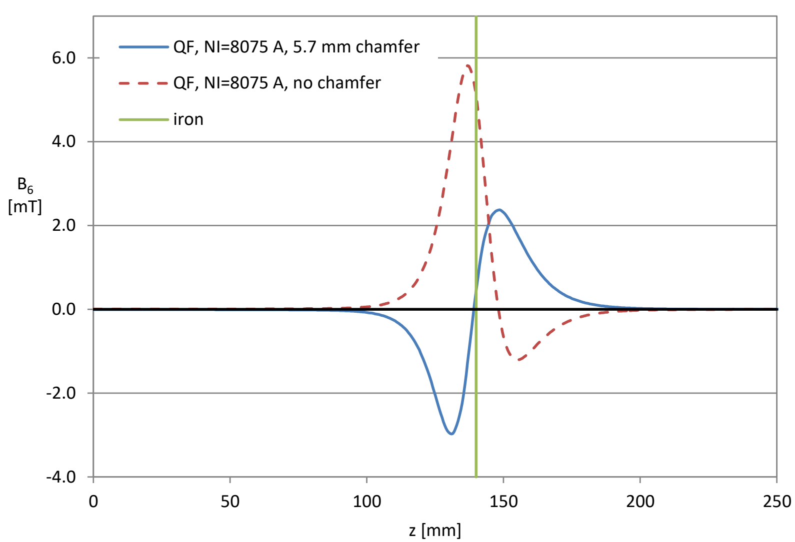

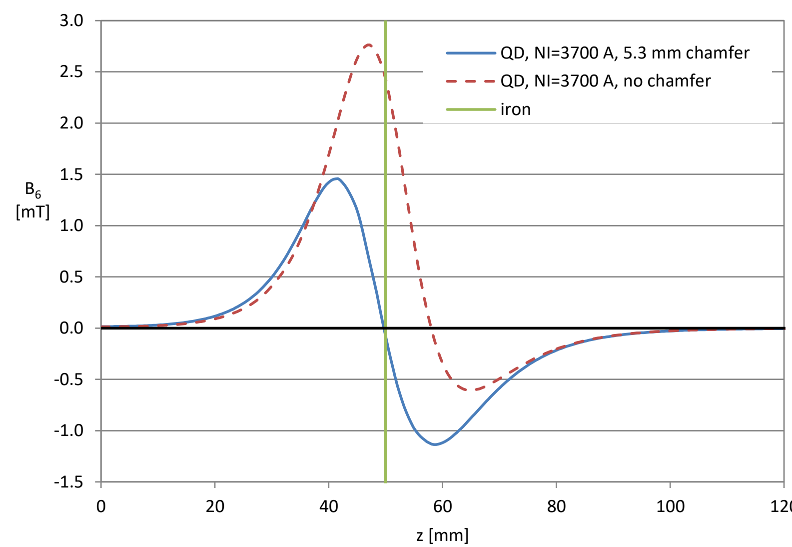

B_6 along the axis (at 24 mm), with and without a chamfer

SESAME sextupoles: no end chamfer, first integrated allowed harmonic compensated with an offset in 2D

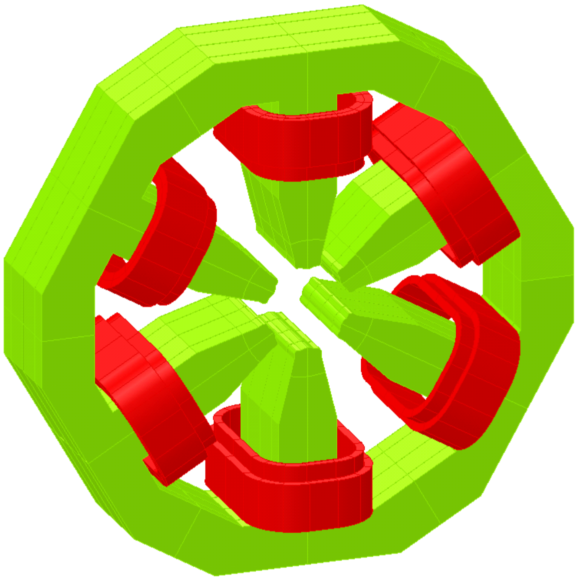

In 2D, $b_9 = 12.8 \cdot 10^{-4}$

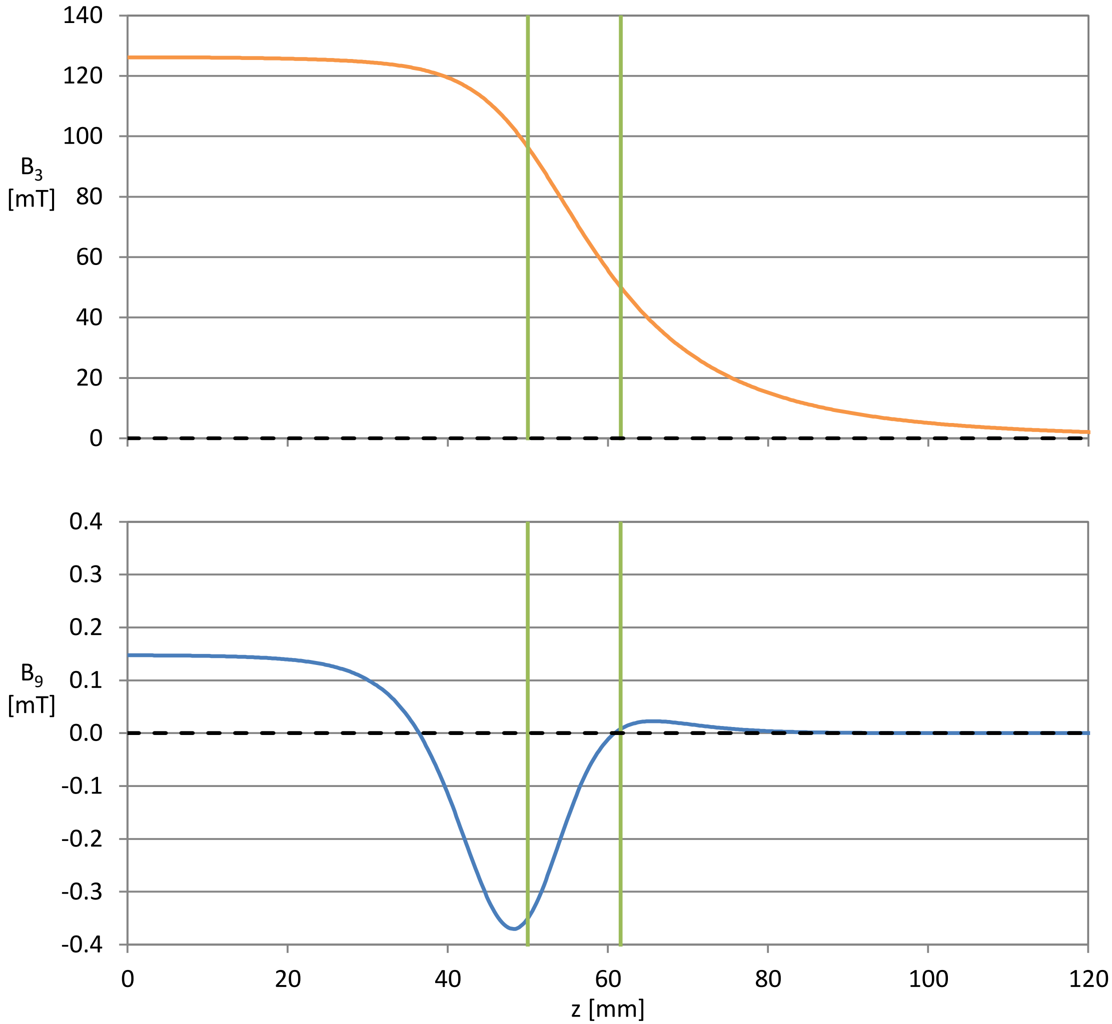

B_3 and B_9 along the axis (at 24 mm), no end chamfer

Solid vs. laminated iron? Simplifying at the extreme, solid ---> dc application, laminated ---> can be pulsed

M200

M200 L

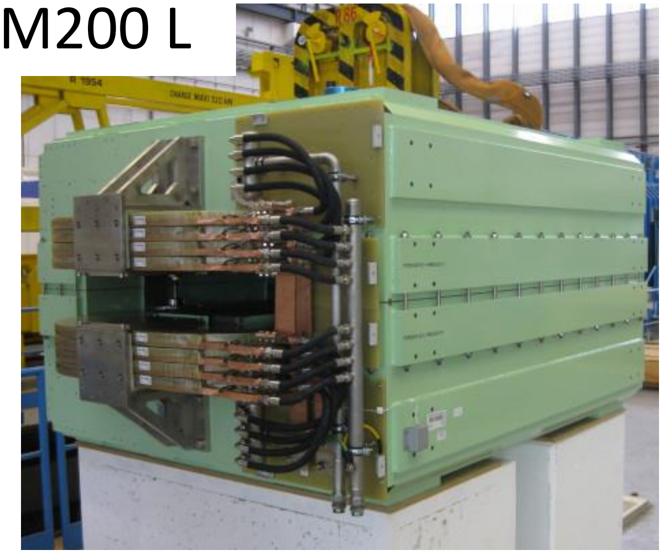

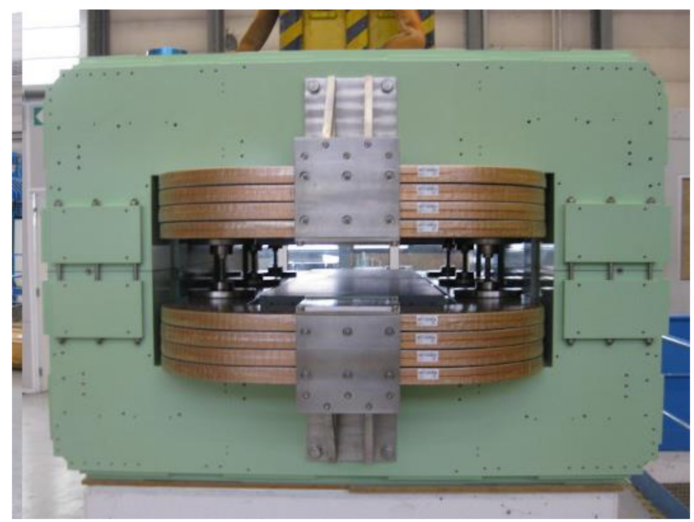

Stacking factor: see below for a formal treatment

In case of anisotropic magnetic material the permeability has the form of a diagonal rank 2 tensor, so that $\mathbf{B} = [\mu]\,\mathbf{H}$ with

$$[\mu] = \begin{pmatrix} \mu_x & 0 & 0 \\ 0 & \mu_y & 0 \\ 0 & 0 & \mu_z \end{pmatrix}. \tag{60}$$

In many materials, such as in rolled metal sheets, the fabrication process produces some regularity in the crystal structure and consequently a dependence of the magnetic properties on the direction. The most well known (and strongest) anisotropy in magnetic materials can be achieved by laminating the iron yokes. Between each of the ferromagnetic laminations of thickness l_{Fe} (magnetically isotropic to first order) there is a non-magnetic ($\mu = \mu_0$) layer of thickness l_0, as shown schematically in Fig. 7.

Consider a lamination in z-direction and the field components $\mathbf{B}_\mathrm{t}$ in the xy-plane. Because of the continuity condition $\mathbf{H}_\mathrm{t}^0 = \mathbf{H}_\mathrm{t}^{\mathrm{Fe}} = \overline{\mathbf{H}}_\mathrm{t}$ we get for the effective macroscopic tangential flux density

$$\overline{\mathbf{B}}_\mathrm{t} = \frac{1}{l_{\mathrm{Fe}} + l_0}\left(l_{\mathrm{Fe}}\mu\overline{\mathbf{H}}_\mathrm{t} + l_0\mu_0\overline{\mathbf{H}}_\mathrm{t}\right). \tag{61}$$

In most cases 0.97-0.98 and in practice no major impact on results

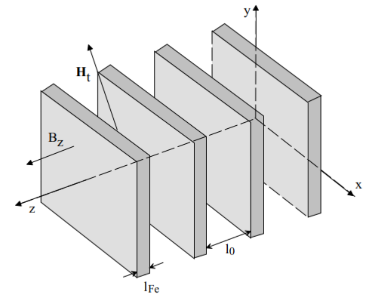

Fig. 7: On the calculation of the μ tensor for laminated materials. The transversal dimensions are large with respect to l_0 and l_{Fe}.

As the normal component of the magnetic flux density is continuous, i.e., $B_z^0 = B_z^{\mathrm{Fe}} = \overline{B}_z$, the average magnetic field intensity can be calculated from

$$\overline{H}_z = \frac{1}{l_{\mathrm{Fe}} + l_0}\left(l_{\mathrm{Fe}}\frac{\overline{B}_z}{\mu} + l_0\frac{\overline{B}_z}{\mu_0}\right). \tag{62}$$

With the packing factor

$$\lambda = \frac{l_{\mathrm{Fe}}}{l_{\mathrm{Fe}} + l_0} \tag{63}$$

which is 0.985 for the LHC yokes, we get for the average permeability in the plane of the lamination

$$\overline{\mu}_\mathrm{t} = \lambda\mu + (1-\lambda)\mu_0 \tag{64}$$

and normal to the plane of the lamination

$$\overline{\mu}_z = \left(\frac{\lambda}{\mu} + \frac{1-\lambda}{\mu_0}\right)^{-1}. \tag{65}$$

We have obtained a simple equation for the packing factor scaling of the material characteristic. For laminations in the x and y direction, i.e, with the plane of the laminations normal to the 2D cross-section, the laminations have a strong directional effect and the packing factor scaling is no longer appropriate. A macroscopic model for these circumstances is developed in [5].

Usually two dipole elements are found in lattice codes: the sector dipole (SBEND) and the parallel faces dipole (RBEND)

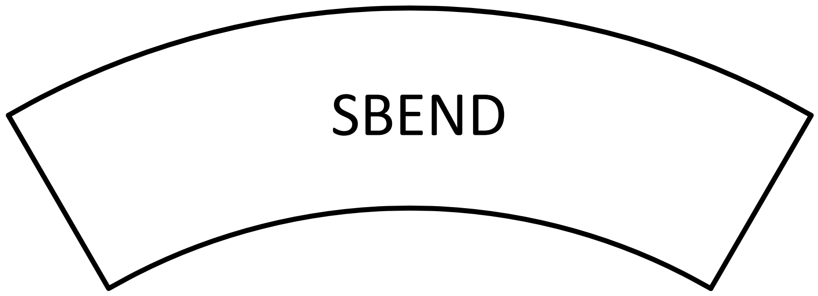

top views

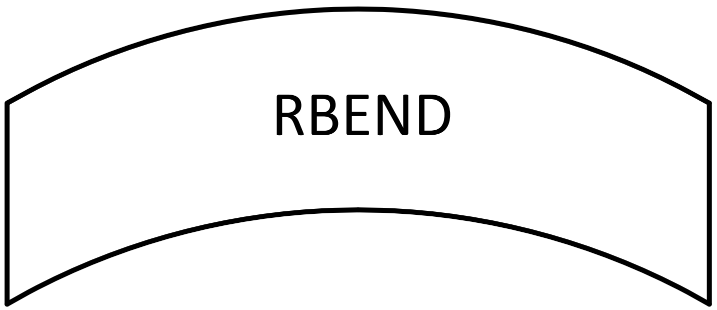

The two types of dipoles are slightly different in terms of focusing, for a geometric effect

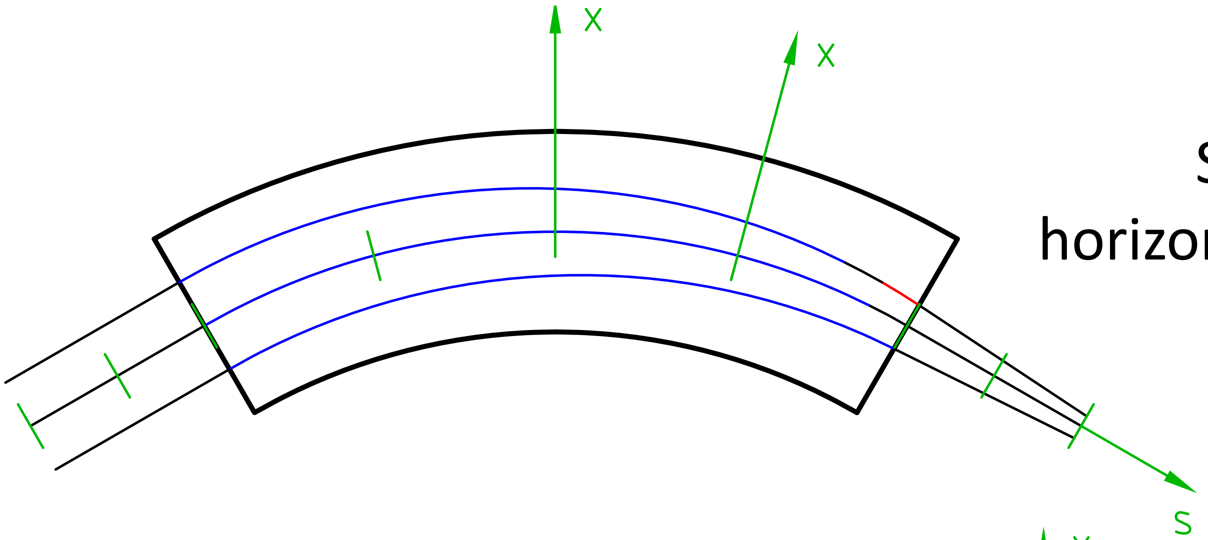

SBEND
horizontal focusing

RBEND
vertical edge focusing

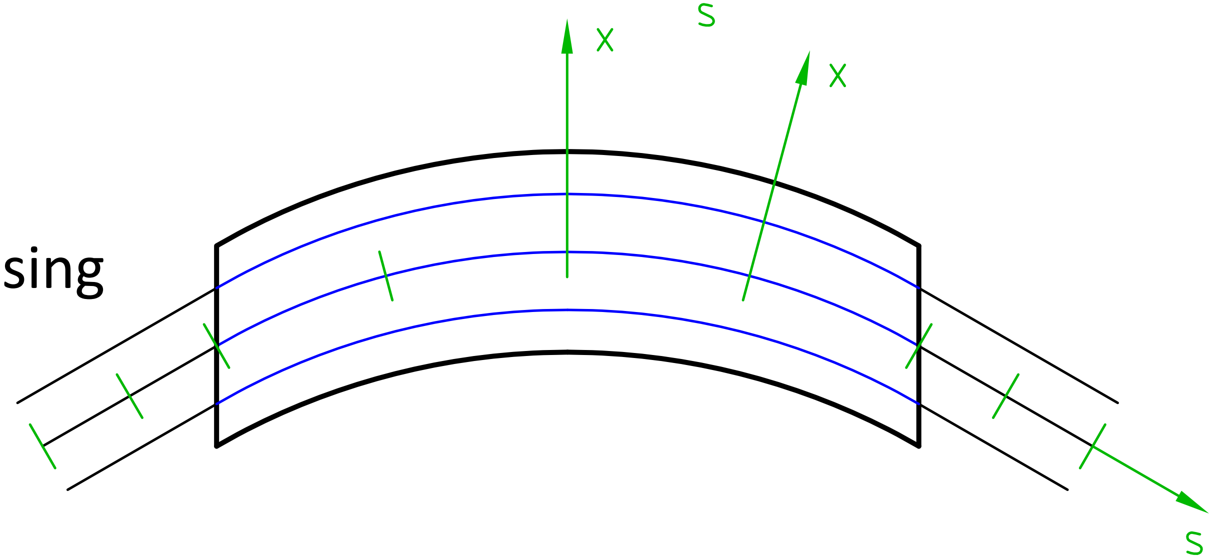

and anything in between, playing with the edges, also curved

Conclusions (yoke design 3D)

The concept of magnetic length is important

- Special attention is needed in crowded lines

As in 2D, several options are possible for the termination of the poles in 3D

- Again, there is not a unique solution
- 3D simulations are powerful tools to check field integrals

Either solid or laminated yokes are used

- The default preference at CERN now is to go for laminated yokes, possibly machined (that is, not stamped)

Coil design

The conductor is either copper (in most cases) or aluminum

Copper

$1.72 \cdot [1 + 0.0039 \cdot (T-20)] \cdot 10^{-8}\ \Omega/m$

$8.9\ kg/dm^3$

Aluminium

$2.65 \cdot [1 + 0.0040 \cdot (T-20)] \cdot 10^{-8}\ \Omega/m$

$2.7\ kg/dm^3$

Some examples of coils with aluminum conductor

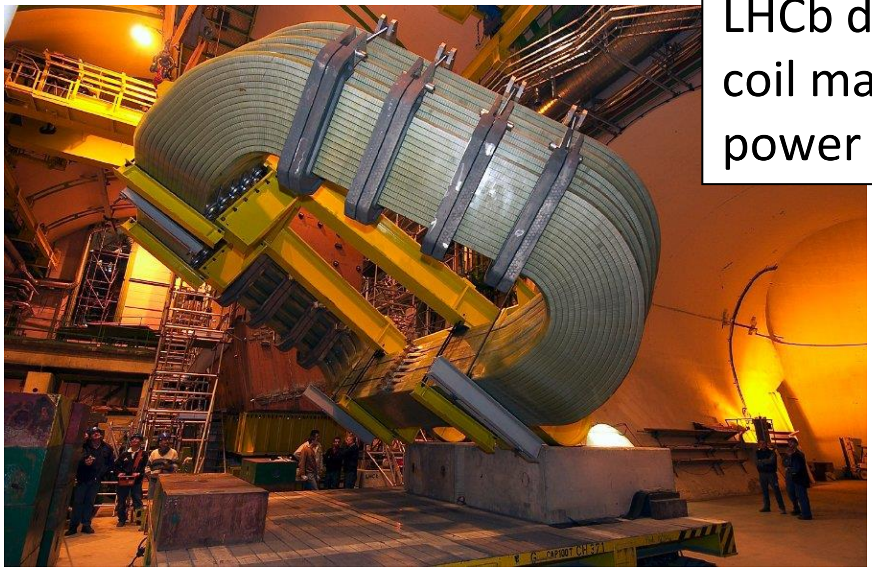

LHCb detector dipole
coil mass 2 × 25 t
power 2 × 2.1 MW

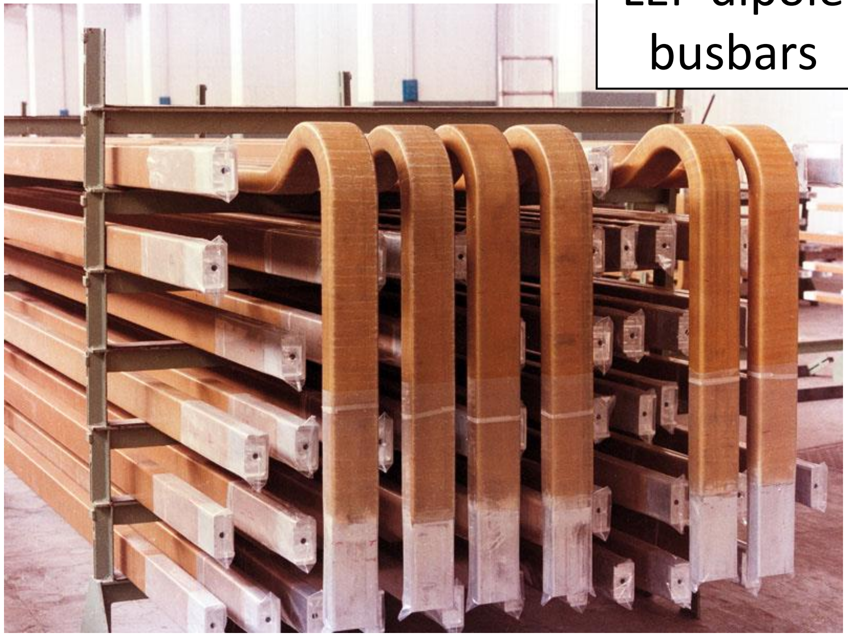

LEP dipole
busbars

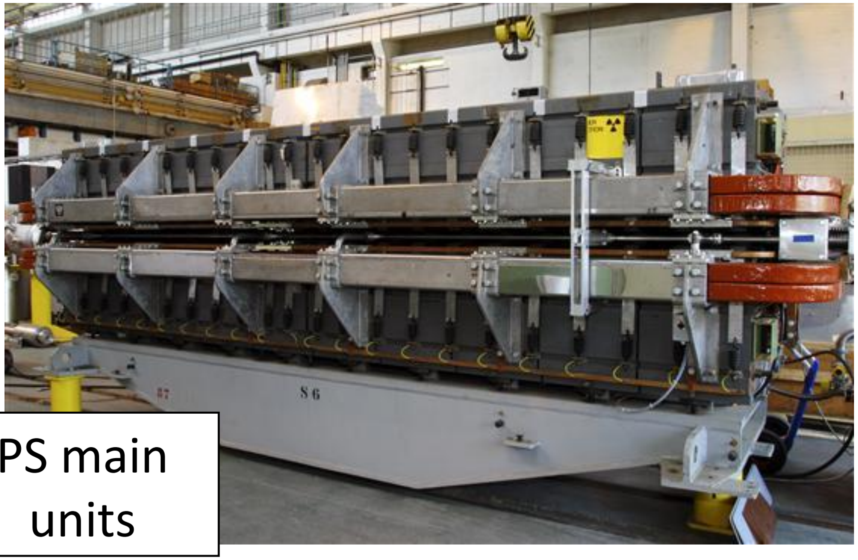

PS main
units

Focusing on copper, both hollow conductors (long length, mostly non-insulated) and solid conductors (also insulated) are commercially available

Standard coil types

Bedstead or saddle coil

Racetrack coil

Tapered quadrupole coil

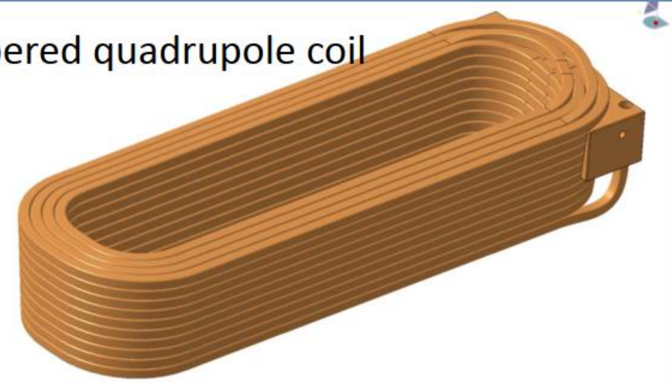

minimum bending radius (in particular for hollow conductor) typically 5x side / 10x the hole diameter – to avoid cooling restrictions and wedging

For a dipole, the Ampere-turns are a linear function of the gap and of the field (at least up to saturation)

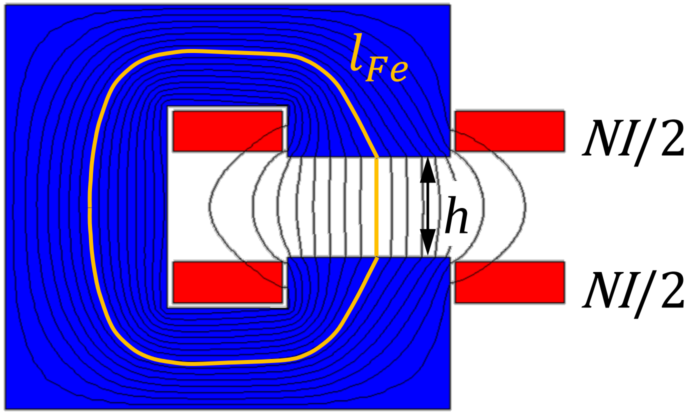

$$NI = \oint \vec{H} \cdot \vec{dl} = \frac{B_{Fe}}{\mu_0 \mu_r} \cdot l_{Fe} + \frac{B_{gap}}{\mu_0} \cdot h \cong \frac{B_{gap} h}{\mu_0}$$

$$NI = \frac{Bh}{\eta \mu_0} \qquad \eta = \frac{1}{1 + \frac{1}{\mu_r} \frac{l_{Fe}}{h}}$$

This formula is very useful, but it also assumes a pure dipole field: see below for ex. when adding a sextupole error

$$\frac{NI}{2} = \frac{B_1}{\mu_0}\frac{h}{2} - \frac{B_3}{3\mu_0 R^2}\left(\frac{h}{2}\right)^3$$

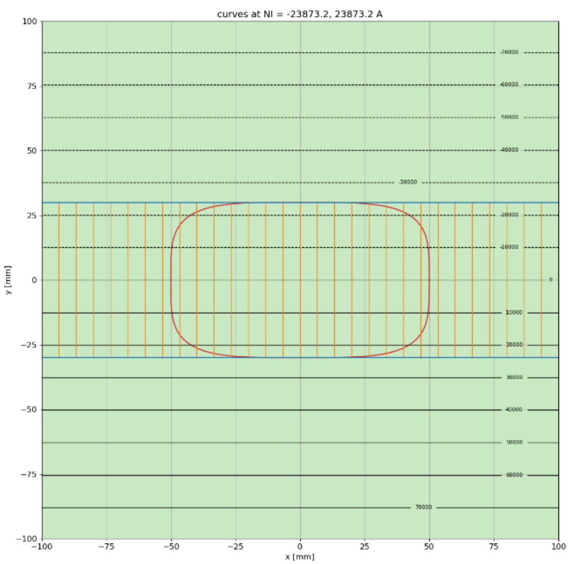

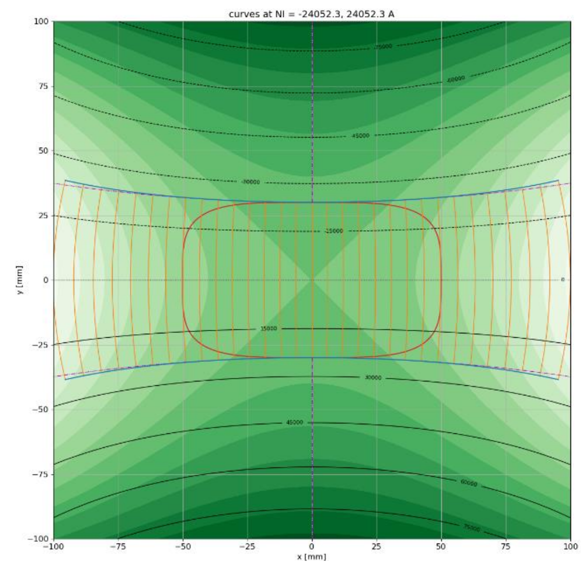

$B_1 = 1\ \mathrm{T}$
$B_3 = 0\ \mathrm{T}$ at $R = 20\ \mathrm{mm}$
$h = 60\ \mathrm{mm}$
$NI = 2 \times 23873.24\ \mathrm{A}$

$B_1 = 1\ \mathrm{T}$
$B_3 = -0.01\ \mathrm{T}$ at $R = 20\ \mathrm{mm}$
$h = 60\ \mathrm{mm}$
$NI = 2 \times 24052.29\ \mathrm{A}$

The same computation can be tackled using magnetic reluctances and Hopkinson's law, which is a parallel of Ohm's law

$$\mathcal{R} = \frac{\mathrm{NI}}{\Phi} \qquad \mathrm{R} = \frac{\mathrm{V}}{I}$$

$$\mathcal{R} = \frac{l}{\mu_0 \mu_r A} \qquad \mathrm{R} = \frac{l}{\sigma S}$$

$$\eta = \frac{1}{1 + \frac{\mathcal{R}_{Fe}}{\mathcal{R}_{gap}}}$$

The Ampere-turns grow with the order of the magnet, so there is an interest in keeping the aperture small

Dipole

$$NI \cong \frac{Bh}{\mu_0}$$

$$\boxed{B \cong \frac{\mu_0 NI}{h}}$$

Quadrupole

$$NI \cong \frac{2B'r^2}{\mu_0}$$

$$B' \cong \frac{\mu_0 NI}{2r^2}$$

Sextupole

$$NI \cong \frac{B''r^3}{\mu_0}$$

$$B'' \cong \frac{\mu_0 NI}{r^3}$$

These are the same formulae – including the more general one – using the fundamental harmonic rather than B, B', B''

<u>Dipole</u>

$$B = B_1 \qquad B_1 \cong \frac{\mu_0 NI}{2r} \qquad NI \cong \frac{2B_1 r}{\mu_0}$$

<u>Quadrupole</u>

$$B' = \frac{B_2}{R} \qquad B_2 \cong \frac{\mu_0 NIR}{2r^2} \qquad NI \cong \frac{2B_2 r^2}{R\mu_0}$$

<u>Sextupole</u>

$$B'' = \frac{2B_3}{R^2} \qquad B_3 \cong \frac{\mu_0 NIR^2}{2r^3} \qquad NI \cong \frac{2B_3 r^3}{\mu_0 R^2}$$

<u>General</u>

$$B_n \cong \frac{\mu_0 NIR^{n-1}}{2r^n} \qquad NI \cong \frac{2B_n r^n}{\mu_0 R^{n-1}}$$

Geometric errors in the pole have a larger impact on the magnetic field in the gap, as the order increases

Dipole

$$\frac{\Delta B}{B} = \frac{B(h + \Delta h) - B(h)}{B(h)} \cong -\frac{\Delta h}{h}$$

Quadrupole

$$\frac{\Delta B'}{B'} = \frac{B'(r + \Delta r) - B'(r)}{B'(r)} \cong -2\frac{\Delta r}{r}$$

Sextupole

$$\frac{\Delta B''}{B''} = \frac{B''(r + \Delta r) - B''(r)}{B''(r)} \cong -3\frac{\Delta r}{r}$$

Example of computation of Ampere-turns and current

central field B = 1.3 T
total gap 80 mm

$$NI = \frac{Bh}{\eta \mu_0}$$

η ≅ 0.90

NI = (1.3*0.080)/(0.90*4*pi*10^-7) = 91956 A total

<u>low inductance option</u>
64 turns, I ≅ 91956/64 = 1437 A
L = 62.9 mH, R = 15.9 mΩ

<u>low current option</u>
204 turns, I ≅ 91956/204 = 451 A
L = 639 mH, R = 172 mΩ

MCA/MCB dipole: same yoke, different coils

32 turns per pole

BEAM TRANSPORT ELEMENTS FOR THE SPS EXPERIMENTAL AREAS

REFERENCE: ISR-MA BEAM TRANSFER LIST 12th OCTOBER 1971

NAME: R. PAGE

DATE: 16-8-74 | REV. DATE:

QUANTITY: 24 | MCA BENDING MAGNET

MAGNETIC FIELD

NOMINAL PEAK FIELD	1,3 T
NOMINAL BENDING POWER	3,38 T.m
APERTURE HEIGHT	80 mm
USEFUL APERTURE WIDTH	160 mm

POWER

D.C. POWER	32,7 kW
CURRENT	1434 A
VOLTAGE	22,8 VOLTS
RESISTANCE	$15,9.10^{-3}\ \Omega$
INDUCTANCE	$62,9.10^{-3}$ H

COOLING

WATER TEMP RISE	25 °C
TOTAL FLOW	$1,12\ m^3\ hr^{-1}$
PRESSURE DROP	$5\ kg.\ cm^{-2}$

WEIGHTS

CORE	18 t
COILS	2,5 t
TOTAL MAGNET ASSY	20,5 t

VACUUM CHAMBER

TOTAL LENGTH (BETWEEN FLANGES)	3,30 m
USEFUL APERTURE	129 / 72,4 mm

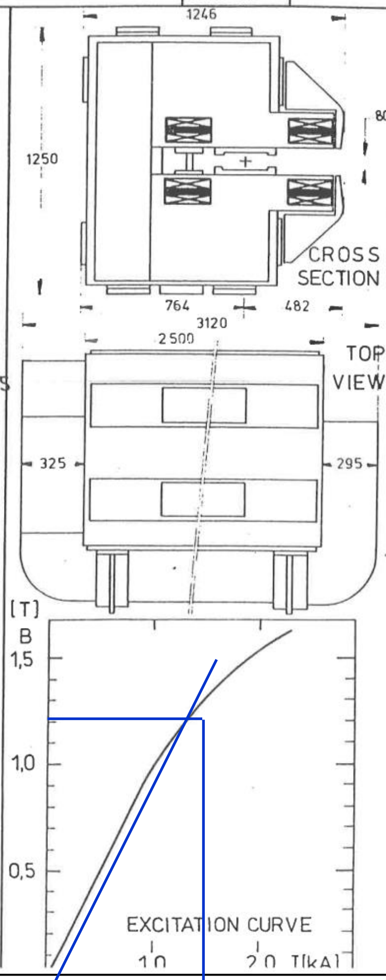

102 turns per pole

BEAM TRANSPORT ELEMENTS FOR THE SPS EXPERIMENTAL AREAS

REFERENCE: LAB I/EA Note 74.10 6.5.74

NAME: R. PAGE

DATE: 16-8-74 | REV. DATE:

QUANTITY: 21 | MCB BENDING MAGNET

MAGNETIC FIELD

NOMINAL PEAK FIELD	1,3 T.
NOMINAL BENDING POWER	3,38 T.m.
APERTURE HEIGHT	80 mm.
USEFUL APERTURE WIDTH	160 mm.

POWER

D C POWER	34,8 kW.
CURRENT	450 A
VOLTAGE	77,4 VOLTS
RESISTANCE	$172.10^{-3}\ \Omega$
INDUCTANCE	639.10^{-3} H.

COOLING

WATER TEMP RISE	25 °C.
TOTAL FLOW	$1,2\ m^3\ hr^{-1}$
PRESSURE DROP	$5\ kg.\ cm^{-2}$

WEIGHTS

CORE	18 t
COILS	2,5 t
TOTAL MAGNET ASSY	20,5 t

VACUUM CHAMBER

TOTAL LENGTH (BETWEEN FLANGES)	3,30 m.
USEFUL APERTURE	129 / 72,4 mm

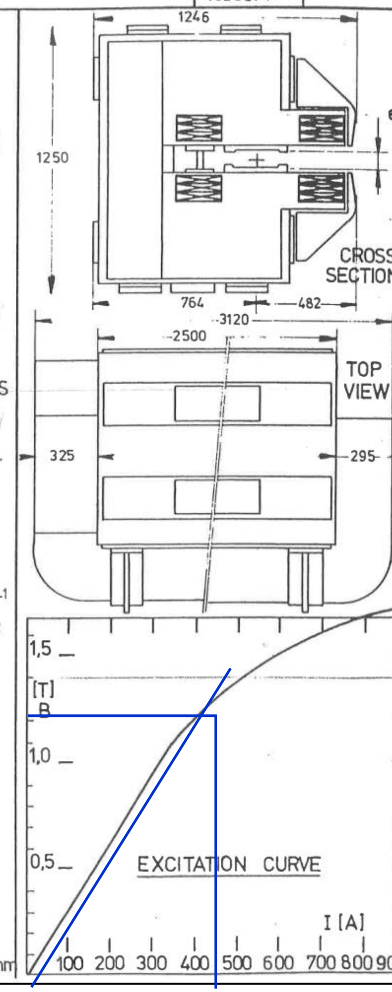

Besides the number of turns, the overall size of the coil depends on the current density, which drives the resistive power consumption (linearly)

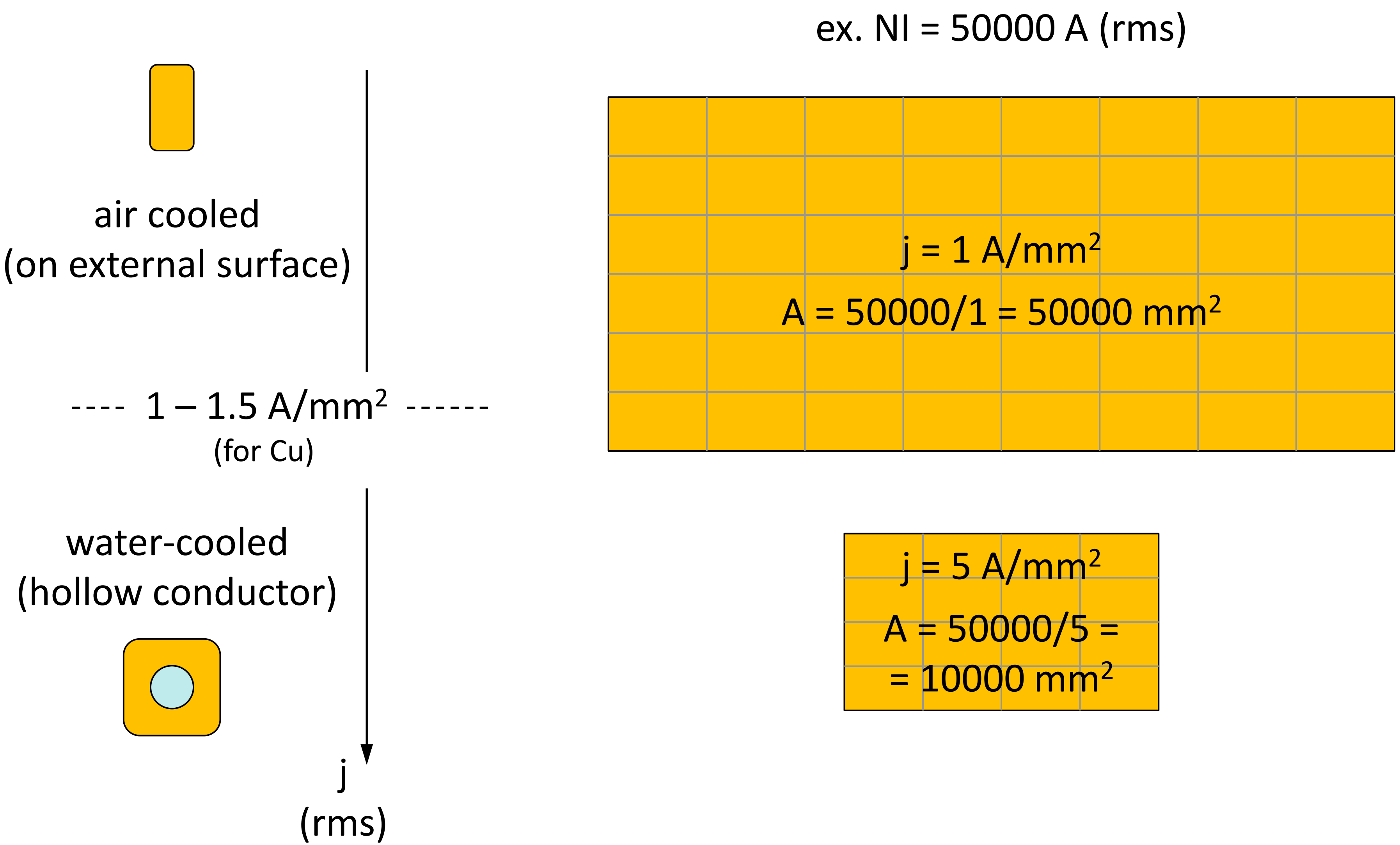

The size of the coil (for large magnets or many in series) is optimized considering capital and running costs (including infrastructure like power converters, cooling, cables, etc.)

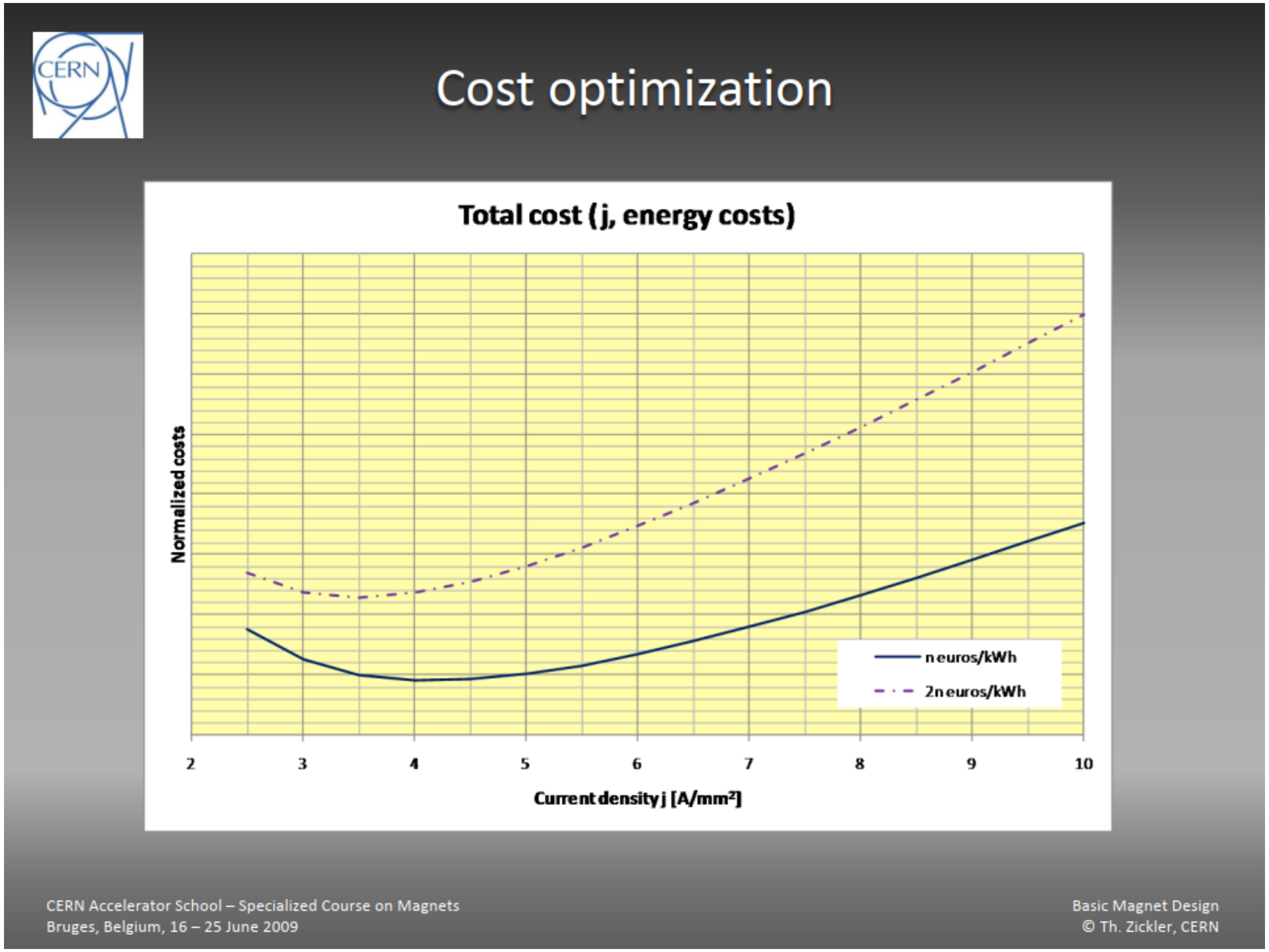

These are common formulae for the main electric parameters of a resistive dipole (1/2)

Ampere-turns (total) $$NI = \frac{Bh}{\eta\mu_0}$$

current $$I = \frac{(NI)}{N}$$

resistance (total) $$R = \frac{\rho N L_{turn}}{A_{cond}}$$

inductance $$L \cong \eta\mu_0 N^2 A/h$$

$$A \cong (w_{pole}+1.2h)(l_{Fe} + h)$$

These are common formulae for the main electric parameters of a resistive dipole (2/2)

voltage

$$V = RI + L\frac{dI}{dt}$$

resistive power (rms)

$$\begin{aligned} P_{rms} &= RI_{rms}^2 \\ &= \rho j_{rms}^2 V_{cond} \\ &= \frac{\rho L_{turn} B_{rms} h}{\eta \mu_0} j_{rms} \end{aligned}$$

magnetic stored energy

$$E_m = \int_0^I Lidi \cong \frac{1}{2} LI^2$$

These are useful formulae for standard resistive quadrupoles

pole tip field $$B_{pole} = B'r$$

Ampere-turns (total) $$NI = \frac{2B'r^2}{\eta\mu_0}$$

current $$I = \frac{(NI)}{N}$$

resistance (total) $$R = \frac{\rho N L_{turn}}{A_{cond}}$$

If the magnet is not dc, then an rms power / current is taken, considering the duty cycle

$$P_{rms} = RI_{rms}^2 = R\frac{1}{T}\int_0^T [I(t)]^2 dt$$

sine wave around 0

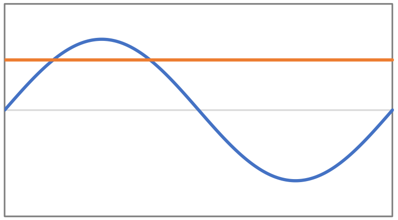

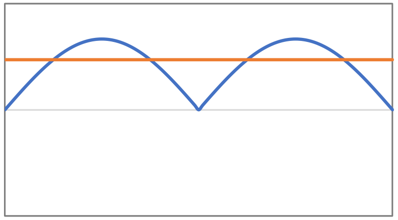

$$I_{rms}^2 = \frac{I_{peak}^2}{2}$$

linear ramp from 0

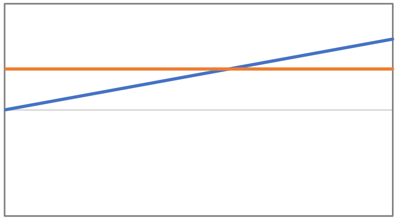

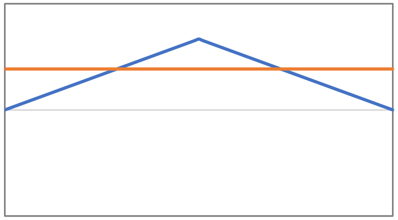

$$I_{rms}^2 = \frac{I_{peak}^2}{3}$$

linear ramp between I_1 and I_2

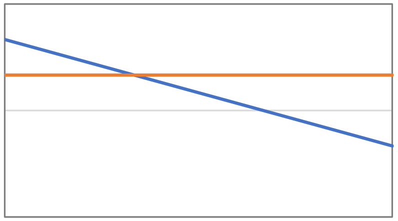

$$I_{rms}^2 = \frac{I_1^2 + I_1 I_2 + I_2^2}{3}$$

The rms power can be computed piecewise, for example with a simple spreadsheet (considering a piecewise linear approximation for the current cycle)

$$I_{rms}^2 = \frac{I_{rms,1}^2 t_1 + I_{rms,2}^2 t_2 + I_{rms,3}^2 t_3 + \cdots}{t_1 + t_2 + t_3 + \cdots}$$

	T	I rms		
	[s]	[A]		
	0	2184.1		
	1.2	2184.1		
	t	I	∫I^2*dt	
	[s]	[A]	[A^2*s]	
	0	0.0	-	
	0.005	137.9	32	
	0.015	200.0	289	
	0.225	200.0	8400	
	0.235	468.5	1177	
	0.245	729.6	3645	
	0.255	967.8	7250	
	0.265	1023.8	9919	
	0.275	1079.9	11067	
	0.285	1107.2	11959	
	0.295	1135.2	12571	

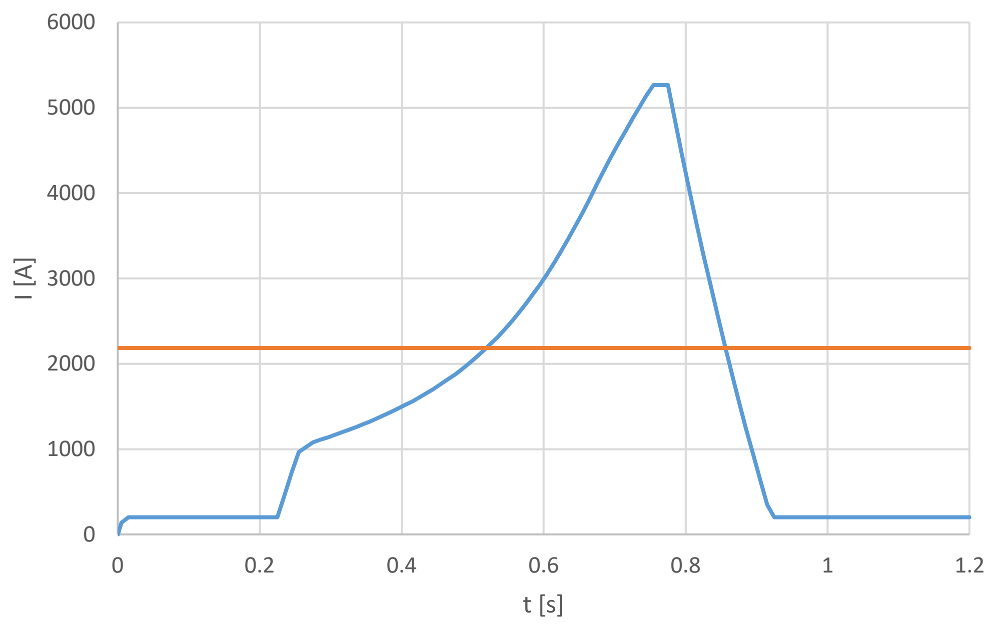

Power requirements

Assuming the magnet cross-section and the yoke length are known, one can calculate the total dissipated power per magnet:

$$P_{dipole} = \rho \frac{Bh}{\eta \mu_0} j l_{avg} \quad (12^*) \qquad P_{qudrupole} = 2\rho \frac{B' r^2}{\eta \mu_0} j l_{avg} \quad (13^*) \qquad P_{sextupole} = \rho \frac{B'' r^3}{\eta \mu_0} j l_{avg} \quad (14^*)$$

- *j*: current density [A/m²]: $j = \frac{NI}{f_c A} = \frac{I}{a_{cond}}$ (15)
- *ρ*: resistivity [Ωm] (for copper: $1.86 \cdot 10^{-8}$ Ωm @ 40°C)
- l_{avg}: average turn length [m]; approximation: $2.5\, l_{iron} < l_{avg} < 3\, l_{iron}$ for racetrack coils
- a_{cond}: conductor cross section [m²]
- *A*: coil cross section [m²]
- f_c: filling factor = $\frac{\text{net conductor area}}{\text{coil cross section}}$ (geometric filling factor, insulation, cooling duct, edge rounding)

Note: for a constant geometry, the power loss P is proportional to the current density j.

Air cooling

Air cooling by natural convection:

- Current density:
  - $j \leq 2$ A/mm² for small, thin coils
  - $j \leq 1$ A/mm² for large, captured coils
- Difficult to calculate analytically
- Numerical computations required to get reasonable results
- Round, rectangular or square conductor
  - Filling factor: 0.63 (round) to 0.8 (rectangular)

grade 1, **2** or 3, that is, simple, double and triple coating

- Conductor pre-impregnated with varnish ($0.02 \leq t \leq 0.1$ mm) or half-lapped polyimide (Kapton®) tape ($0.1 \leq t \leq 0.2$ mm)
- Outer coil insulation: epoxy impregnated glass fibre tape

Cooling enhancement:

- Heat sink with enlarged radiation surface
- Forced air flow (cooling fan)

Only for magnets with limited strength (correctors, steering magnets....)

Water cooling

Direct water cooling:

- Current density typically up to $j = 10$ A/mm^2
- $j = 80$ A/mm^2 have been realized,
  but difficult and risky (single turn cooling)
- Rectangular or square copper (or aluminium) conductor with central cooling duct for demineralised water
- Inter-turn and ground insulation: one or more layers of half-lapped epoxy impregnated glass fibre tape
- Inter-turn insulation thickness: $0.3 \le t \le 1.0$ mm
- Ground insulation thickness: $0.5 \le t \le 3.0$ mm

Indirect water cooling:

- Current density $j \le 2$ A/mm^2
- Tap water can be used

Cooling water properties

Water properties:

- For the cooling of hollow conductor coils demineralised water is used (exception: indirect cooled coils)
- Water quality essential for the performance and the reliability of the coil (corrosion, erosion, short circuits)
- Resistivity > 0.1×10^6 Ωm
- pH between 6 and 6.5
- Dissolved oxygen below 0.1 ppm
- Filters to remove particles, loose deposits and grease to avoid cooling duct obstruction

Cooling parameters

Recommendations and canonical values:

- Water cooling: $2\ A/mm^2 \leq j \leq 10\ A/mm^2$
- Pressure drop: $0.1 \leq \Delta p \leq 1.0$ MPa (possible up to 2.0 MPa) 1 to 10 bar
- Low pressure drop might lead to more complex and expensive coil design
- Flow velocity should be high enough so flow is turbulent
- Flow velocity $u_{av} \leq 5$ m/s to avoid erosion and vibrations < 3 m/s as a target
- Acceptable temperature rise: $\Delta T \leq 30°C$ thermoswitch protection
- For advanced stability: $\Delta T \leq 15°C$

Assuming:

- Long, straight and smooth pipes without perturbations
- Turbulent flow = high Reynolds number
- Good heat transfer from conductor to cooling medium
- Temperature of inner conductor surface equal to coolant temperature
- Isothermal conductor cross section

Hydraulic parameters for cooling can be computed using different formulae

They assume all Joule heating is removed by the water

- No contribution from air convection

Several sets of formulae are reported next

- D. Tommasini --- more direct
- T. Zickler, from J. Tanabe --- need iterative solution
- both work in the turbulent regime

Friction Factors for Pipe Flow

By LEWIS F. MOODY,[1] PRINCETON, N. J.

The object of this paper is to furnish the engineer with a simple means of estimating the friction factors to be used in computing the loss of head in clean new pipes and in closed conduits running full with steady flow. The modern developments in the application of theoretical hydrodynamics to the fluid-friction problem are impressive and scattered through an extensive literature. This paper is not intended as a critical survey of this wide field. For a concise review, Professor Bakhmeteff's (1)[2] small book on the mechanics of fluid flow is an excellent reference. Prandtl and Tietjens (2) and Rouse (3) have also made notable contributions to the subject. The author does not claim to offer anything particularly new or original, his aim merely being to embody the now accepted conclusions in convenient form for engineering use.

IN the present pipe-flow study, the friction factor, denoted by f in the accompanying charts, is the coefficient in the Darcy formula

$$h_f = f \frac{L}{D} \frac{V^2}{2g}$$

with numerical constants for the case of perfectly smooth pipes or those in which the irregularities are small compared to the thickness of the laminar boundary layer, and for the case of rough pipes where the roughnesses protrude sufficiently to break up the laminar layer, and the flow becomes completely turbulent.

The analysis did not, however, cover the entire field but left a gap, namely, the transition zone between smooth and rough pipes, the region of incomplete turbulence. Attempts to fill this gap by the use of Nikuradse's results for artificial roughness produced by closely packed sand grains, were not adequate, since the results were clearly at variance from actual experience for ordinary surfaces encountered in practice. Nikuradse's curves showed a sharp drop followed by a peculiar reverse curve,[3] not observed with commercial surfaces, and nowhere suggested by the Pigott chart based on many tests.

Recently Colebrook (11), in collaboration with C. M. White, developed a function which gives a practical form of transition curve to bridge the gap. This function agrees with the two extremes of roughness and gives values in very satisfactory agreement with actual measurements on most forms of commercial piping and usual pipe surfaces. Rouse (12) has shown that it is a reasonable and practically adequate solution and has plotted a chart based upon it. In order to simplify the plotting, Rouse

The spreadsheet below is an example of cooling computations

INPUTS						
A_cable	[mm^2]	49	conductor dimensions (overall)		CONSTANTS	
d_hole	[mm]	3.7	cooling hole diameter			
r_fillet	[mm]	1	conductor round fillet		density of water	
L	[mm]	32860	length of the circuit		T	ρ
T_inlet	[°C]	24	water inlet temperature		[°C]	[km/m^3]
		Cu	material (Cu or Al)		4	1000.0
I	[A]	235	current		10	999.7
P	[kW]	0.851	power to be dissipated		15	999.1
ε	[mm]	1.50E-03	surface roughness		20	998.2
ΔT	[°C]	10	temperature rise		22	997.8
					25	997.0
COMPUTED QUANTITIES					30	995.7
T_ave	[°C]	29	average temperature		40	992.2
A_curr	[mm^2]	37.4	Cu area per conductor		60	983.2
m_cable	[kg]	11.0	mass of the conductor		80	971.8
ρ	[Ohm*m]	1.75E-08	resistivity			
R	[mOhm]	15.35	resistance		kinematic viscosity	
P	[kW]	0.851	R*I^2		T	ν
j	[A/mm^2]	6.3	current density		[°C]	[m^2/s]
ρ	[km/m^3]	996	water mass density		15.4	1.13E-06
ν	[m^2/s]	8.21E-07	kinematic viscosity		21.0	9.85E-07
cp	[kJ/(kg*K)]	4.179	specific heat capacity		26.6	8.64E-07
					32.1	7.66E-07
OUTPUT (Colebrook)					37.7	6.87E-07
Δp	[bar]	5.24	pressure drop			
v	[m/s]	1.90	cooling water speed		specific heat capacity	
Re	[/]	8568	Reynolds number		T	cp
q	[L/min]	1.227	cooling water flow		[°C]	[kJ/(kg K)]
					10	4.192
OUTPUT (Blasius)					20	4.182
Δp	[bar]	5.26	pressure drop		30	4.178
v	[m/s]	1.90	cooling water speed		40	4.179
Re	[/]	8568	Reynolds number		50	4.181
q	[L/min]	1.227	cooling water flow		60	4.184
					70	4.190
OUTPUT (Davide)						
Δp	[bar]	5.56	pressure drop			
v	[m/s]	1.89	cooling water speed			
Re	[/]	9771	Reynolds number			
q	[L/min]	1.217	cooling water flow			

Formulae for coil cooling computations

Notation

p	[Pa]	pressure drop	ν	[m²/s]	kinematic viscosity
f	[/]	friction coefficient	ε	[m]	surface roughness
l	[m]	length	q	[m³/s]	volume flow rate
d	[m]	hole diameter	ΔT	[°C]	temperature increase
ρ	[kg/m³]	mass density	P	[W]	extracted power
v	[m/s]	velocity	c_p	[kJ/(kg K)]	specific heat capacity

Darcy equation

$$\Delta p = f \frac{l}{d} \frac{\rho v^2}{2}$$

Reynolds number

$$Re = \frac{vd}{\nu}$$

Colebrook formula

$$\frac{1}{\sqrt{f}} = -2\log_{10}\left(\frac{\varepsilon}{3.7d} + \frac{2.51}{Re\sqrt{f}}\right)$$

The first part is a Nikuradse term whereas the second one is of the Prandtl-v.Karman form.

$$\Delta p \;\Rightarrow\; k_v = \sqrt{\frac{2}{\rho}\frac{d}{l}\Delta p} \;\Rightarrow\; f = \left[-2\log_{10}\left(\frac{\varepsilon}{3.7d} + \frac{2.51}{\frac{d}{\nu}\sqrt{k_v}}\right)\right]^{-1/2} \;\Rightarrow\; v = \frac{k_v}{\sqrt{f}}$$

Blasius formula

$$f = \frac{0.3164}{\sqrt[4]{Re}}$$

$$\Delta p \;\Rightarrow\; v = \left[\frac{d^{1.25}\Delta p}{0.1582\nu^{0.25} l \rho}\right]^{1/1.75}$$

Volume flow rate

$$q = v\frac{\pi d^2}{4}$$

Temperature increase

$$\Delta T = \frac{P}{c_p \rho q}$$

These are "Davide's" formulae for the main cooling parameters of a water-cooled resistive magnet

cooling flow $$Q_{tot} \cong 14.3\frac{P}{\Delta T} \qquad Q_{tot} \cong N_{hydr}Q$$

water velocity $$v = \frac{1000}{15\pi d^2}Q$$

Reynolds number $$Re \cong 1400dv$$

pressure drop $$\Delta p = 60L_{hydr}\frac{Q^{1.75}}{d^{4.75}}$$

derived from Blasius' formula for the friction coefficient

Cooling parameters

Pressure drop through a water circuit: $\Delta p = f \frac{l}{d} \frac{\delta u_{av}^2}{2}$ (16)

Darcy equation

- *p:* pressure [Pa, N/m^2]
- *f*: friction factor [.]
- *l,d*: cooling circuit length and diameter [m]
- δ: coolant mass density [kg/m^3] (for water: 1000 kg/m^3 = 1 kg/liter)
- u_{avg}: average coolant velocity [m/s]

Friction factor *f* depends on the Reynols number *Re* $\mathrm{Re} = \frac{u_{avg} d}{\nu}$ (17)

Laminar flow: *Re*< 2000 and *f*=64/*Re*

- *ν:* kinematic viscosity of coolant is temperature depending, for simplification it is assumed to be constant ($9.85 \cdot 10^{-7}$ m^2/s @ 21°C for water)

Turbulent flow: Re > 4000 and f is transcendental:

$$\frac{1}{\sqrt{f}} = -2\log_{10}\left(\frac{\varepsilon}{3.7d} + \frac{2.51}{\mathrm{Re}\sqrt{f}}\right) \quad (18)$$

Colebrook formula (Nikuradse + Prandtl-v.Karman)

- *ε:* roughness of cooling channels (~$1.5 \cdot 10^{-3}$ mm)

Cooling parameters

Velocity and friction factor using $Re(u_{avg}) \rightarrow u_{avg}$ to be solved iteratively:

$$u_{avg} = \sqrt{\frac{2\Delta p}{\delta f}\frac{d}{l}} \qquad (19)$$

$$\mathrm{Re} = \frac{d}{\nu}\sqrt{\frac{2\Delta p}{\delta f}\frac{d}{l}} \qquad (20)$$

Substituting *Re* in (18) with (20) leads to:

$$u_{avg} = -2\sqrt{\frac{2\Delta p}{\delta}\frac{d}{l}}\log_{10}\left(\frac{\varepsilon}{3.7d} + \frac{2.51}{\frac{d}{\nu}\sqrt{\frac{2\Delta p}{\delta}\frac{d}{l}}}\right) \qquad (21)$$

Simplified approach using water as cooling fluid:

$$u_{avg} \approx 0.3926 \cdot d^{0.714}\left(\frac{\Delta p}{l}\right)^{0.571} \qquad (22^*)$$

Cooling parameters

Heat absorbed by coolant medium across a heated surface:

$$P = \dot{m} c_p \Delta T \qquad \dot{m} = \delta Q$$

Technically, the power P is a function of the ΔT, as the resistance changes with T

- c_p: heat capacity [W s/kg °C] (4.19 kW s/kg °C for water)
- Q: flow rate [liter/s]
- P: power [W]
- ΔT: temperature increase [°C]

energy balance

Flow *Q* necessary to remove heat *P*: $Q = \frac{P}{\delta c_p \Delta T} \qquad Q_{water} = 0.2388 \frac{P}{\Delta T}$ (22)

Coolant flow inside a round tube with a bore diameter *d*: $Q = u_{av} \frac{\pi d^2}{4} 10^3$ (23)

Temperature increase using water as cooling fluid: $\Delta T = 0.304 \frac{P}{u_{avg} d^2} \cdot 10^{-6}$ (24)

Cooling parameters

Number of cooling circuits per coil: $\Delta p \propto \frac{1}{K_W^3}$

→ Doubling the number of cooling circuits reduces the pressure drop by a factor of eight for a constant flow

Diameter of cooling channel: $\Delta p \propto \frac{1}{d^5}$

→ Increasing the cooling channel by a small factor can reduce the required pressure drop significantly

Cooling circuit design

Already determined: current density *j*, power *P*, current *I*, # of turns *N*

1. Select # of layers *m* and # of turns per layer *n*
2. Round up *N* if necessary to get reasonable m and n
3. Define coil height *c* and coil width *b*: $A = bc = \frac{NI}{j f_c}$ (Aspect ratio *c* : *b* between 1 : 1 and 1 : 1.7 and $0.6 \leq f_c \leq 0.8$)
4. Calculate l_{avg}= pole perimeter + 8 x clearance + 4 x coil width
5. Start with single cooling circuit per coil: $l = \frac{K_c N l_{avg}}{K_w}$ (25)
6. Select ΔT, Δp and calculate cooling hole diameter *d*: $d = 5.59 \cdot 10^{-3} \left(\frac{P}{\Delta T\, K_w} \right)^{0.368} \left(\frac{l}{\Delta p} \right)^{0.21}$ (26*)
7. Change Δp or number of cooling circuits, if necessary
8. Determine conductor area a: $a = \frac{I}{j} + \frac{d^2 \pi}{4} + r_{edge}(4 - \pi)$ (27)
9. Select conductor dimensions and insulation thickness
10. Verify if resulting coil dimensions, N, I, V, ΔT are still compatible with the initial requirements (if not, start new iteration)
11. Compute coolant velocity and coolant flow using (21) and (22)
12. Verify if Reynolds number is inside turbulent range (Re > 4000) using (17)

Basic principles : force

On a conductor immerged in magnetic field

$$\mathbf{F} = \mathrm{I}\cdot \boldsymbol{L} \times \mathbf{B}$$

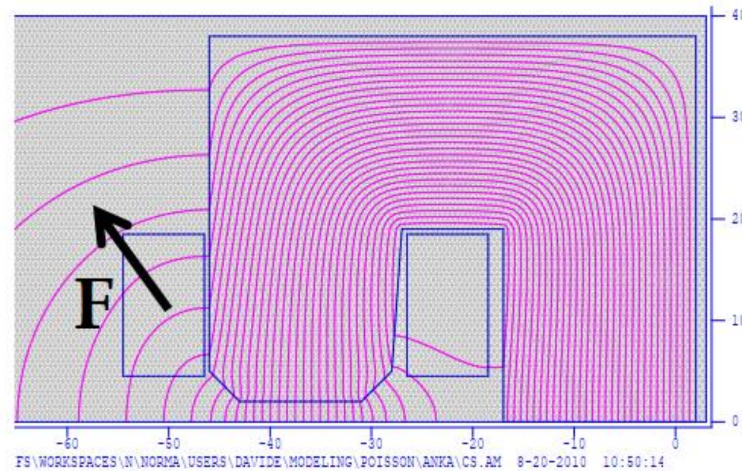

Example for the Anka dipole:
On a the external coil side with N=40 turns, I= 700A, L~2.2 m
in an average field of B= 0.25 T

$$F = 40 \cdot 700 \cdot 2.2 \cdot 0.25 = 15400\ \mathrm{N} \sim 1.5\ \mathrm{tons}_f$$

Proper shimming of the coils is important – it also called for dedicated campaigns in CERN magnets

Pole face windings are sometimes (now more rarely) used to correct / shape the magnetic field

PS main units

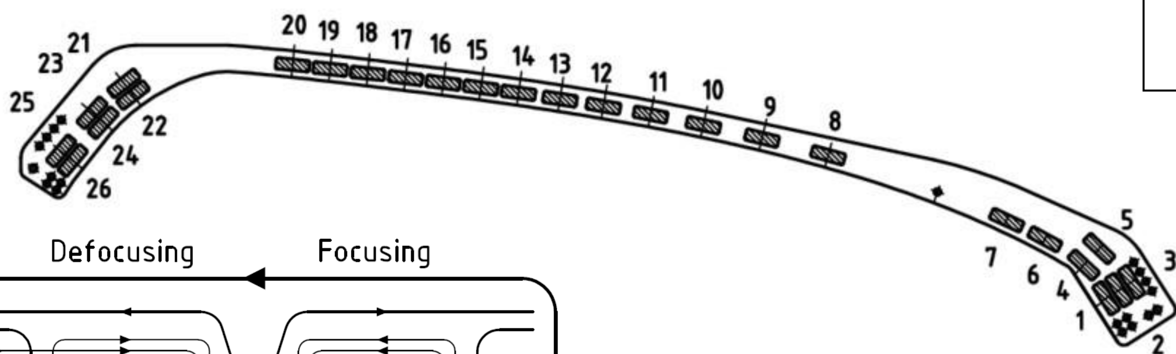

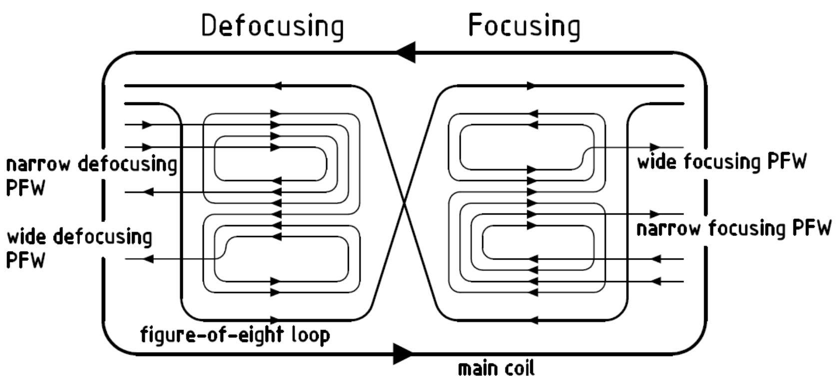

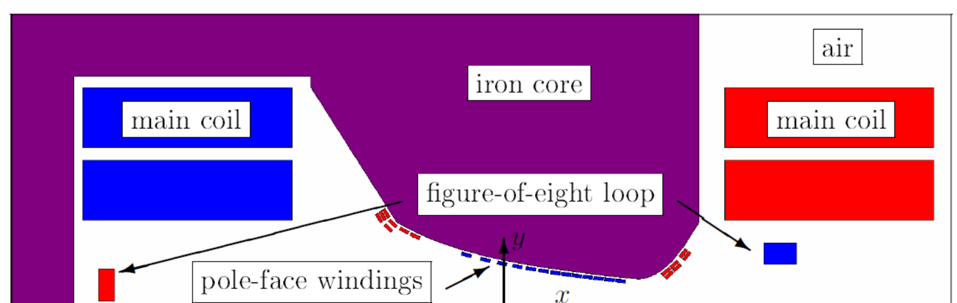

Conclusions (coil design)

Ampere-turns can be computed analytically with very good approximation

- Power law scaling with order of the magnet

Several coil geometries are possible

- Again, no unique solution

Typically, either copper (in most cases) or aluminum is used

Resistive power, as Joule heating, is dissipated either by forced flow of demineralized water, or by air convection

- The main parameter is the current density in the conductor

Lorentz forces on the conductor shall be checked

- Proper shimming is important, even more for cycled operation

Gallery of cross-sections

see separate file

Fabrication (hints)

In many cases, the fabrication is subcontracted to (specialized) companies – below are examples of technical specifications

ORGANISATION EUROPÉENNE POUR LA RECHERCHE NUCLÉAIRE
CERN EUROPEAN ORGANIZATION FOR NUCLEAR RESEARCH

CERN EDMS N° 1279694 IT-3941/TE/SESAME
TE Department / SESAME Project

Invitation to Tender

Technical Specification

SESAME Storage Ring
Combined Function Dipole Magnets

This technical specification concerns the supply of 17 combined function dipole electromagnets (including pre-series) and a set of spare coils for the storage ring of the SESAME synchrotron. The cores of the magnets are laminated steel yokes; the coils are water cooled, wound from hollow copper conductor, and epoxy impregnated. Their mass is approximately 6.5 tonnes. Delivery shall be completed within 24 months after placement of the contract.

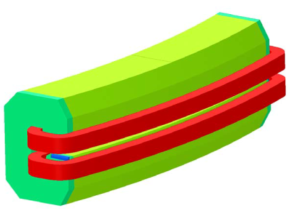

June 2013

EDMS 1279694

ORGANISATION EUROPÉENNE POUR LA RECHERCHE NUCLÉAIRE
CERN EUROPEAN ORGANIZATION FOR NUCLEAR RESEARCH

CERN EDMS N° 1257262 IT-3940/TE/SESAME
TE Department / SESAME Project

Invitation to Tender

Technical Specification

SESAME Storage Ring
Quadrupole Magnets

This technical specification concerns the supply of 33 focusing and 33 defocusing quadrupole electromagnets (including pre-series) for the storage ring of the SESAME synchrotron. The cores of the magnets are laminated steel yokes; the coils are water cooled, wound from hollow copper conductor, and epoxy impregnated. Their mass is approximately 400 / 150 kg. Delivery shall be completed within 20 months after placement of the contract.

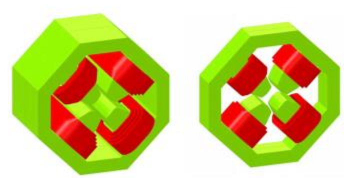

June 2013

EDMS 1257262

ORGANISATION EUROPÉENNE POUR LA RECHERCHE NUCLÉAIRE
CERN EUROPEAN ORGANIZATION FOR NUCLEAR RESEARCH

CERN EDMS N° 1279686 TE Department / SESAME Project

Price Enquiry

Technical Specification

Coils for the
SESAME Storage Ring
Quadrupole Magnets

This technical specification concerns the supply of 140 coils for the focusing quadrupole and 140 coils for the defocusing quadrupole electromagnets for the SESAME storage ring. These coils are water cooled, wound from hollow copper conductor and epoxy impregnated under vacuum. Their mass is approximately 18 / 6 kg. Delivery shall be completed within 14 months after signing the contract.

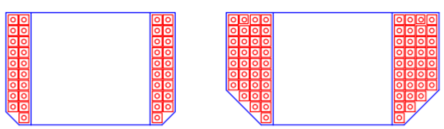

June 2013

EDMS 1279686

Manufacture : coils


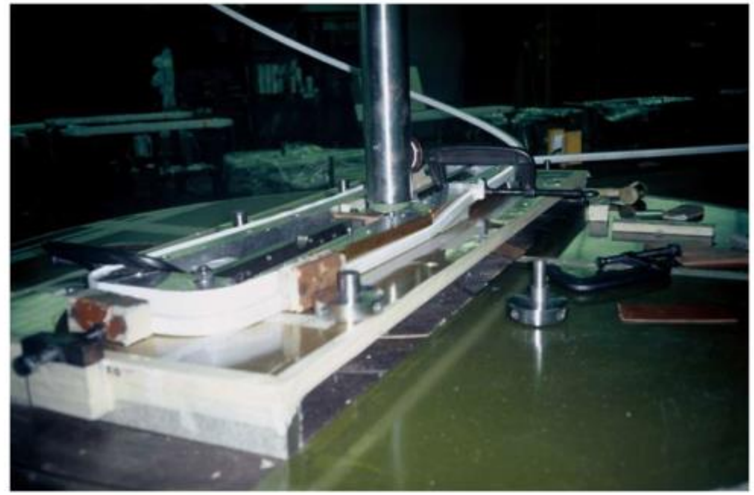

Manufacture : yoke

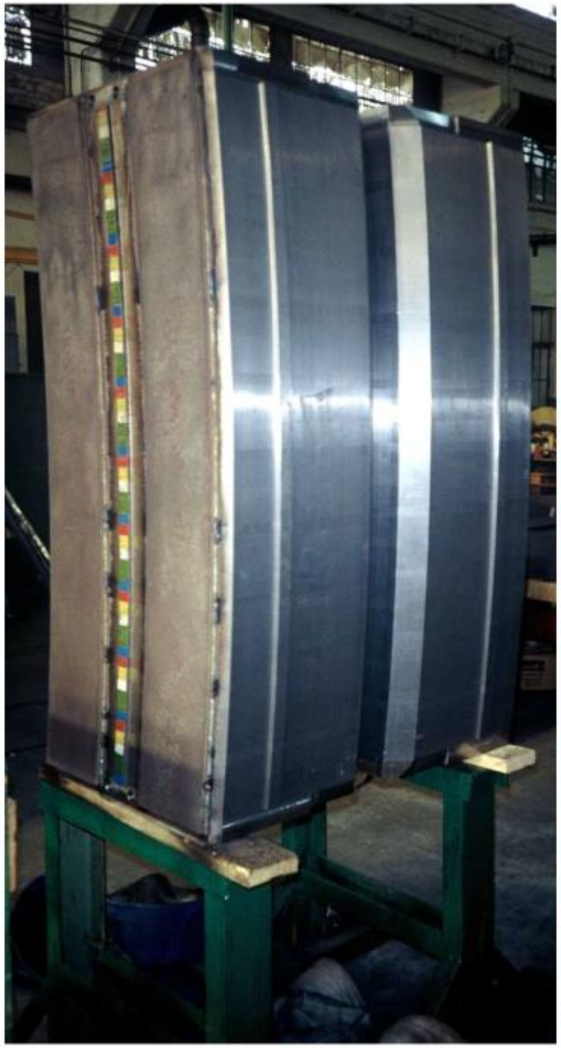

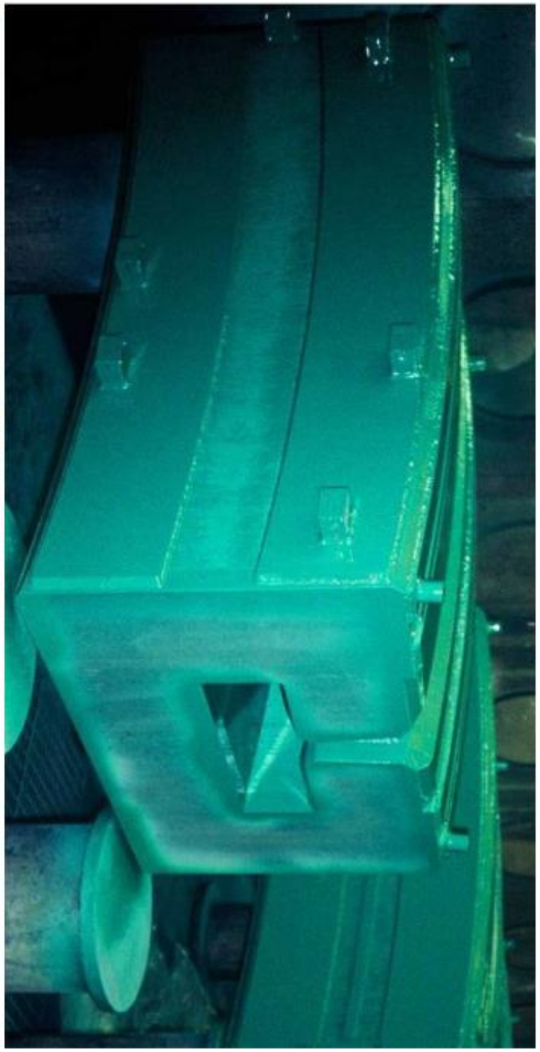

Manufacture : yoke

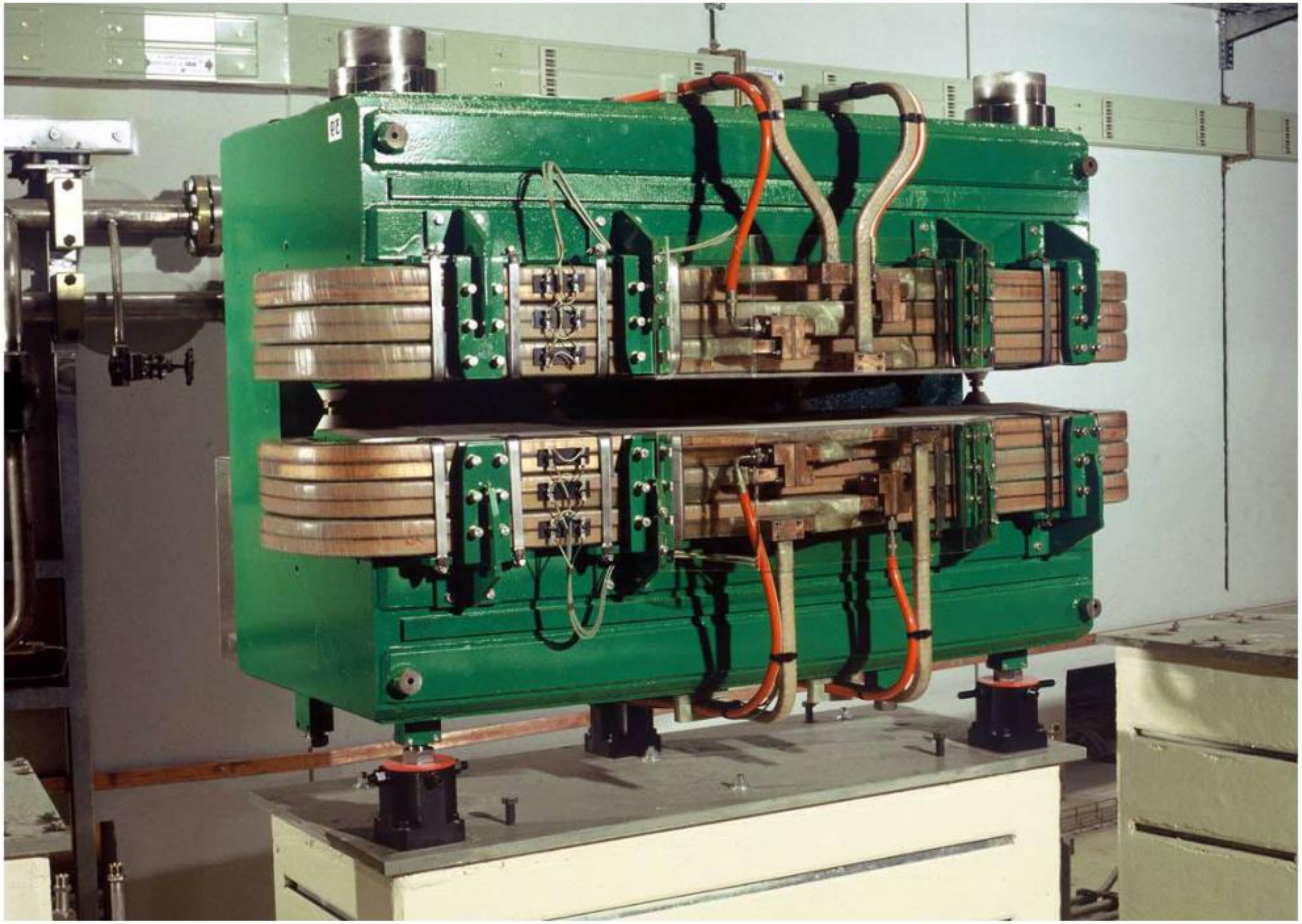

Corrector dipole North Experimental area

Magnet with solid yoke parts assembled with bolts.

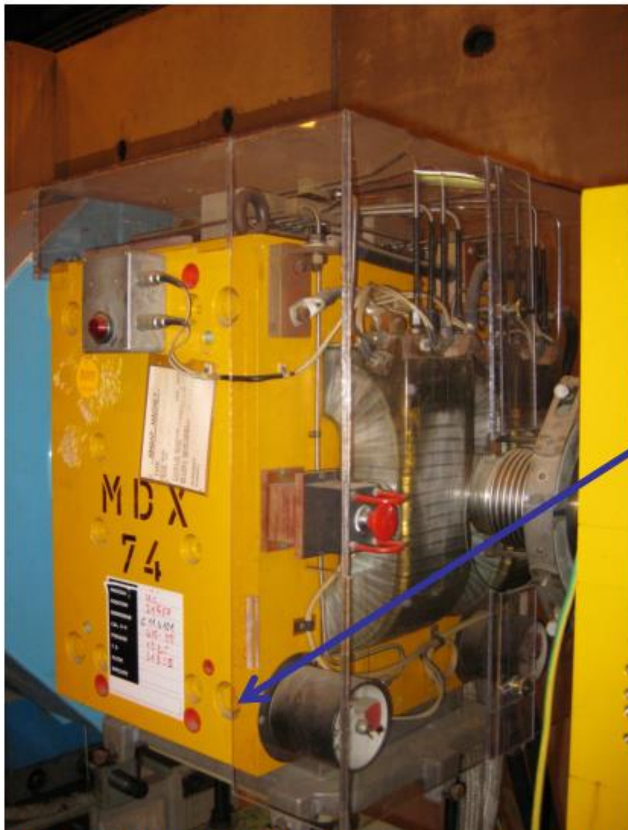

Main parameters	
Name	MDX
Type	Vertical correcting dipole
Installation	SPS experimental area
Nominal peak field [T]	1.33
I_{max} [A]	240
Résistance [Ω]	0. 305
Inductance [H]	0. 221
Yoke lenght [mm]	400
Gap [mm]	80
Total weight [kg]	1000

Corrector dipole in TI2 and TI8 LHC injection lines

Magnet with glued laminated yokes assembled with bolts.

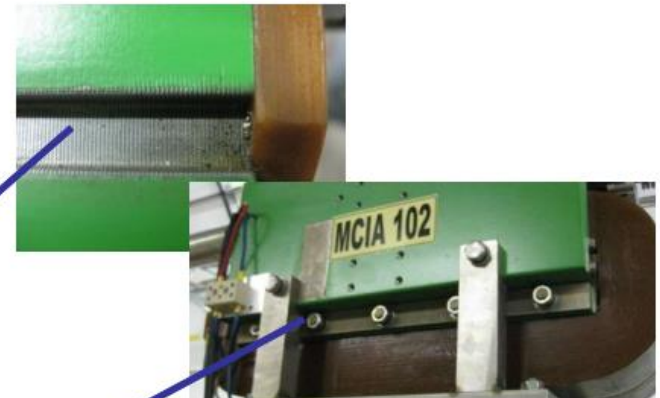

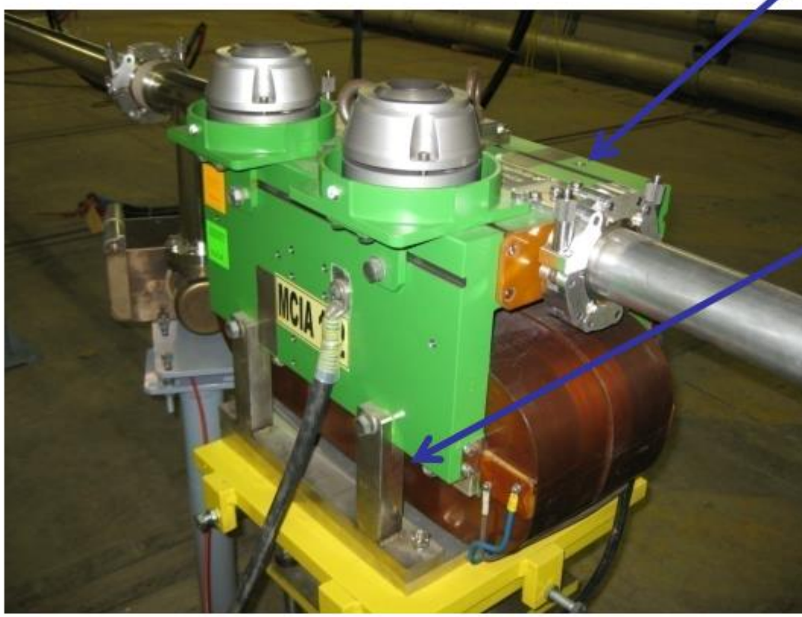

Main parameters	
Name	MCIA V
Type	Vertical correcting dipole
Nominal peak field [T]	0.26
I_{max} [A]	3.5
N. Of turns	1014
Résistance [Ω]	13.9
Yoke lenght [mm]	450
Gap [mm]	32.5
Total weight [kg]	300

Corrector dipole for E-Cloud experiment in SPS

Magnet with laminations welded in a steel envelope
half-yokes assembled with bolts.

Main parameters	
Name	MDVW
Type	Vertical correcting dipole
Nominal peak field [T]	0.266
I_{max} [A]	55
N. Of turns	2 x 50
Résistance [Ω]	1.76
Inductance [H]	1.12
Yoke lenght [mm]	429
Gap [mm]	200
Total weight [kg]	1100

Acceptance tests

Acceptance tests: ex. from CERN standard template

Water Cooled Magnet Certification Report

Template EDMS Document 1103493

EDMS Document number: ____
To be filled by the QA

MTF identifier	
Another identifier	
Manufacturer	
Construction year	
Requested by	

Previous certification?	☐ No	
	☐ Yes	EDMS Document ____

To be filled by the magnet responsible

FINAL RESULT

☐ Certified Good
☐ Certified Fair
☐ To be Refurbished
☐ Discontinued

Non-conformities?	☐ No	
	☐ Yes	EDMS Document ____

If yes, provide nonconformity report — *To be filled by the QA*

	Name	Date
Operator		
Workshop / certifications responsible		
Technical responsible		
QA responsible		

1 – GENERAL INFORMATION

Yokes identifiers	Coils identifiers

To be filled in order accordingly to the Polarity convention for normal conducting magnets (EDMS 1105981)

Presence of a vacuum chamber	☐ No
	☐ Yes, picture:
Interlock circuit	☐ WIC Number of channels:
	☐ Other

Interlock circuit details

Box picture: ____
Connector picture: ____

Electrical power connection	Picture:
	Dimensions of holes or terminal block:
Hydraulic circuit	Connecter type:
	Connecter picture:
	Circuit grounded? ☐ Yes ☐ No
IP2X protective covers	☐ Yes, picture:
	☐ No
Magnet weight	

Acceptance tests: ex. from CERN standard template

2 – VISUAL INSPECTION

General state (impacts, oxidation presence, etc.)
Coils state (insulation, conductor, etc.)
Interlock circuit, etc.

Indicate the name of the pictures if necessary

3 – HYDRAULIC TESTS

50 bar

Static pressure	Test pressure =	bar
	Duration =	minute
No leakage and maintained pressure for the duration of the test		☐ Ok

Flow measurement	Nominal pressure ΔP =	bar
	Nominal flow =	l/min
at 2xΔP or maximum ΔP	ΔP =	Flow =
at nominal ΔP	ΔP =	Flow =
at ΔP/2	ΔP =	Flow =

4 – ELECTRICAL TESTS

⚠ **Before starting the electrical tests**
Make sure the **yoke is grounded**
and that the hydraulic system is properly **flushed and bled**

Interlock dielectric test	Test voltage = 0.5 kV	Duration = 1 min
⚠ During the test, connect the magnet coil(s) to the ground		
Interlock circuit details	Insulation resistance R =	Leakage current Ic =
Thermo-switches		

5 kV dc

Coils insulation	Test voltage = kV	Duration = min
⚠ During the test, connect the magnet interlock circuit to ground		
Insulation resistance	R =	
Leakage current	Ic =	

Capacitive discharge	Test voltage(s)	
Magnet = kV	Half-magnet = kV	Coil(s) = kV

Name of the curves saved in TXT and PNG format	
☐ Magnet:	☐ Coil 5:
☐ Half-magnet 1:	☐ Coil 6:
☐ Half-magnet 2:	☐ Coil 7:
☐ Coil 1:	☐ Coil 8:
☐ Coil 2:	☐ Coil 9:
☐ Coil 3:	☐ Coil 10:
☐ Coil 4:	☐ Other:

Inductance measurement	Nominal inductance =	
	Nominal frequency =	Hz
at 1Hz =	at 20Hz =	at 100Hz =

Resistance measurement at I = 1 A	Nominal resistance =
$R_{20} = R / (1+0.004x(T-20))$	Measured room temperature = °C
	Measured resistance =
Corrected resistance at 20°C:	R_{20} =

Acceptance tests: ex. from CERN standard template

5 – POWER TESTS

Thermo-switches trigger test

Power the magnet at I = A, until the temperature is stabilized, then

reduce the flow rate until the 1st trigger	Q (l/min) =
and/or increase the current	I (A) =
Thermo-switch type	

TS	Details	Nominal temperature (˚C)	Trigger temperature (˚C)
1			
2			
3			
4			
5			
6			
7			
8			
9			
10			
11			
12			
13			
14			
15			
16			
17			
18			
19			
20			
21			
22			
23			
24			

Maximum temperature recorded by the thermal camera, when the last thermos-switch has triggered	˚C Picture:
All thermo-switches closed after cool down	☐ Ok
Interlock circuit continuity test after disconnected	☐ Ok

Page 5 of 8

Trigger test of the interlock system
WITHOUT WATER

Perform test? ☐ Yes ☐ No

- **MANDATORY** supervision of a CERN STAFF for the entire duration of the test
- Do not exceed 80°C on the coils

Name of the person supervising the test:

Stop the water flow, then

power the magnet at I = A, or A/mm²

Converter stop

thermo-switch triggering	Or	Manually (Temperature too high without trigger)
☐ Ok		☐ Ok

Maximum temperature reached =	˚C Picture:

At the end of the test, let the magnet cool down WITHOUT CIRCULATING WATER

DC Power test

Before starting the test
connect the interlock system straight to the converter

Applied current I = A ΔP = bar

Coils temperature stabilization at	˚C
Water inlet temperature	˚C
Water outlet temperature	˚C
☐ Temperature curve:	

Thermal pictures:

- Indicate the magnet orientation with an arrow - Indicate the power connections A and B - Check the polarity accordingly to the convention EDMS 1105981	☐ Ok

Page 6 of 8

Acceptance tests: ex. from CERN standard template

Pulsed Power test			
⚠ Before starting the test connect the interlock system directly to the converter			
Applied current I =	A	ΔP =	bar
Duration ON =	s		
Duration OFF =	s		
Valid coils shimming	☐ Ok		

⚠

- At the end of the certification tests, check the **continuity** and the **insulation/ground at 0.5 kV for 1 min** of the interlock circuit.
- Make sure the hydraulic system is properly bled.

Checks performed	☐ Ok

6 – COMMENTS

7 – DOCUMENTS COMPILATION

The documents requested into the first table below ***must be provided***

☐	Picture(s) of the magnet without covers:	
☐	Picture(s) of the magnet opening:	
☐	Picture of the interlock box	
☐	Picture of the interlock connector	
☐	Picture of the power connections	
☐	Picture of the hydraulic connections	
☐	Capacitive discharge files	
☐	Thermal pictures from DC power test	
☐	Thermal pictures from trigger test	
☐	Trigger file and DC power	

☐	Picture of the vacuum chamber
☐	Visual inspection picture(s)
☐	Picture of the magnet with protective covers
☐	Other pictures and files:

Acceptance tests: ex. mechanical checks (extract)

MQDSE #12

2 – YOKE CONTROL MEASUREMENTS OPPOSITE QUADRANTS (DIAMETERS)

Nominal value 70.00 mm					
[mm]	Distance from hydraulic connection side [mm]				Average
	15	40	60	85	
d_{13}	70.048	70.042	70.035	70.008	70.033
d_{24}	70.011	70.04	70.04	70.05	70.035

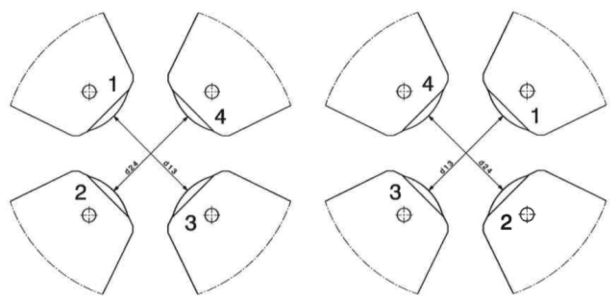

Hydraulic connections side — Non-connection side

[mm]	measured	target	
max – avg	0.001	≤ 0.05	☒ Ok
avg – min	0.001	≤ 0.05	☒ Ok
Measured with	☐ Vertical measuring column ___ ☐ Mechanical dial gauge ___ ☐ Electronic dial gauge ___ ☐ Measuring arm ___ ☐ Other		

page 3 / 8

MQDSE #12

3 – YOKE CONTROL MEASUREMENTS ADJACENT QUADRANTS

Nominal value 23.568 mm					
[mm]	Distance from hydraulic connection side [mm]				Average
	15	40	60	85	
d_{12}	-0,015	0	+0,02	+0,03	23,577
d_{23}	+0,02	-0,01	+0,01	+0,01	23,576
d_{34}	-0,02	-0,01	0	0	23,561
d_{41}	0	-0,01	-0,04	-0,03	23,548

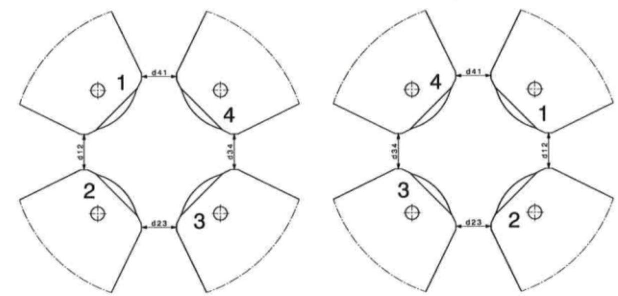

Hydraulic connections side — Non-connection side

[mm]	measured	target	
max – avg	0,012	≤ 0.03	☒ Ok
avg – min	0,017	≤ 0.03	☒ Ok
Measured with	☐ Vertical measuring column ___ ☐ Mechanical dial gauge ___ ☐ Electronic dial gauge ___ ☐ Measuring arm ___ ☐ Other		

page 4 / 8

Thank you

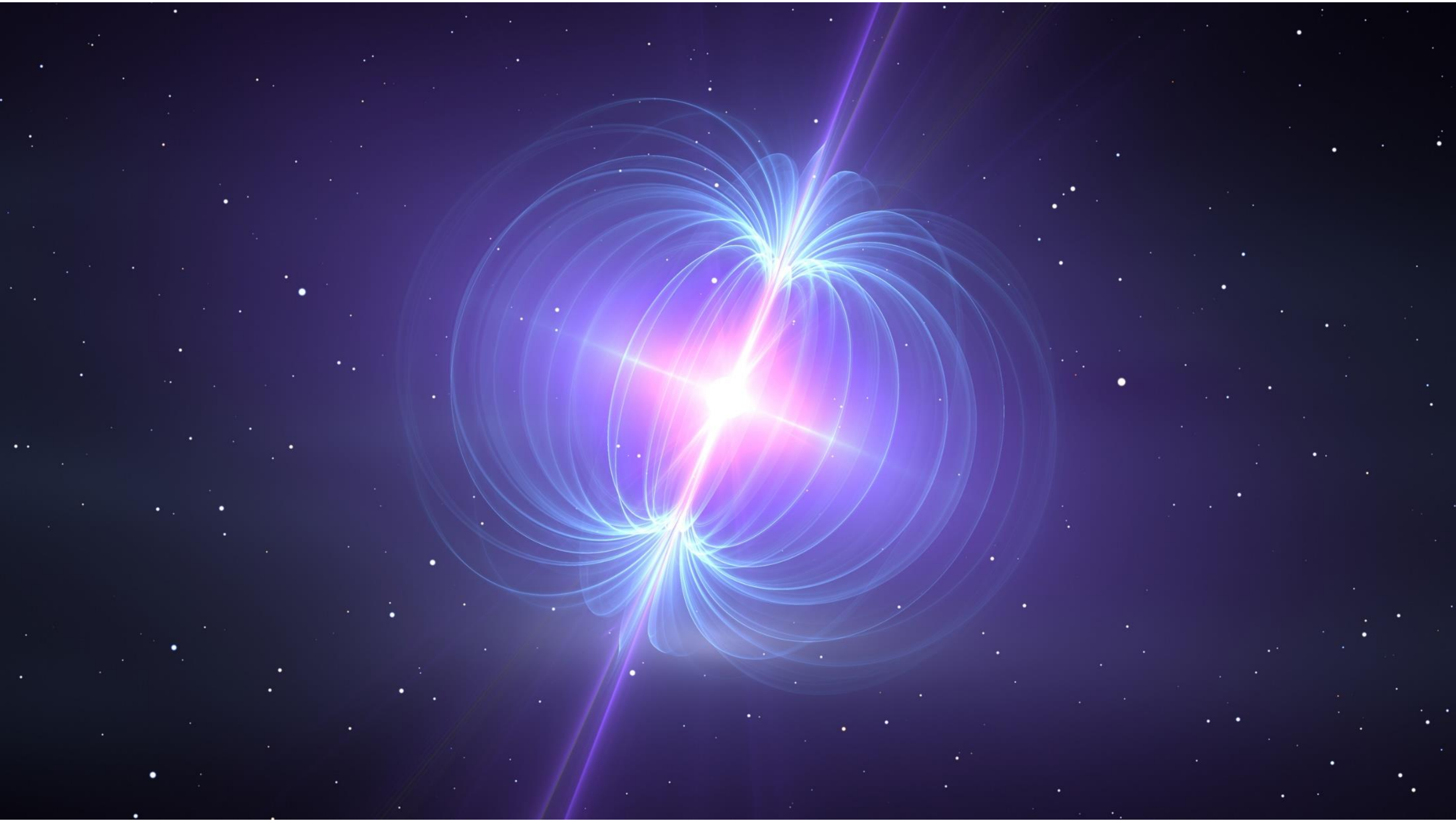

Bonus

LINAC4 solenoids

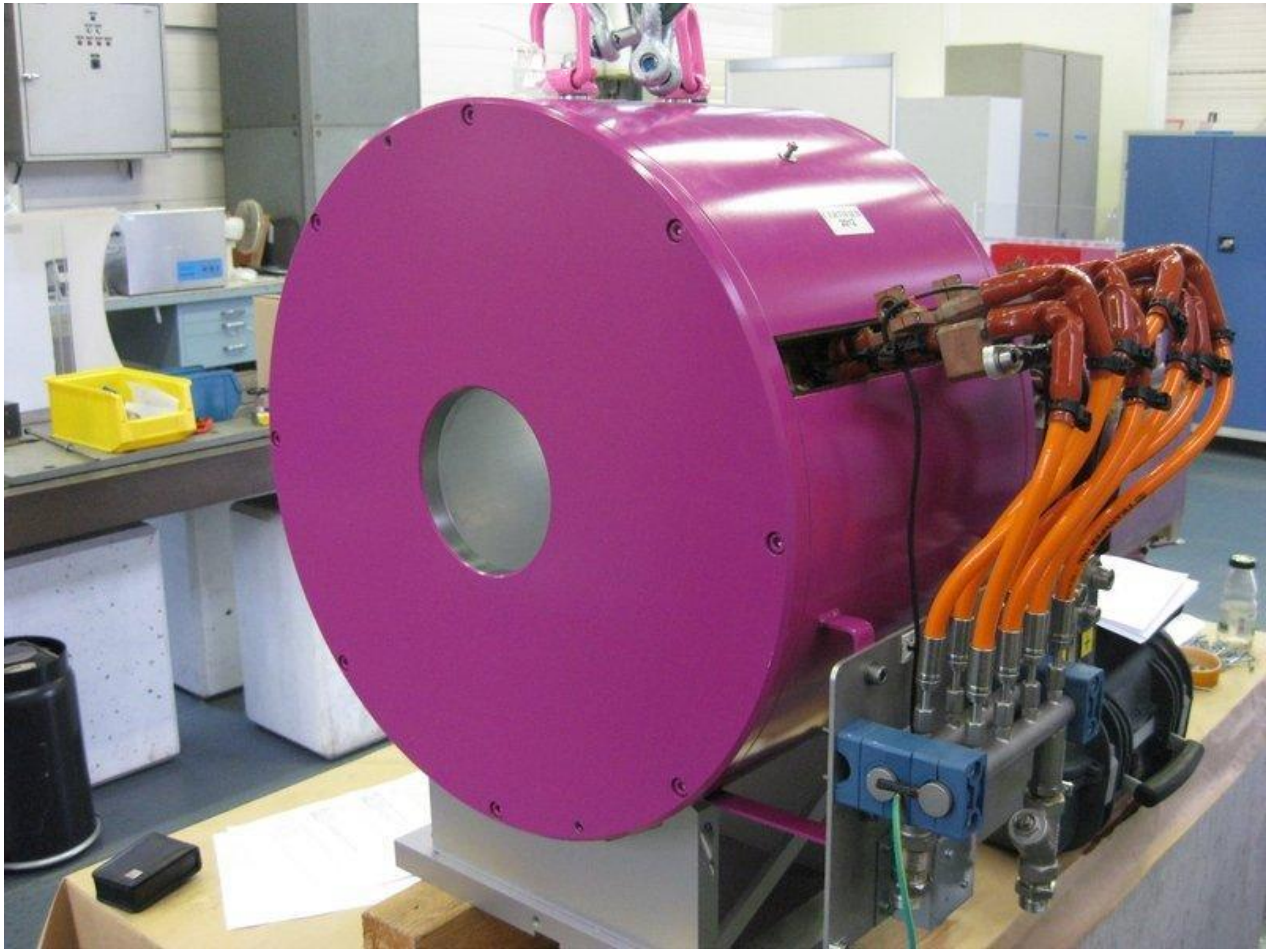

0.26 T, 122 A
aperture diameter 140 mm

Experimental magnets: ALICE dipole

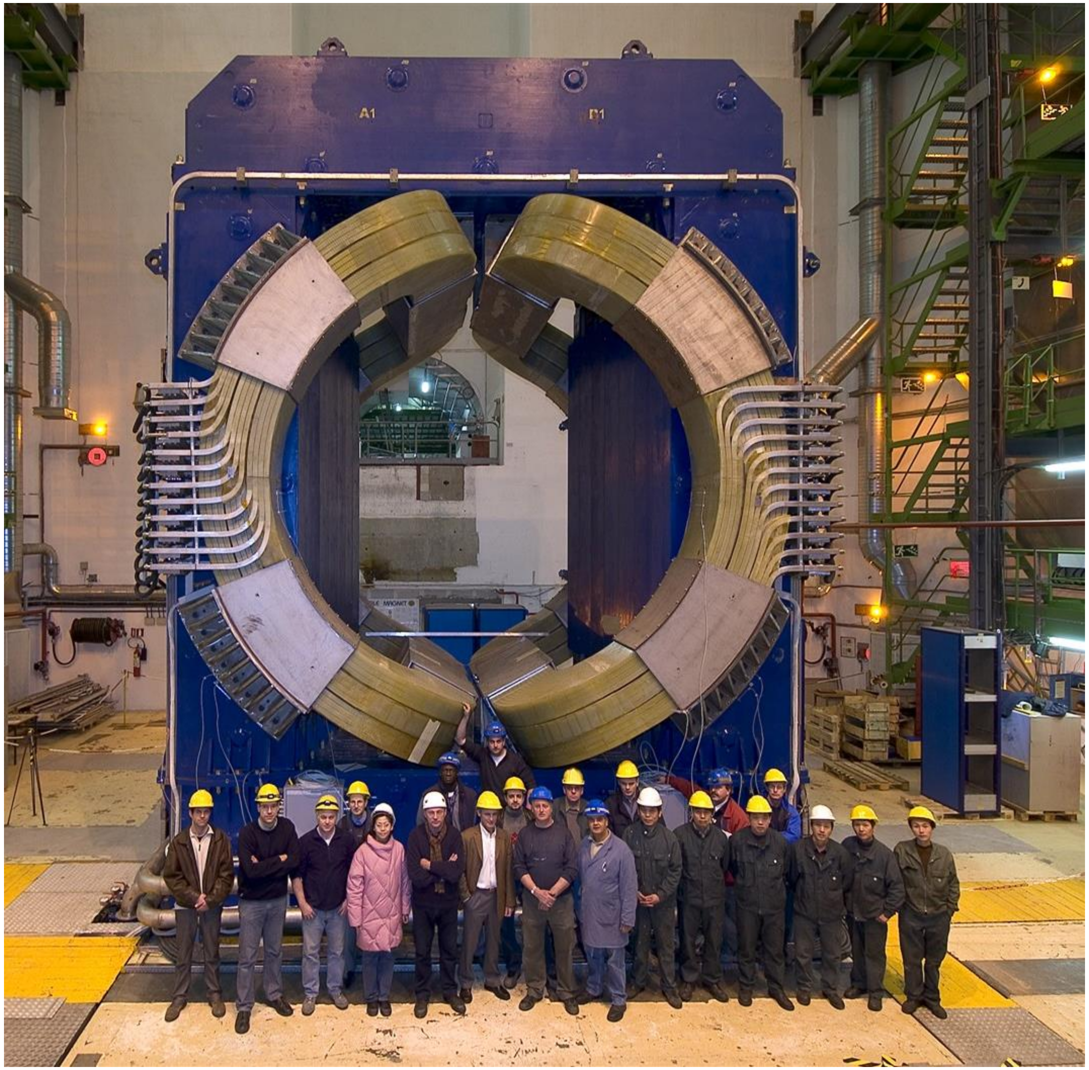

Experimental magnets: the Open Axial Field Magnet, ISR

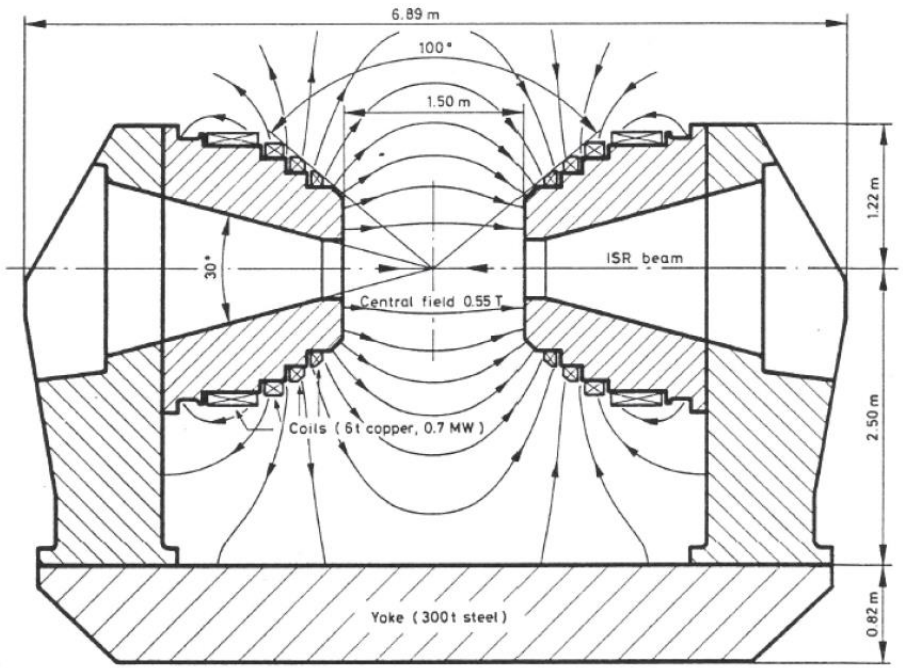

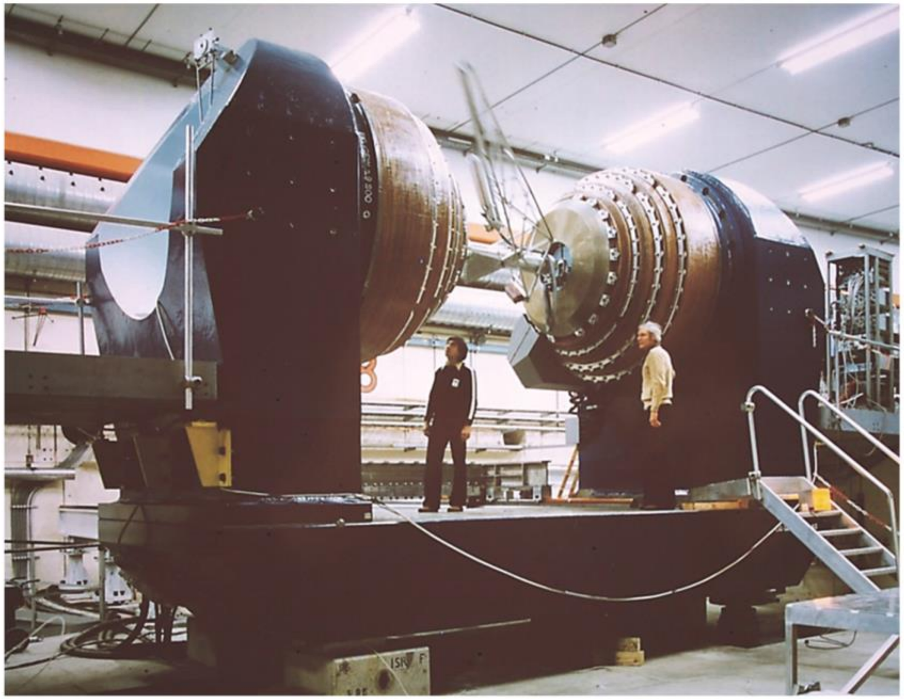

Experimental magnets: toroid for NA10

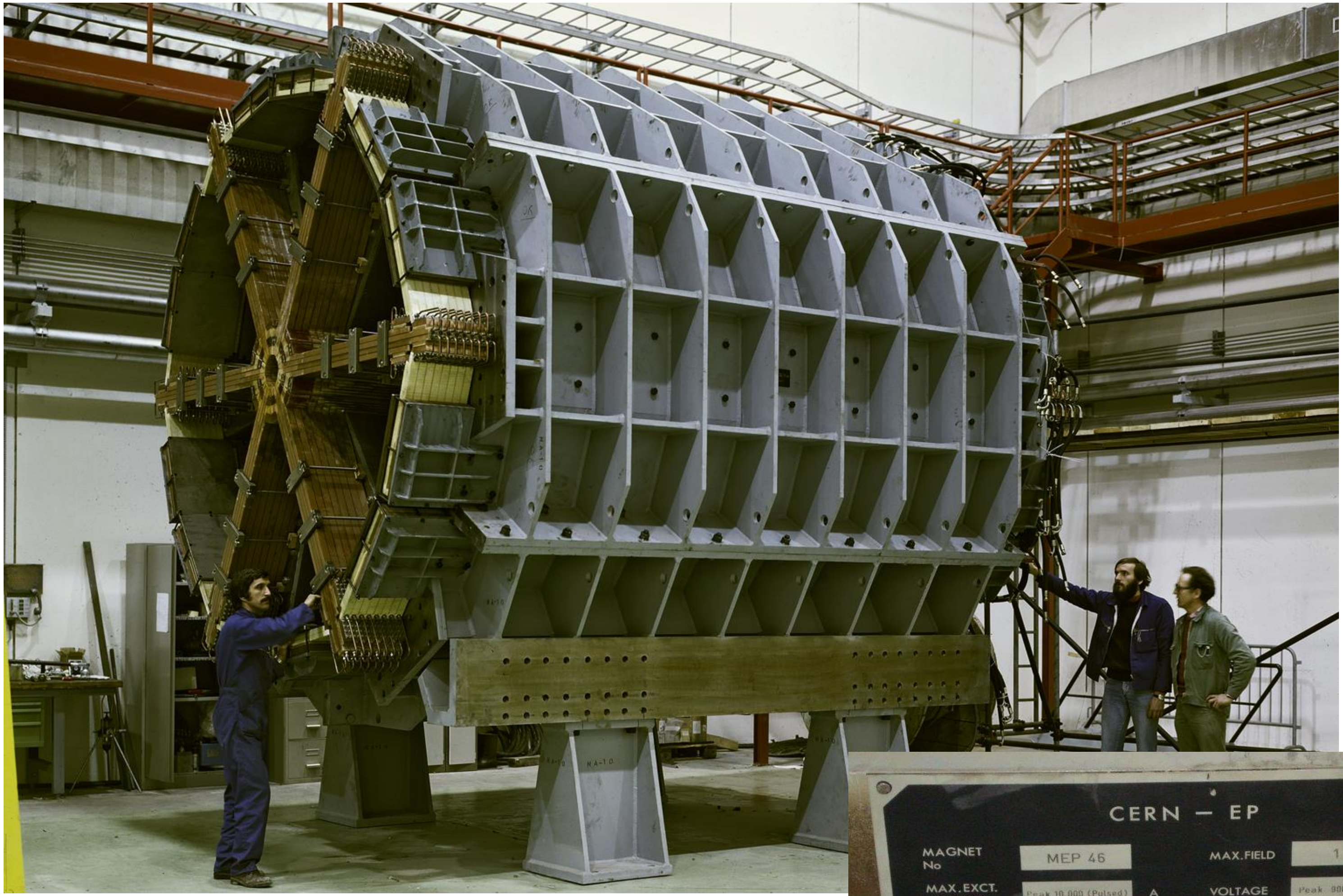

Main magnets in synchrotrons before strong focussing: Cosmotron (1953) and SATURNE (1956)

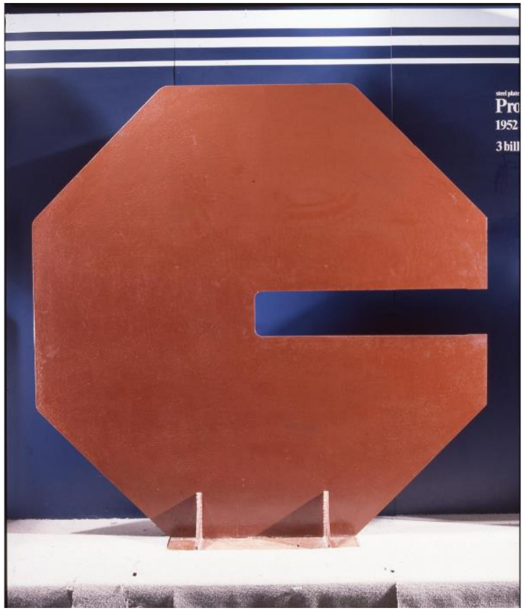

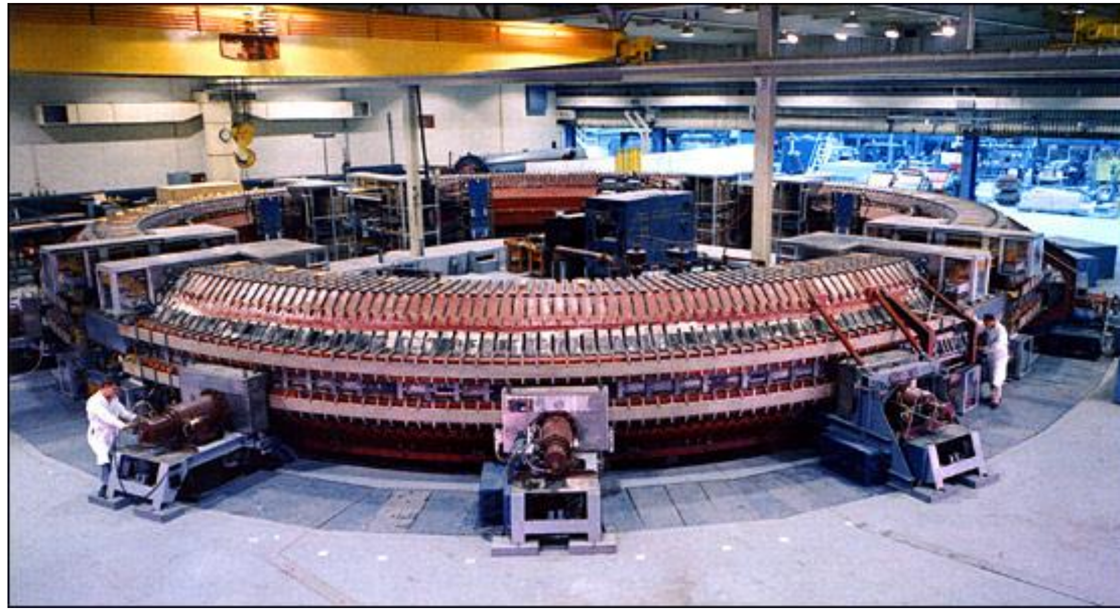

Dipole correctors embedded in quadrupoles (just two examples)

MOPAS074 Proceedings of PAC07, Albuquerque, New Mexico, USA

COMBINED PANOFSKY QUADRUPOLE & CORRECTOR DIPOLE *

George H. Biallas[#], Nathan Belcher, David Douglas, Tommy Hiatt, Kevin Jordan, Jefferson Lab, Newport News, Virginia, U.S.A.

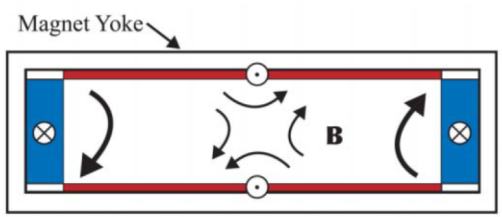

Rectangular Panofsky Quadrupole with Coil Currents (Looking Downstream, Focusing Electrons)

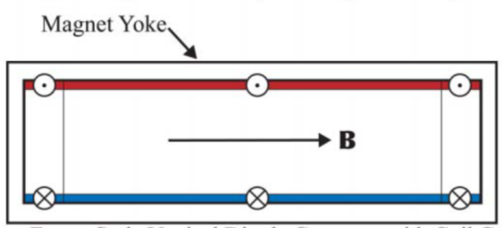

Window Frame Style Vertical Dipole Corrector with Coil Currents (Looking Downstream, Bending Electrons Up)

OPEN ACCESS
IOP Publishing | International Atomic Energy Agency Nuclear Fusion
Nucl. Fusion **62** (2022) 086024 (21pp) https://doi.org/10.1088/1741-4326/ac733f

Design and manufacturing of the combined quadrupole and corrector magnets for the LIPAc accelerator high energy beam transport line

B. Brañas[1,*], J. Castellanos[1,a], C. Oliver[1], J. Campmany[2], F. Fernández[3], M. García[3], I. Kirpitchev[1], J. Marcos[2], V. Massana[2], P. Méndez[1], J. Mosca[4], F. Toral[1], F. Arranz[1], O. Nomen[5] and I. Podadera[1]

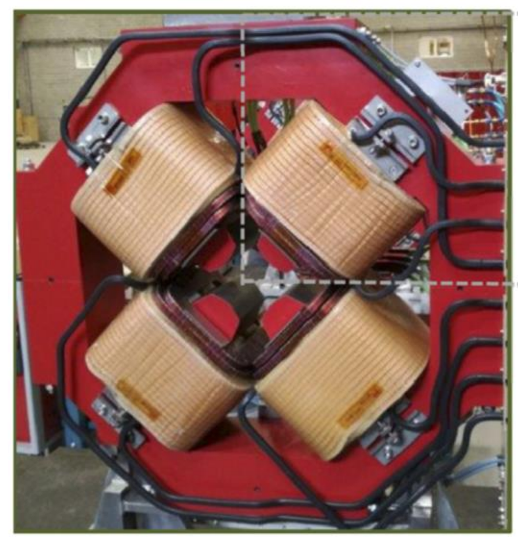

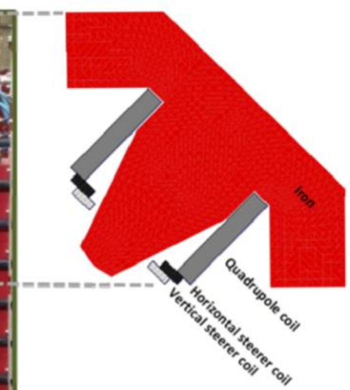

Several correctors embedded in an octupole (an example)

IPAC22

APSU Corrector/Octupole

Dipole (H,V) and Skew Quad Corrector

Parameter	Value
Bore radius	15.5 mm
Yoke (laminated) length	84.6mm
DC correction	0.44 mrad
Steering (1 kHz)	4.4 μrad
Integ. skew gradient	0.73 T

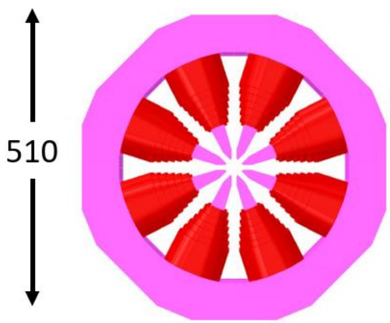

Pole Segment

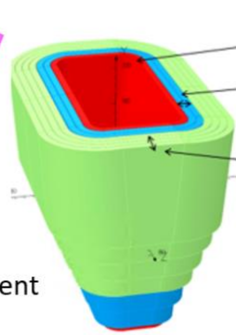

NSLS-IIU Octupole:

- Bore radius: 14 mm
- Pole-tip gap: 8 mm
- Solid Yoke: 206 mm x 206 mm
- Octupole strength (B'''/6) = 121,000 T/m^3
- (Efficiency of 99%)

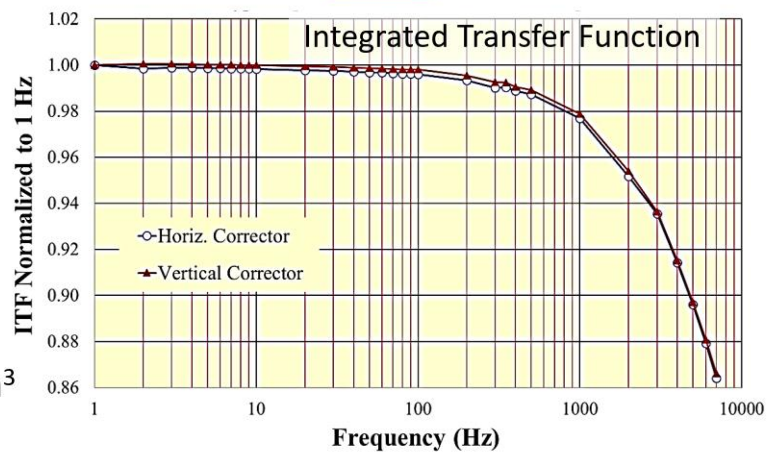

At 1 kHz. drop in ITF = 2%, phase lag < 4^o

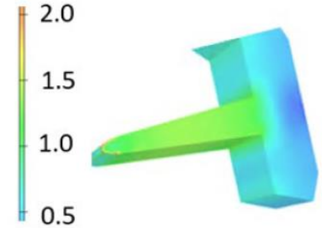

Flux plot
NSLS-IIU Octupole

U.S. DEPARTMENT OF ENERGY

S. Sharma
June 16, 2022

30

BROOKHAVEN NATIONAL LABORATORY

Claw-pole magnet by Malyshev, then revamped by several colleagues, in particular Kashikhin (FNAL) and Volpini (INFN) for superconducting designs

Союз Советских Социалистических Республик

ОПИСАНИЕ ИЗОБРЕТЕНИЯ **402171**

К АВТОРСКОМУ СВИДЕТЕЛЬСТВУ

Зависимое от авт. свидетельства № —

Заявлено 02.VIII.1971 (№ 1689890/26-25)

с присоединением заявки № —

Приоритет —

Опубликовано 12.X.1973. Бюллетень № 41

Дата опубликования описания 27.II.1974

М. Кл. H 05h 7/00
H 01j 3/20

УДК 621.384.6(088.8)

Государственный комитет Совета Министров СССР по делам изобретений и открытий

Автор изобретения — И. Ф. Малышев

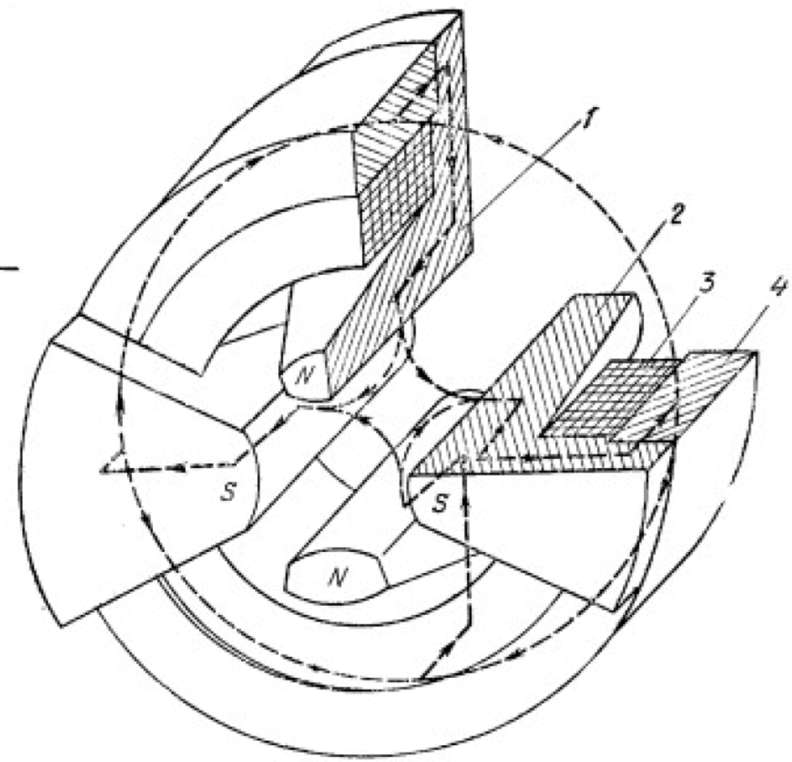

The poles can extend past the coils – this is more rare, but it is done – below a couple of examples

TU1RAI01 Proceedings of PAC09, Vancouver, BC, Canada

SPECIAL MAGNET DESIGNS AND REQUIREMENTS FOR NEXT GENERATION LIGHT SOURCES*

R. Gupta[#] and A. Jain
Brookhaven National Laboratory, Upton, NY 11973, U.S.A.

Figure 1: Prototype magnet for NSLS-II with "*extended pole*" or "*nose*". The dotted line shows the boundary between the nose piece and the main laminations.

DEVELOPMENT OF EXTENDED POLE QUADRUPOLE MAGNET

Kailash Ruwali[#], Ritesh Malik, Navin Awale, Bhim Singh, Anil Kumar Mishra, B. Srinivasan, Gautam Sinha and S. N. Singh

Accelerator Magnet Technology Division, Raja Ramanna Centre for Advanced Technology, Indore, India

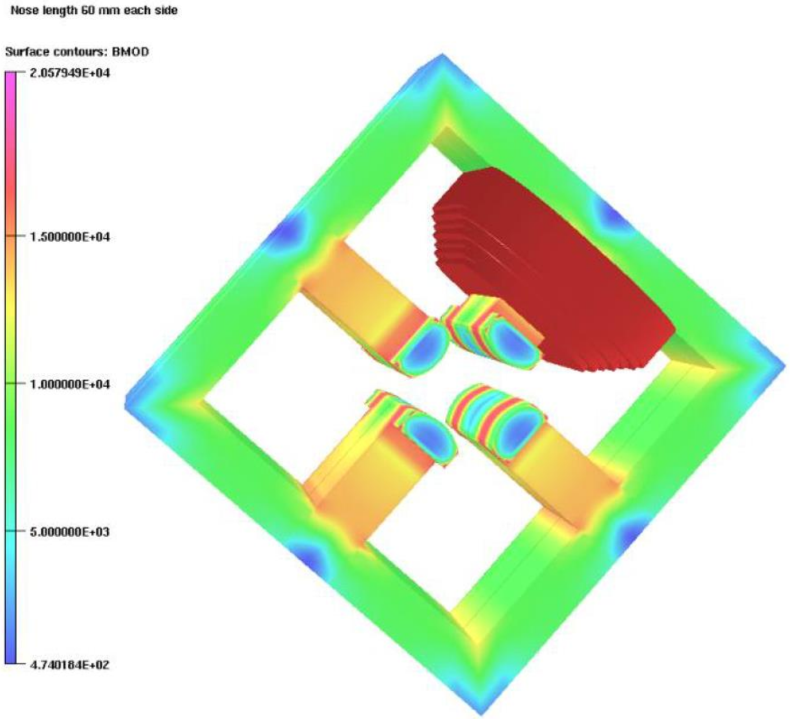

The smallest quadrupole?

PHYSICAL REVIEW SPECIAL TOPICS - ACCELERATORS AND BEAMS **18,** 023501 (2015)

High-gradient microelectromechanical system quadrupole electromagnets for particle beam focusing and steering

Jere Harrison,* Yongha Hwang, Omeed Paydar, and Jimmy Wu
Department of Electrical Engineering, University of California, Los Angeles, California 90095, USA

Evan Threlkeld, James Rosenzweig, and Pietro Musumeci†
Department of Physics, University of California, Los Angeles, California 90095, USA

Rob Candler‡
Department of Electrical Engineering, University of California, Los Angeles, California 90095, USA
and California NanoSystems Institute, Los Angeles, California 90095, USA
(Received 14 August 2014; published 17 February 2015)

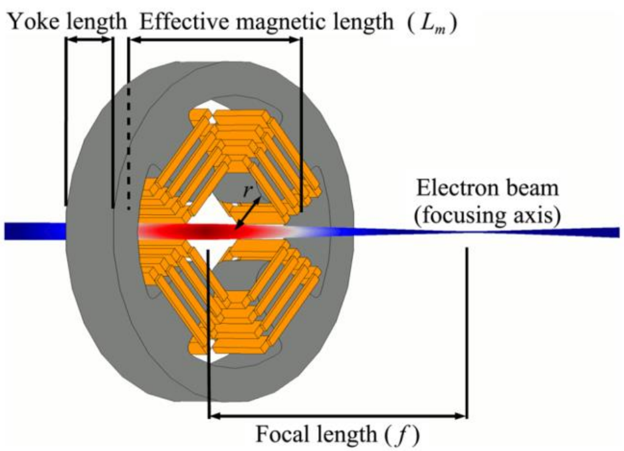

FIG. 1. Particle-tracking illustration of a 0.3 mm electromagnet gap radius, 0.2 mm yoke length MEMS quadrupole acting on an electron beam. The magnitude of the force on the electron beam is illustrated in color (e.g., red = max force). The illustration perspective shows electron beam focusing on-axis of the quadrupole; a perspective from the top would show defocusing of the electron beam.

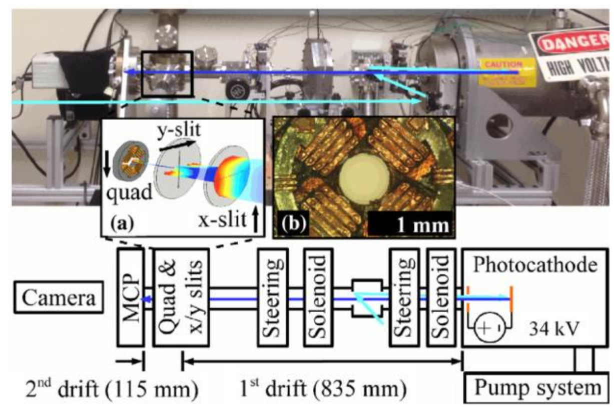

FIG. 9. Photograph and illustration of the electron beam experiment. Inset (a) shows an illustration of the inside of the experiment chamber with an electron beam (colored) entering the chamber from the right, striking a horizontal slit (x-slit) that is inserted into the chamber from below, a vertical slit (y-slit) that is inserted into the chamber from the left, and passing through a MEMS quadrupole (quad) that is inserted into the chamber from above. Inset (b) shows a photograph of a MEMS quadrupole. Cyan arrows illustrate the UV laser path from left to right and blue arrows illustrate the electron beam path from right to left.

SESAME combined function (dipole + quadrupole) magnet: (half of) the cross-section

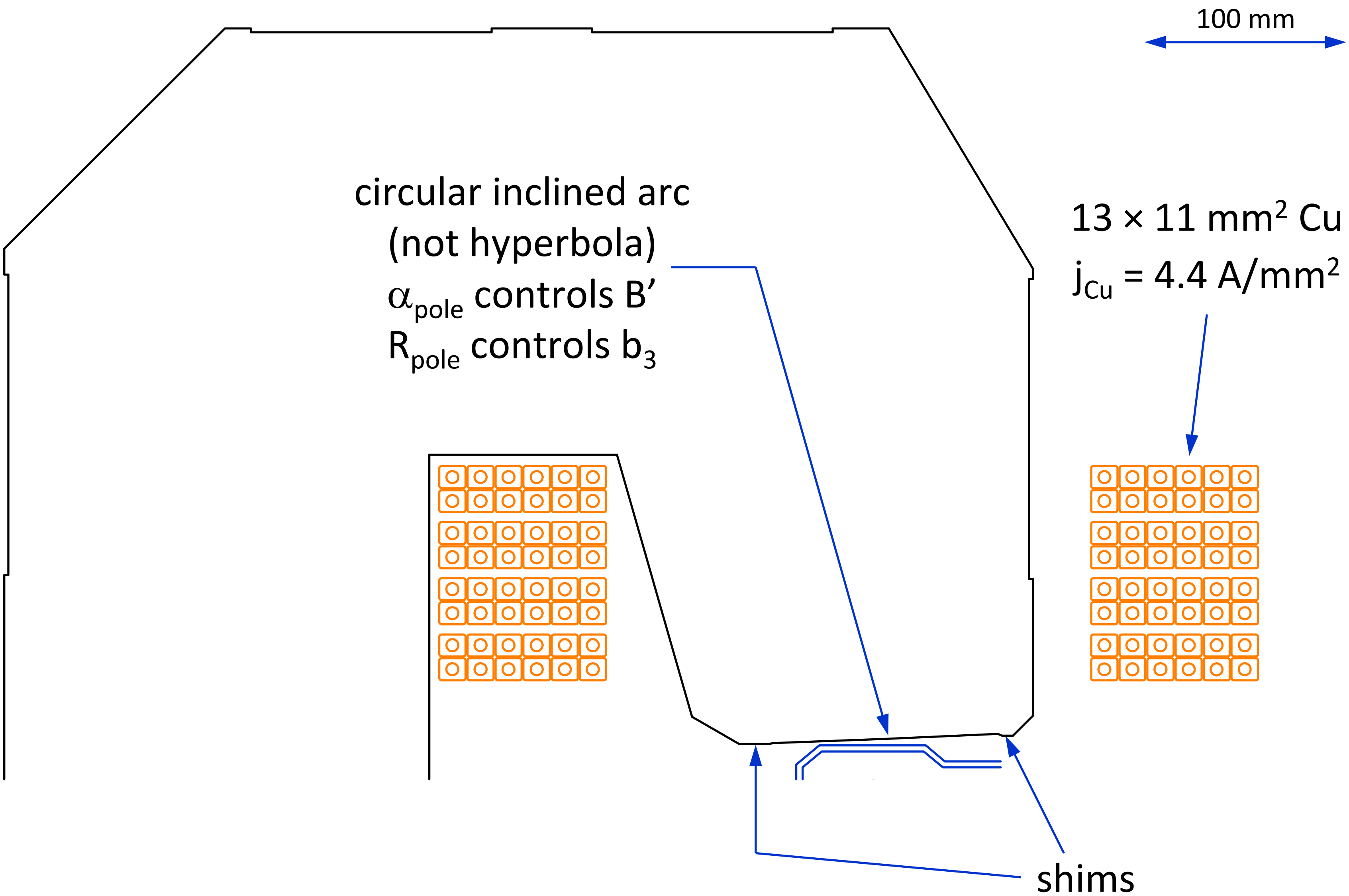

SESAME main bending: the pole is tapered to be gradually filled by flux at 2.5 GeV; at injection energy, the flux lines in the iron are rather different

2.5 GeV, B = 1.45 T

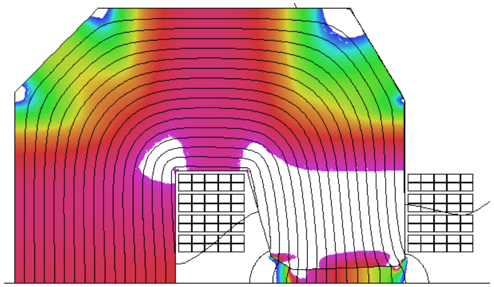

1.0 T to 1.60 T

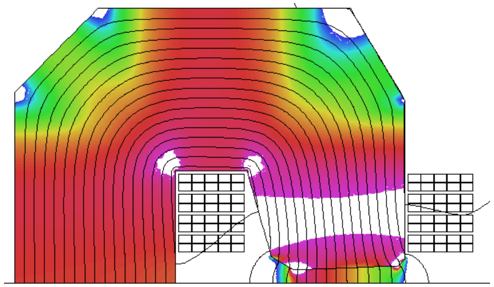

1.0 T to 1.65 T

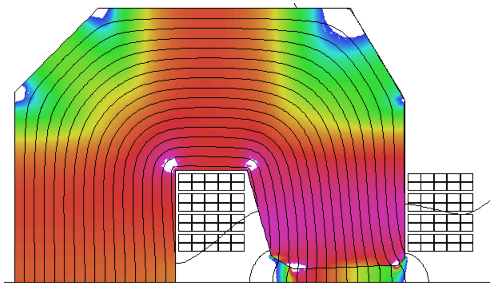

1.0 T to 1.70 T

0.8 GeV, B = 0.47 T

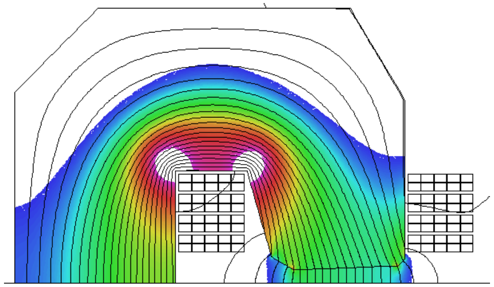

0.25 T to 1.0 T

SESAME main bending: the poles are terminated with three sets of shims, mounted in the endplates, to adjust ∫B, ∫B’ and ∫b_3 (if needed)

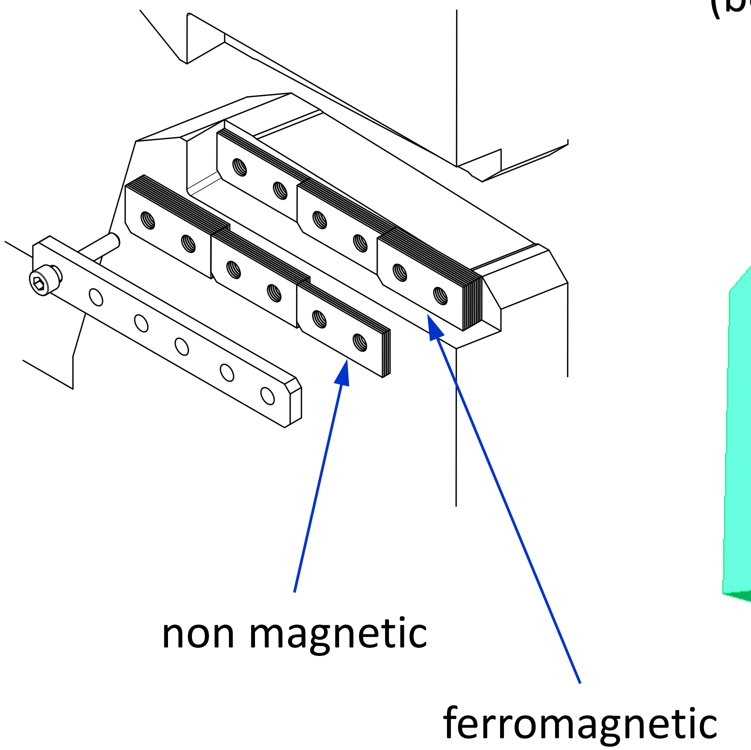

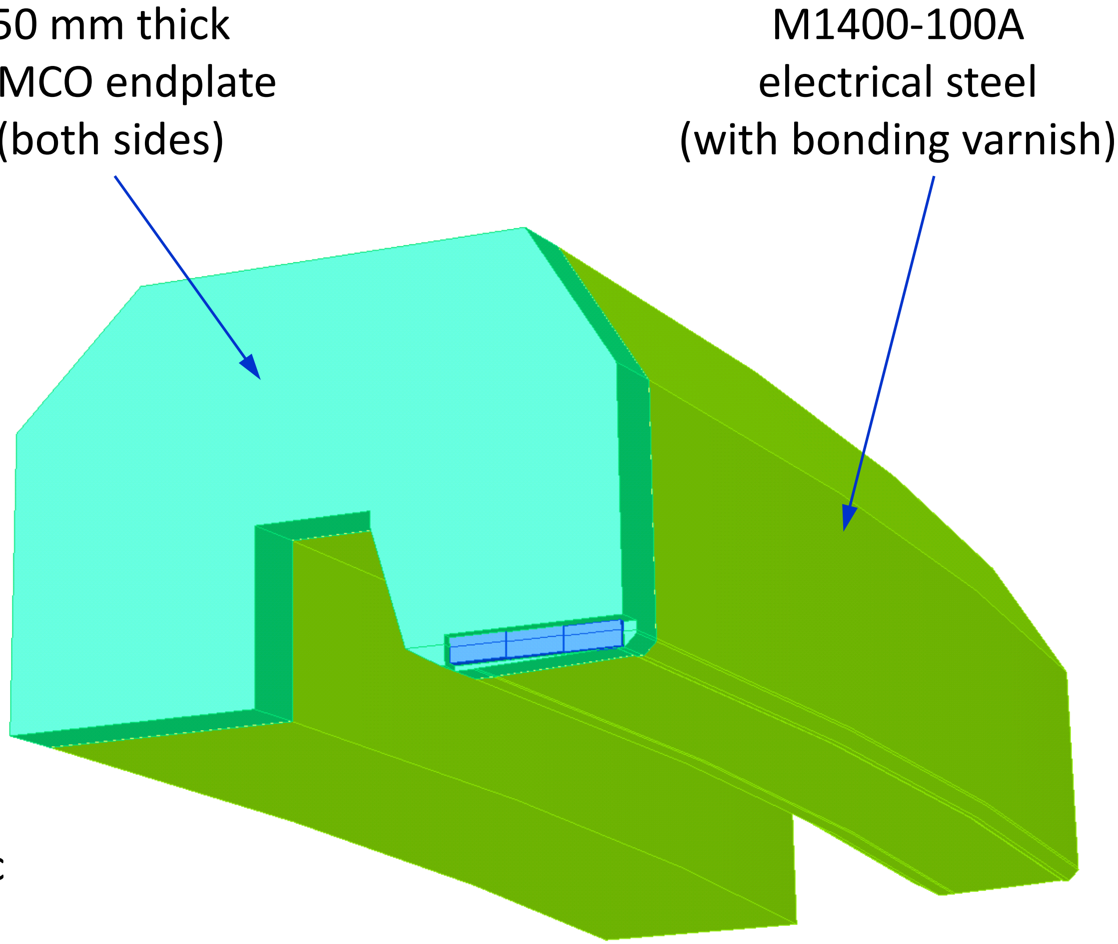

SESAME main bending: the field maps also allowed an optimal alignment, for repeatability of ∫B, and to cancel skew dipole and quad terms

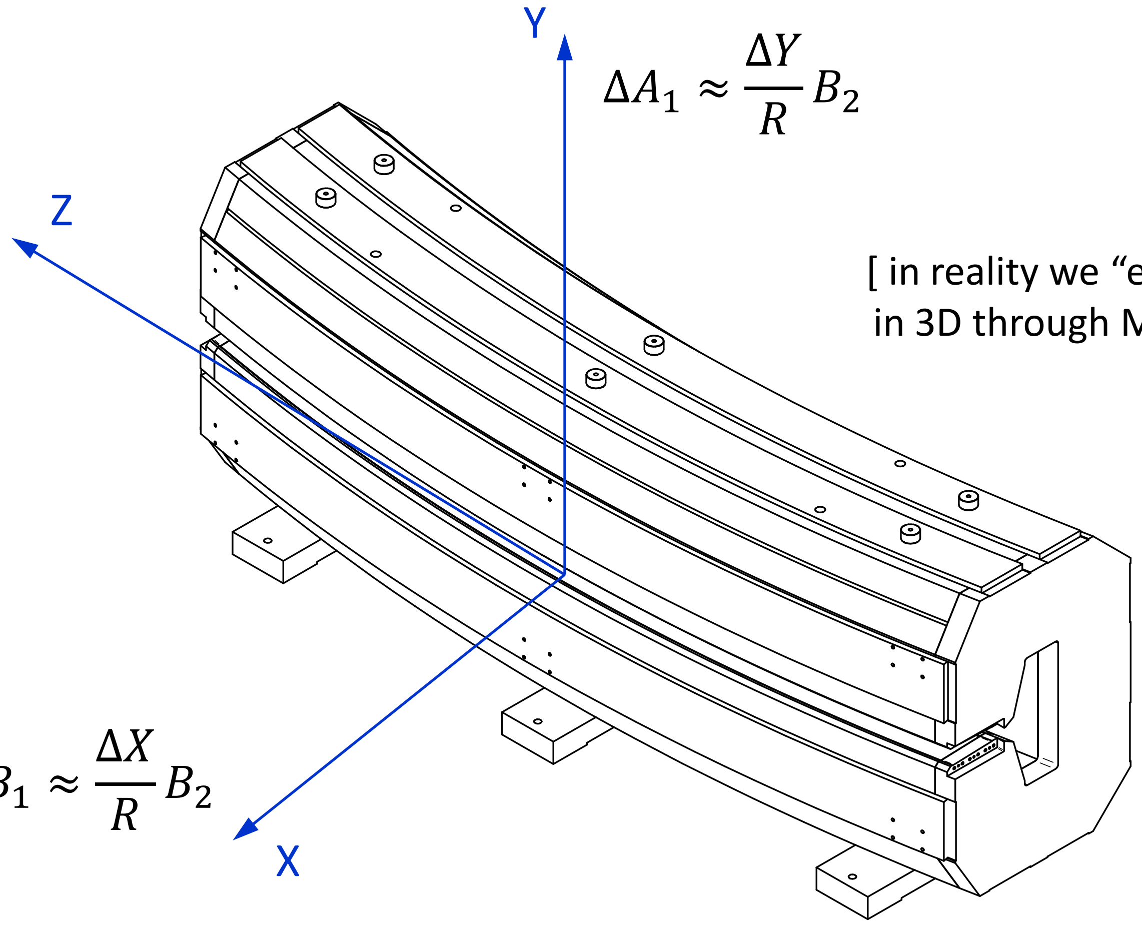

$$\Delta A_1 \approx \frac{\Delta Y}{R} B_2$$

$$\Delta A_1 \approx \Delta\theta_Z B_1$$

$$\Delta A_2 \approx 2\Delta\theta_Z B_2$$

$$\Delta B_1 \approx \frac{\Delta X}{R} B_2$$

[in reality we "extended" the maps in 3D through Maxwell equations]

∫ omitted everywhere

SESAME quadrupoles: as part of the acceptance procedure, we checked on all 66 magnets the key dimensions of the gap

MQDSE #05		ELYTT	
[mm]	hydr. connection side	non-connection side	average
d13	70.004	70.022	70.013
d24	70.040	70.018	70.029
max - average		average - min	
0.008		0.008	
[mm]	hydr. connection side	non-connection side	average
d12	23.536	23.588	23.562
d23	23.564	23.571	23.568
d34	23.609	23.596	23.603
d41	23.579	23.586	23.583
max - average		average - min	
0.024		0.017	

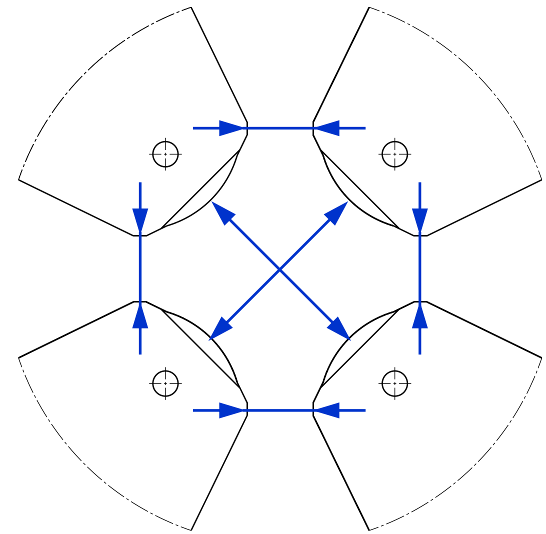

MQDSE #05			Carlos / Michel		10/07/2015
[mm]	hydr. connection side		non-connection side		average
d13	70.030	70.017	70.008	70.005	70.015
d24	70.016	70.018	70.022	70.025	70.020
max - average			average - min		
0.003			0.003		
[mm]	hydr. connection side		non-connection side		average
d12	23.643	23.498	23.508	23.568	23.554
d23	23.548	23.558	23.568	23.568	23.561
d34	23.593	23.588	23.568	23.558	23.577
d41	23.578	23.583	23.598	23.598	23.589
max - average			average - min		
0.019			0.016		

opposite poles ≤ 0.05 mm
adjacent poles ≤ 0.03 mm

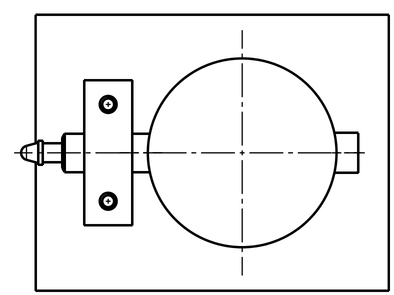

SESAME quadrupoles: the allowed harmonics are well controlled, with b_6 cancelled by the end pole chamfers

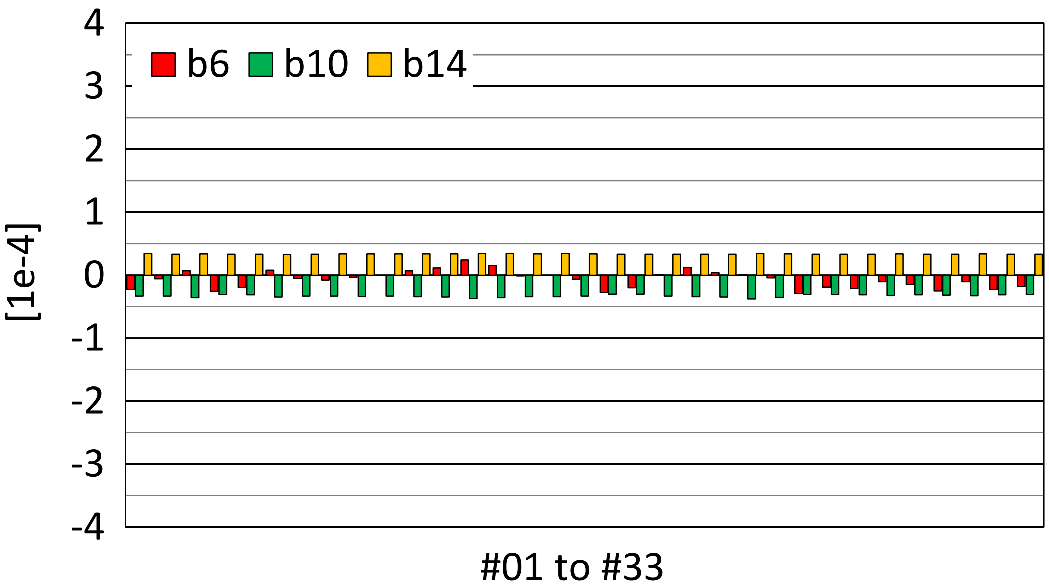

QF (long) @ 250 A

b_6 = -0.1 ± 0.1 rms

b_{10} = -0.3 ± 0.0 rms

b_{14} = 0.3 ± 0.0 rms

harmonics in 10^{-4}
@ 24 mm radius

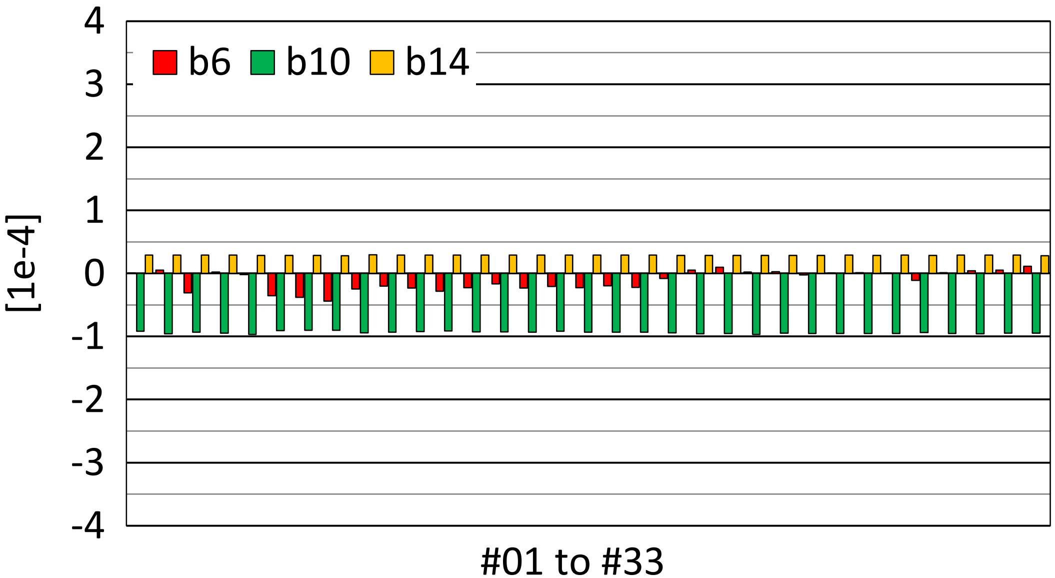

QD (short) @ 215 A

b_6 = -0.1 ± 0.2 rms

b_{10} = -0.9 ± 0.0 rms

b_{14} = 0.3 ± 0.0 rms

SESAME quadrupoles: the random harmonics are also very satisfactory, witnessing the mechanical symmetry of the assembly

mean ± rms	QF (long) @ 250 A	QD (short) @ 215 A
b_3	-0.2 ± 0.8	0.0 ± 1.1
a_3	-0.1 ± 0.9	0.1 ± 1.2
b_4	0.3 ± 0.4	0.9 ± 0.9
a_4	-0.3 ± 0.1	-1.0 ± 0.2
b_5	0.0 ± 0.1	0.0 ± 0.1
a_5	0.0 ± 0.1	0.0 ± 0.1

solenoidal loop in the connection (→ a_4)

harmonics in 10^{-4} @ 24 mm radius

SESAME sextupoles: the correctors are embedded, using extra (10 A) windings – a popular trick in light sources

vertical dipole
(0.5 mrad kick @ 2.5 GeV)

horizontal dipole
(0.5 mrad kick @ 2.5 GeV)

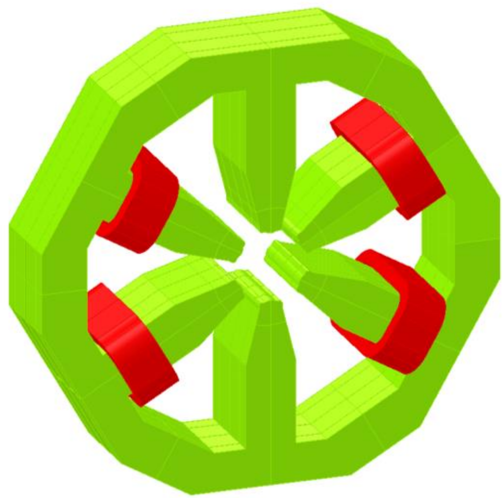

skew quadrupole

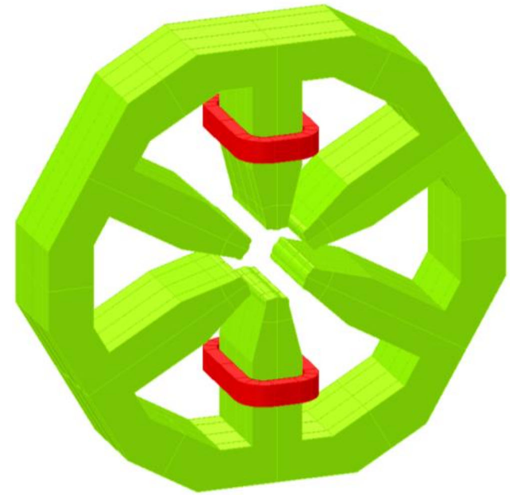

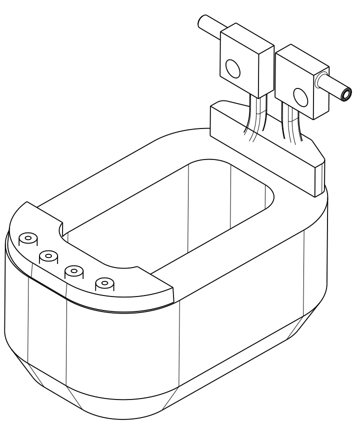

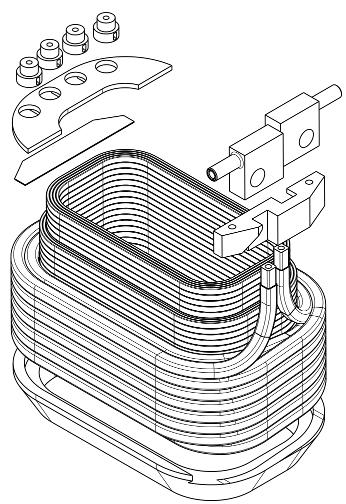

3 windings per coil package:
main (water cooled) one +
two wound with solid conductor

SESAME sextupoles: the field quality of the sextupoles (with the correctors off) is very good

mean ± rms	firm 1 @ 215 A	firm 2 @ 215 A
b_4	-0.5 ± 1.5	0.3 ± 1.6
a_4	-0.8 ± 1.5	-0.7 ± 1.5
b_5	0.8 ± 0.9	0.8 ± 1.1
a_5	0.0 ± 0.7	0.3 ± 1.2
b_6	0.0 ± 0.5	-0.1 ± 0.8
a_6	-0.5 ± 0.2	-0.5 ± 0.1
b_9	0.4 ± 0.1	0.8 ± 0.1
b_{15}	-0.1 ± 0.0	-0.1 ± 0.0

solenoidal loop in the connection (→ a_6)

“allowed” (→ b_9, b_{15})

harmonics in 10^{-4} @ 24 mm radius

SESAME sextupoles: also for each of the 66 sextupoles we re-checked at CERN the key dimensions of the gap

MSXSE #002			CNE TECHNOLOGY CENTER		
[mm]	hydr. connection side		non-connection side		average
d14	75.010	75.020	75.040	75.030	75.025
d25	75.020	75.025	75.025	75.025	75.024
d36	75.040	75.030	75.010	75.030	75.028
max - average			average - min		
0.002			0.002		
[mm]	hydr. connection side		non-connection side		average
d12	19.770	19.770	19.770	19.770	19.770
d23	19.760	19.760	19.765	19.760	19.761
d34	19.810	19.810	19.800	19.810	19.808
d45	19.760	19.770	19.780	19.770	19.770
d56	19.780	19.790	19.780	19.785	19.784
d61	19.780	19.770	19.765	19.770	19.771
max - average			average - min		
0.030			0.016		

MSXSE #002			Greg		11/05/2015
[mm]	hydr. connection side		non-connection side		average
d14	74.997	75.013	75.030	75.042	75.021
d25	75.010	75.012	75.015	75.014	75.013
d36	75.046	75.038	75.035	74.998	75.029
max - average			average - min		
0.008			0.008		
[mm]	hydr. connection side		non-connection side		average
d12	19.759	19.771	19.753	19.763	19.762
d23	19.756	19.749	19.758	19.753	19.754
d34	19.772	19.757	19.763	19.750	19.761
d45	19.763	19.773	19.777	19.778	19.773
d56	19.753	19.777	19.774	19.768	19.768
d61	19.745	19.750	19.741	19.740	19.744
max - average			average - min		
0.013			0.016		

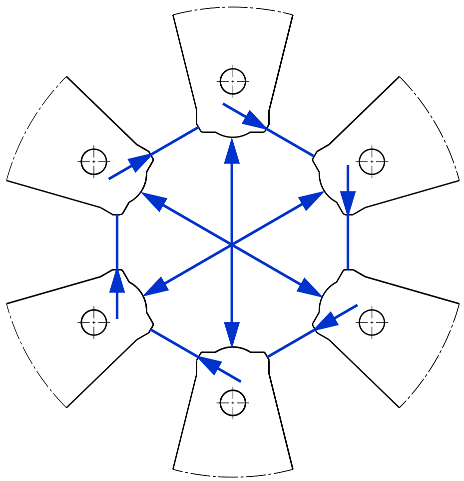

opposite poles ≤ 0.05 mm

adjacent poles ≤ 0.03 mm